# Perspective of Perovskite Solar Cells Through Stability, Safety, Sustainability, Scalability, and Storage (5S) Criteria

*JinKiong Ling, Pradeep Kumar Koyadan Kizhakkedath, Trystan M. Watson, Ivan Mora-Sero*, Lukas Schmidt-Mende, Thomas M. Brown and Rajan Jose**

JinKiong Ling, Professor Dr. Rajan Jose
Nanostructured Renewable Energy Material Laboratory, Faculty of Industrial Sciences & Technology, Universiti Malaysia Pahang, 26300 Kuantan, Pahang Darul Makmur, Malaysia
*E-mail: Rajan Jose (rjose@ump.edu.my)

Dr. Pradeep Kumar Koyadan Kizhakkedath
Research and Development Department, Rex-Tone Industries Ltd. Mumbai, Maharashtra, India

Professor Dr. Trystan M. Watson
SPECIFIC, College of Engineering, Swansea University, Baglan Bay Innovation and Knowledge Centre, Central Avenue, Baglan, SA12 &AX, UK

Professor Dr. Ivan Mora-Sero
Institute of Advanced Materials (INAM), Universitat Jaume I, 12071, Castelló de la Plana, Spain
*E-mail: Ivan Mora-Sero (sero@uji.es)

Professor Dr. Lukas Schmidt-Mende
Department of Physics, University of Konstanz, Universitaetsstr. 10, 78457 Konstanz, Germany

Professor Dr. Thomas M. Brown
CHOSE (Centre of Hybrid and Organic Solar Energy), Department of Electronic Engineering, University of Rome Tor Vergata, Italy.

Keywords: organometallic halide perovskite, lead-free perovskite, multifunctional photovoltaic, tandem photovoltaic, circular economy, solution-based deposition

Perovskite solar cells (PSCs) have received large amount of research funds due to their potential as a front runner in a new generation of solar cells; consequently, desire towards commercializing this technology is mounting. In this roadmap, the knowledge and the technological gaps between laboratory and industry are critically analyzed from the perspective of a 5S criterion (Stability, Safety, Sustainability, Scalability, and Storage). To avoid any favoritism in the arguments toward commercializing this technology, herein, the average parameters of PSCs (photoconversion efficiency, durability, cost, manufacturability, and sustainability) estimated from previous studies are analyzed and discussed. We identify unique

opportunities for PSCs in their current stage of achievements, where application-driven, instead of performance-driven developments are shown to favor their commercialization. Efforts required for improving the average performance indicators of PSCs to the level of the state-of-the art in photovoltaics are also identified and discussed.

**Table of Content**

## 1. Introduction

Share of photovoltaics (PV) in the energy industry has witnessed a drastic increase ever since the introduction of the Paris Agreement to cut down the emission of greenhouse gases. A 2019 report of International Energy Agency estimates ~30% growth in global PV power capacity for subsequent five years, mainly due to cost reduction and coordinated government policy efforts.[1] However, PV and other renewable energy technologies are still not popular than traditional fossil fuels as the latter can supply cheaper energy at higher densities. Besides, concerns over the increasing silicon PV wastes and related photovoltaic waste management after its operational lifetime are mounting.[2-3] Perovskite solar cells (PSCs) discovered in 2009 are viewed as one of the promising sources for future flexible, wearable, and low-cost solar energy production devices. Ever since their discovery in a dye-sensitized solar cells (DSSCs) architecture, reporting a photoconversion efficiency (PCE) of 3.8%,[4] PSCs have experienced large increases in efficiency (arriving at PCEs of over 25%) in much shorter time than any other PV technologies.[5-6] The photovoltaic performance of PSCs can be attributed to the superior optoelectronic properties of halide perovskites, even in polycrystalline films, such as long electron diffusion length,[7-9] ambipolar charge transport properties,[10-12] high absorption coefficient,[13-15] low exciton binding energy,[16-20] the possibility of limiting defect states,[21-25] as well as tuneable energy gap.[26-27] Halide perovskites have the lowest open-circuit voltage ($V_{OC}$)-deficit (defined as $E_g/eV_{OC}$, where $E_g$ is the energy gap of the active material and $e$ is the electron charge) compared to other light absorbing materials (organic molecules and inorganic semiconductors), giving a $V_{OC}$ of ~1.26 and ~1.4 V from a low energy gap perovskite (~1.55 eV) and wide energy gap perovskite (~1.92 eV), respectively.[28-30] In addition, perovskite films can be deposited via low-cost solution processing methods;[31-33] full PSCs (excluding top and bottom electrodes) can be fabricated via coating and printing techniques such as slot die and inkjet,[34-36] allowing low-cost roll-to-roll processing in PSCs fabrication. The capability to integrate PSCs in other devices (tandem cell) offer yet wider opportunities.

The Helmholtz-Zentrum Berlin team have successfully demonstrated a perovskite/silicon tandem cells with efficiency >29%, approaching the magic threshold of 30% efficiency.[37] With certified performance improvement and low-cost solution processing fabrication in laboratory scale, PSCs are expected to advance from laboratory to industry and commercial domain as soon as stability and large scale yields and performance follow suit.

In order for PSCs to be successfully deployed and commercialized, factors such as the environmental factors (lead toxicity), energy payback time (durability), reliability (undisturbed energy supply), etc. need to be taken into account. One major bottleneck in PSCs' practicality is the stability of device; fortunately, after a decade's research, the stability of PSCs has improved to >10,000 hours under constant one sun illumination while retaining a PCE of 13%.[38] Still PSC stability leaves huge gap behind that of silicon PV. Toxicity of PSCs especially the use of lead (Pb) is yet another hurdle to be dealt with. Even though few recovery and recycling techniques were suggested to reduce lead leakage and environmental pollution after service life of PSCs,[39-41] a completely lead-free PSC is preferred for practical applications. Similar to silicon PV, the disposal of end-of-life PSCs modules needs also to be addressed. For constant energy supply, the intermittency of PV requires the technology to be coupled with other energy sources either from National Electric Grid (NEG) or from secondary battery. Recently, companies such as APB Corporation (Japan) and Tesla have started focusing on developing stationary battery power station for constant energy supply. Unfortunately, the high cost of battery could increase the overall cost of PSCs installation as well. The techniques to reduce the cost of battery do not fall within the scope of this paper and are not discussed here; interested readers are directed to other publications.[42-43] With regard to the present article, based on their current state of development, several applications of PSCs are discussed herewith as the low barrier point for their commercialization. The most widely discussed architecture is the PSCs/Si tandem device[44-47] where PSCs are used as a low-cost top cell to improve the

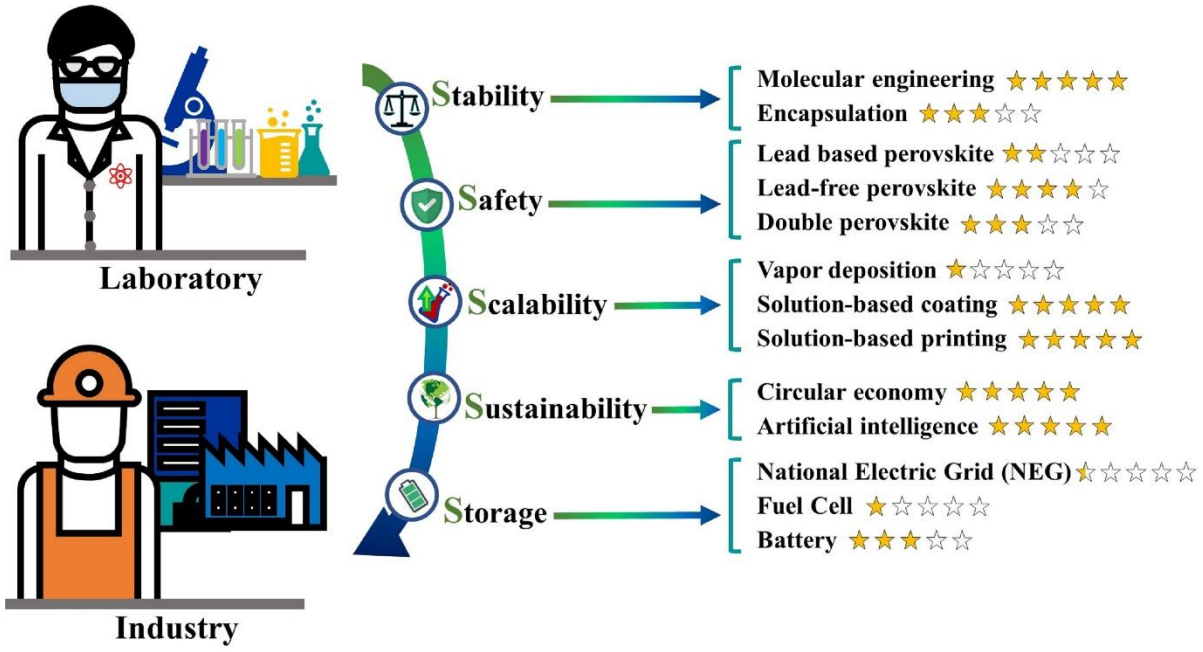


**Figure 1. 5S consideration prior to commercialization of PSCs.** The performance, stability, and safety of PSCs were widely discussed to identify the maturity of this technology for commercialization. Here, production scalability, PSCs sustainability, and intermittency factor (energy storage) are as important in measuring maturity of PSCs technology for commercialization.

performance of Si PV to PCE >29%.[37] Few other applications such as indoor photovoltaics to power smart sensors and the internet-of-things, flexible devices, breathable as well as self-powered consumer electronics could pave the way for successful practical implementation of PSCs even with their current level of performance indicators. However, due to the complexity in producing PSCs fabric, it is expected that the market interest in wearable PV to be interesting only for premium customers (such as astronauts and military). Flexible PSCs to serve as rollable, portable solar panels or with aesthetic purposes in building facades have also been studied extensively.[14,48-50] Flexible PSCs can also be placed on currently installed Si solar farm via mechanical attachment (4-junction tandem device) to boost the performance of Si PV,[51-53] which can then be easily removed for recovery or recycling. In fact, these could serve as the low barrier points of entry for PSCs in the commercial domain.

The purpose of this article is to review the progress of halide perovskite materials and PSCs based on five main considerations (5S) (**Figure 1**) for a roadmap towards their market

entry. The 5S' are Stability, Safety, Scalability, Sustainability, and Storage. All the five criteria are ranked important (5 stars) due to their respective undivided role in commercializing the PSCs technology. The coloured star designates (in our opinion) the importance of respective criteria to bring PSCs one step closer towards low-cost, environmental-friendly, toxicity-free, long-lasting and a highly competitive photovoltaic device. Typically, this article concentrates on the laboratory-to-industrial gap of PSCs technology according to the 5S criteria, including areas lacking research. With focus only on the roadmap toward commercializing PSCs, the commercialization of other applications for halide perovskites, such as perovskite light-emitting diodes (PLEDs), lasers, field-effect transistors (FETs), etc, do not fall into the scope of this discussion. A roadmap toward commercialization is provided, unravelling gaps that need to be closed toward widespread commercialization of PSCs.

## 2. A Brief Overview of PSCs

In general, perovskites refer to a crystal class shared by a wide group of materials showing the broadest range of physical properties from insulator to superconducting, dielectric to ferroelectric, multiferroic and so on; the latest in this addition is the optoelectronic and photovoltaic properties in halide perovskites. The crystal structure of perovskite can be visualized with cation A occupying the dodecahedral position (12-fold coordination) and cation B occupying the octahedral position (6-fold coordination), as shown in **Figure 2a**. Formation of the perovskite crystal structure depends on the size of the cations and anions forming the material. A relatively good indicator to predict the formation and stability of the perovskite phase for a given material is the Goldschmidt tolerance factor ($t$)[54] defined as:

$$t = \frac{r_A + r_X}{\sqrt{2}(r_B + r_X)} \quad (1)$$

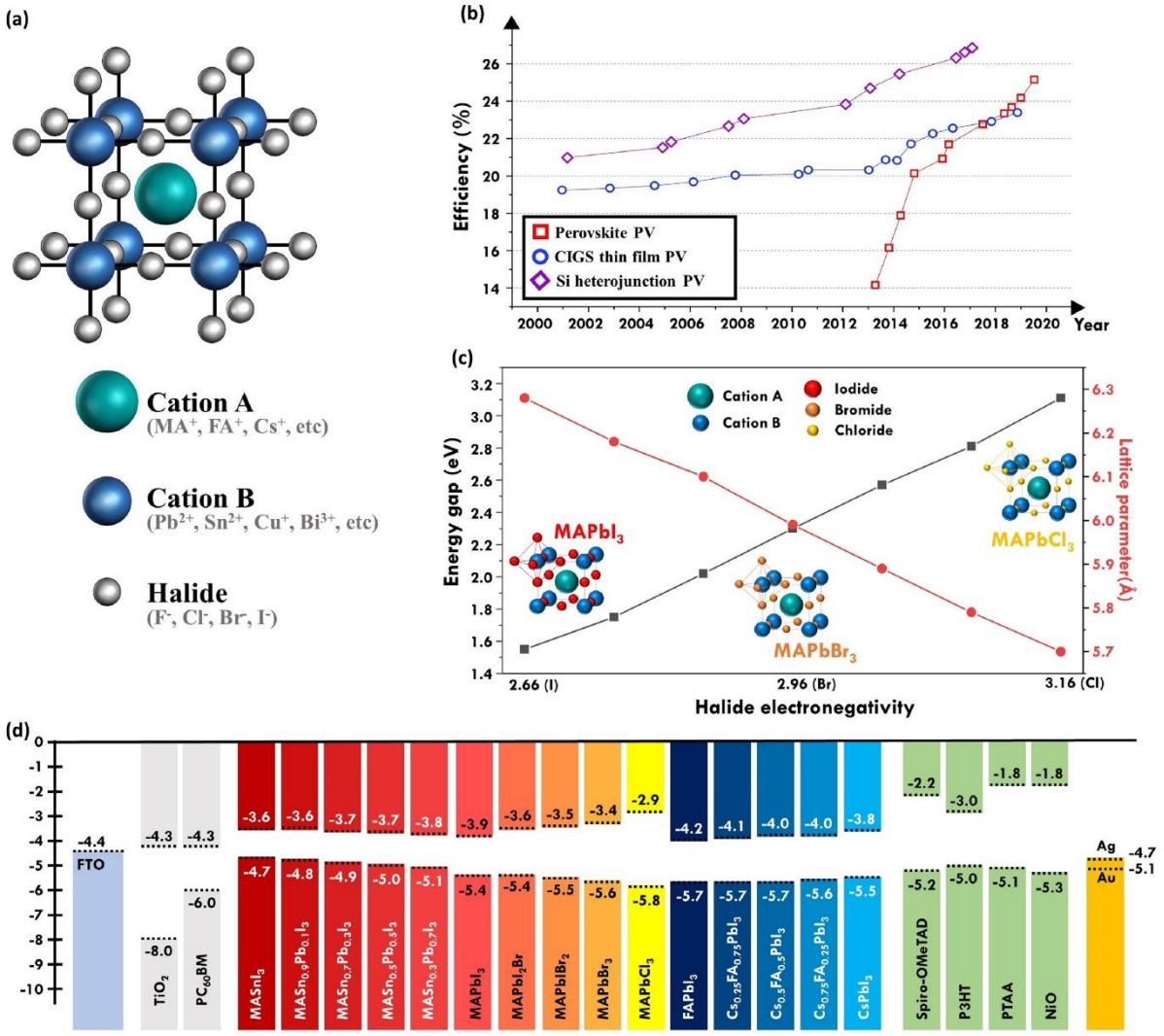


**Figure 2. Structure and opto-electronic energy gap of halide perovskite.** (a) Crystal structure of halide perovskite where few possible candidates for each position stated in blanket. (b) Comparison of efficiency improvement between perovskite, thin film, and Si PVs, showing unique drastic increase in PSCs. (Adopted from NREL photovoltaic efficiency chart). (c) Manipulation of energy gap and lattice parameter during partial substitution of halide anion. (d) Few examples of halide perovskite with wide range of energy gap achieved through ion substitution.

where $r_A$, $r_B$, and $r_X$ are the Goldschmidt ionic radii of cation A, cation B, and anion X, respectively. Generally, the *t* needs to be in the 0.75-1 range to tolerate perovskite phase, with $r_A > r_B > r_X$ and $r_A \sim 1.4r_B + 0.4r_X$ for maintaining the stable cubic phase (favourable phase for photoactive halide perovskite).[55-56] Ideally, cation B is positioned at the centre of the anion octahedral cage. However, the mismatch of radii between the cations and anion could either realign the position of cation B away from the centre position or tilts the octahedral cage at an angle.[57-59] This misalignment of cation B or tilting of octahedral cage could be accounted for

the origin of optoelectronic properties in halide perovskite.[60-62] Nevertheless, tremendous amount of research and development efforts has led to skyrocketing efficiency in PSCs over short time-span, compared to other photovoltaics as shown in **Figure 2b**.

One of the attractive properties of halide perovskite is its energy gap tuneability in the ~1.3-3.1 eV range simply via ion substitution, **Figure 2c-d**.[26-27,63-65] A simple substitution of iodide with bromide ($ABI_{3-X}Br_X$) has widened the energy gap from 1.55 to 2.33 eV (x = 0 and 3, respectively).[26,66-67] Similarly, the energy gap of $ABBr_{3-X}Cl_X$ increased from 2.35 to 3.11 when $x = 0 \rightarrow 3$.[27,68-69] Shrinkage of the crystal volume was observed during I-Br substitution,[70] which is related to the increase in the energy gap of the materials,[71-72] see **Figure 2c**. The shrinkage of the cell volume as well as larger difference in electronegativity between cation B and halide anion were confirmed to widen the energy gap of halide perovskite.[73] Such scenario can be attributed to the increase in electron binding energy of halide ions, where more energy is required to excite the electrons to conduction band (CB).[74] Otherwise, iodide-chloride substitution can only occur at low Cl concentration (only 3-4% iodide ion was replaced), due to the large difference in the ionic radii between both ions.[75-77] As a result, only small increase in the energy gap of the iodide-chloride hybrid perovskite was observed. Fascinatingly, the hybrid halide perovskite containing more than one type of halide ions showed improved stability as well as charge transport properties compared to their mono-halide counterpart.[75,78] The reposition of CB in hybrid iodide-bromide halide perovskite also offered a higher $V_{OC}$ and charge recombination resistance compared to their mono-halide analogue.[79-80] Substitution of lead (Pb) by tin (Sn) in the B site of the perovskite lattice further narrowed the energy gap from 1.31 to 1.1 eV (**Figure 2d**), with a PCE of ~12% for Pb:Sn = 1:1.[81-85] Even though pure tin-based halide has a narrower energy gap compared to its lead based counterpart, with highest PCE recorded at 12.4%, their stability need to be further improved for them to be commercialized.[86-88]

Other than flexibility in energy gap tuning, ambipolar transport properties of halide perovskite materials also attracted considerable attention for this material to be developed into application other than photovoltaics.[10,89-90] In halide perovskites, both electron and hole carriers have almost identical effective mass ($m_e^* = 0.23m_o$ and $m_h^* = 0.29m_o$, respectively), resulting in balanced charge transport properties.[91-95] In other words, the halide perovskite can exhibit properties of both n-type (electron-rich) and p-type (electron-deficient) at the contact interfaces with electron transport layer (ETL) and hole transport layer (HTL), respectively.[12,96-97] A perspective by Kerner and Rand correlated the ambipolar transport properties in the halide perovskite to ionic diffusion; the authors further suggest that unveiling the coupled ionic-electronic ambipolar transport properties is crucial to further understand perovskite materials.[98] This ambipolar transport properties allow smooth diffusion for both negative and positive charges, ensuring promising performance even without selective charge transport materials.

### 2.1. Device architecture

The device architectures of PSCs have undergone many revisions and improvement ever since its discovery in a dye-sensitized solar cell (DSSC) configuration. Different architectures of PSCs are illustrated in **Figure 3** and summarized in **Table 1**. In the first report, perovskite was used to broaden the absorption cross-section (sensitization) of $TiO_2$ photoanode in DSSCs, which otherwise was routinely done using dye-molecules or quantum dots. Kojima et al. reported that such replacement resulted in PCE of 3.8% from $MAPbI_3$ based DSSCs, with an open-circuit voltage ($V_{OC}$) of ~0.96 V, using a liquid electrolyte and DSSC configuration.[4] The photovoltaic performance was further improved to 6.5% by synthesizing quantum dot perovskite and with liquid electrolyte DSSCs device structure.[99] However, low stability was observed due to the dissolution of perovskite in liquid electrolyte, with photovoltaic

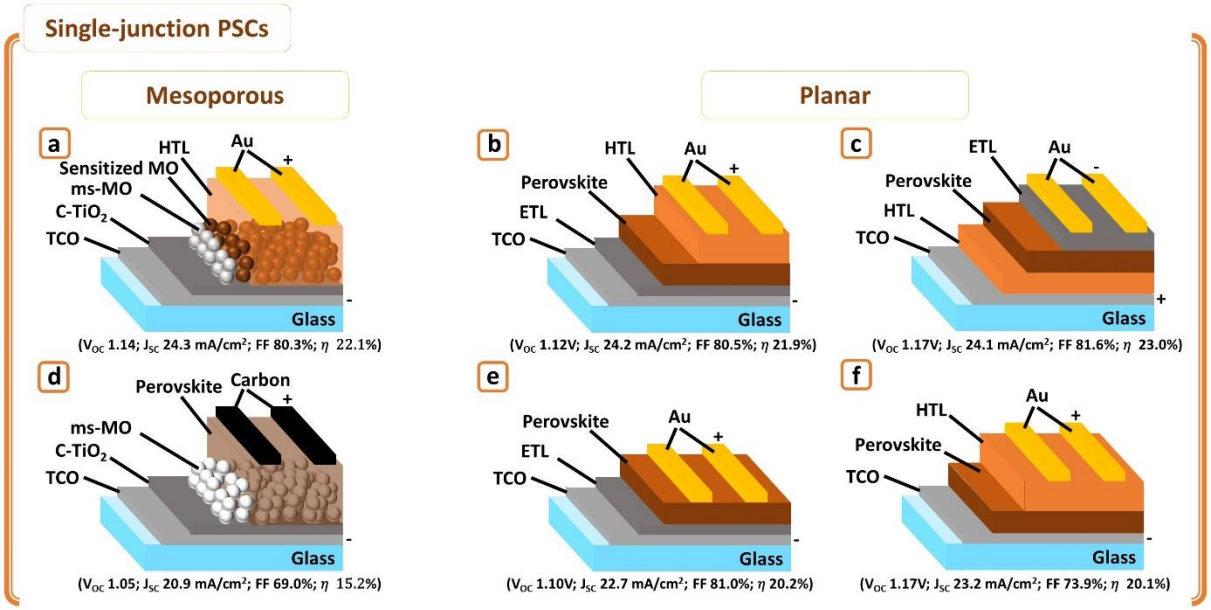


**Figure 3. Device architectures for single-junction PSCs.** Two main branches of device architectures were developed for single-junction PSCs, namely mesoporous and planar devices. The former device adopts mesoporous metal oxide as the scaffold for the deposition of halide perovskite whereas the latter utilized thin metal oxide film with thickness ~400 nm as the photoanode. The photovoltaic parameter inserted in this figure is adopted from: (a) Mesoporous super-structure PSCs. Ref[100] (b) Planar PSCs. Ref[101] (c) Inverted planar PSCs. Ref[102] (d) HTL-free mesoporous carbon-based PSCs. Ref[103] (e) HTL-free planar PSCs. Ref[104] and (f) ETL-free planar PSCs. Ref[105]

performance lasting only for few minutes. The next step in the development of perovskite photovoltaic is obviously improving the stability of the device (or halide perovskite material to be more specific). One of the techniques was to substitute the liquid electrolyte with solid-state hole transporting material, which constituted a significant enhancement on the device stability with durability retained for more than 500 hours.[106] Readers are redirected to cited literatures for further study on hole transport layer for perovskite solar cells.[107-110] Subsequently, the device architecture of PSCs underwent extensive modifications, with only a few suitable for industrial scale roll-to-roll production. The device architectures can be generally categorized either into mesoporous, super-structure or planar designs.

Similar to that of DSSCs configuration, mesoporous metal oxides were deployed as a high surface area photoanode to accommodate more perovskite crystals as an effort to increase the current density (**Figure 3a**). A systematic comparison between semiconducting $TiO_2$ and

insulating $Al_2O_3$ as the ETL then reveal that the mesoporous photoanode merely act as the scaffold for the deposition of halide perovskite.[111] Recently, mesoporous carbon-based PSCs were extensively studied (**Figure 3d**), with PCE reaching ~17% and superior durability owing to the hydrophobicity of carbon electrode.[103,112-113] In fact, PSCs with the longest recorded durability (negligible degradation for 10,000 h in large module with size of 10 × 10 $cm^2$) was deposited based on the mesoscopic device architecture with carbon as its electrode, recording a PCE of ~13%.[38] An in-depth review on the functionality of carbon materials in PSCs is reported elsewhere.[114-116] Apart from its hydrophobicity that offer excellent durability, mesoporous carbon-based PSCs have attracted tremendous attention due to its low-cost compared to metal electrode and HTL. However, the carbon-based PSC PCE need to be further improved to 20% for it to compete with other architectures. Surprisingly, when the metal oxide scaffold layer was removed, a PSC with PCE of 1.8% (currently exceeding 22%) was obtained (known as a planar device) (**Figure 3b**).[101,117-120] Even though metal oxide scaffold has been removed from the mesoporous architecture an additional compact $TiO_2$ layer is present to effectively block the diffusion of hole, which significantly improved the electron extraction and transport efficiency. Planar device showed higher open-circuit voltage ($V_{OC}$) owing to the larger electrochemical potential difference between the conduction band of halide perovskite and valence band of the HTL.[121-123] The combination of both ambipolar transport properties and low exciton binding energy also allow the diffusion of photo-excited charges over longer distances, enabling the deposition of thick halide perovskite layer which is beneficial for high photon absorption and photocurrent degeneration.[124-126] Inverse to the planar design, the components of PSCs can be arranged in the Glass‖FTO‖HTL‖Perovskite‖ETL‖Electrode manner, known as the inverted planar architecture (**Figure 3c**).[127-129] The inverted planar PSCs demonstrated lower J-V hysteresis behaviour compared to its planar counterpart, with PCE as high as 23% (12.8% without the HTL layer).[102,130] Several factors causing the hysteresis were discussed previously,[131-133] with the space charge accumulation at the interface pointed out as

one of the main culprits.[134-136] The J-V hysteresis posted significant uncertainties in the measurement of the photovoltaic performance of the PSCs; different efficiencies are obtained when measured under different measurement conditions.[137-142] However, drawback from the J-V hysteresis is just limiting the efficiency determination by the most extended methodology but it is not affecting the solar cell working condition in DC.

Following the removal of scaffold layer, researches then demonstrated that PSCs without the hole transport layer (HTL) is also functionable, resulting in the HTL-free architecture (**Figure 3e**).[143-145] However, the large offset between the valence band of halide perovskite and the working potential of the metal electrode could significantly reduce the hole extraction efficiency, detrimental to the photovoltaic performance.[146-147] The offset can be overcame either via depositing double layer transparent conducting oxide (TCO) for enhanced charge separation[148-150] or doping in halide perovskite to realign the energy band.[104,113,147] The current highest recorded PCE for HTL-free PSCs (PCE ~20%) was achieved by energy band realignment through p-type doping in halide perovskite. [104,113,147] Motivated by the HTL-free design, removal of metal oxide ETL was also investigated to avoid high temperature annealing requirement (**Figure 3f**). To be clear, the notation of ETL-free included the removal of compact $TiO_2$ layer as well. Similar to that of HTL-free design, removal of ETL significantly reduced the fill factor (**Table 1**), a clear indication of poor charge extraction. Surface defect passivation in halide perovskite was, thus far, the most effective technique in ensuring efficient charge extraction in ETL-free devices,[105,151-152] where perfect surface coverage (close to 100%) is essential in preventing the short circuit between the FTO and HTL.[153-155] Surprisingly, 3-fold enhancement in stability was observed in ETL-free devices compared to their mesoporous metal oxide counterpart,[105,151-152] which we attributed to the elimination of $OH^-$ ions from water splitting under illumination of near ultra-violet light.[156-159] The mechanism of this degradation will be further discussed in **Section 3**. Even though ETL-free devices demonstrating better

durability, their low photovoltaic performance (PCE ~13%) due to poor charge transport properties (FF ≤ 65%) does not favour commercialization. Polymeric ETL was utilized to replace metal oxide, given that no annealing was required during deposition, beneficial for flexible devices, roll-to-roll production, and less energy consumption.[160-162] However, these polymeric ETL are not as cost effective, in term of raw material, lower electronic conductivity as well as poorer thermal, moisture, and light stability compared to the metal oxide counterparts.[163-164] In order to completely understand the stability of PSCs in different device architectures, devices fabricated using $MAPbI_3$ as the absorber materials can be selected from **Table 1** for comparison. To ensure reliable comparison, devices with interface modification, charge transport layer engineering, two-dimensional absorber materials, as well as stability tested under inert atmosphere or encapsulation, is excluded from been compared due to the fact that any improvement in stability could arises from factors other than device architecture. Among the architectures, inverted-planar device offered promising advantages for large-scale production given its superior photovoltaic performance as well as durability, possibly attributed to the enhanced hole diffusion coefficient.[165-166] However, if these devices are compared from a holistic approach, both planar and mesoporous-based architecture also show promising advantages, with the later demonstrating superior operation durability due to the hydrophobicity of the carbon materials. With further work on efficiency enhancement, mesoporous carbon-based device would take over the production owing to its low-cost as well as excellent durability.

### 2.2. Low barrier points for commercialization

#### *2.2.1. Tandem cells*

*PSCs/Si Tandem Device.* Other than standalone PV, PSCs could also be stacked on the other PVs to form multijunction cell, also known as tandem cell. The device architectures of tandem PV are illustrated in **Figure 4a-d** and a brief comparison of tandem cell design in these three architectures is given in **Table 2**. This smart approach can take benefit of the current

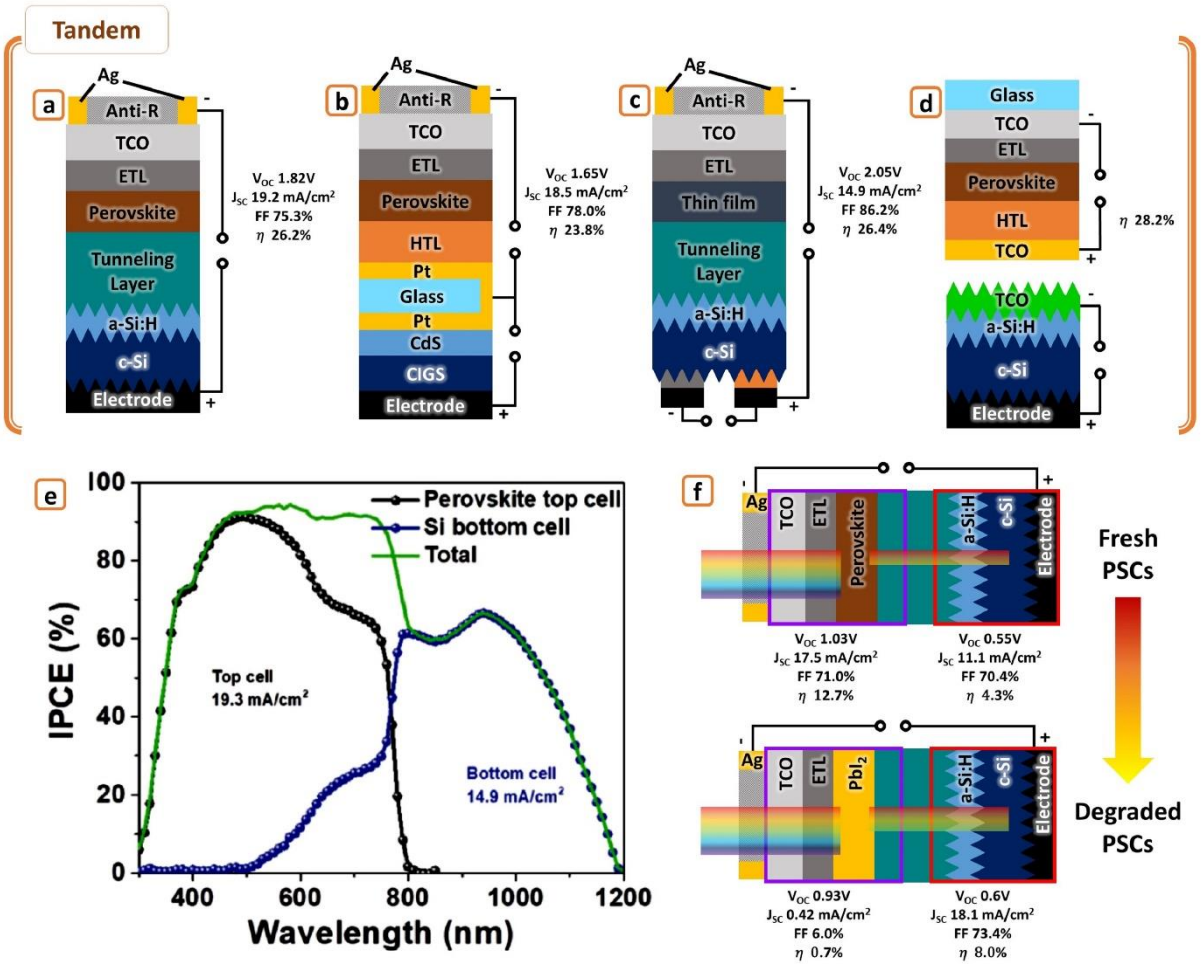


**Figure 4. PSCs/Si tandem devices.** Device architectures of PSCs/Si tandem device for (a) 2-terminal, (b-c) 3-terminal, and (d) 4-terminal devices. (e) The external quantum efficiency curve for PSCs/Si tandem devices showing the contribution of both sub-cells in total photocurrent generation. Reproduced with permission.[167] Copyright 2020, Wiley. (f) Expected performance of PSCs/Si tandem cells when the top perovskite sub-cells degraded.

mature PV technology, as Si or CIGS solar cells, to improve their performance and use their production platforms. The ease in energy gap ($E_g$) tuning allowed the perovskite to be configurated into either the top or bottom sub-cell, using wider or narrower $E_g$ photon absorber, respectively (**Figure 4e**). Tandem devices offer higher photovoltaic performance compared to the single-junction PSCs,[168-171] coupled with reduced thermalization loss (loss of energy in the form of phonon when excited electrons are relaxed back to conduction band edge).[172-175] A certified PCE (~29%) surpassing that of single junction silicon solar cells was recently achieved,[176] indicating that PSCs could function as a low-cost additional cell to improve the

PCE of Si-based PV. Insightful reviews on the efforts to improve the performance of tandem PV above 30% are available elsewhere.[177-178] Even though a PCE of ~29% (31% from simulations) strengthen the PSCs/Si tandem cells as one of the most promising routes for commercialization, the low durability of PSCs remains an obstacle for PSCs/Si to be widely accepted. The mismatch of durability between PSCs (400 days under constant illumination) and Si (22 years) results in severe performance deterioration once perovskite started to degrade. To estimate the performance of the PSCs/Si tandem device after the degradation of perovskite sub-cell, we first look into the photovoltaic performance of Si PV as the bottom sub-cell of the tandem cell. In single-junction Si PV, the photovoltaic performance is approximately ~0.72 V, ~37.0 mA/cm$^2$, ~80.0%, and ~20.5% for $V_{OC}$, $J_{SC}$, FF, and PCE, respectively.[179] However, the performance of Si PV bottom sub-cell dropped drastically to ~0.55 V ($V_{OC}$), ~11.1 mA/cm$^2$ ($J_{SC}$), ~70.4% (FF), and ~4.3% (PCE),[172,180] most likely due to both parasitic absorption from previous layers as well as shortened absorption range (**Figure 4f**). It is expected that the bottom Si PV sub-cell could not acquire the optimum operation as that of its single-junction counterpart after degradation of PSCs top sub-cell. Conversion of perovskite ($E_g$ ~1.7 eV) to $PbI_2$ ($E_g$ ~2.3 eV)[181-182] will broaden the absorption range of the bottom Si sub-cells, thereby slightly increasing it photocurrent. However, the formation of $PbI_2$ during perovskite decomposition would most likely reduce the transparency of the top sub-cell and the increase in shunt resistance could severely affect the overall PCE of the tandem device. In this case, PSCs fail in bringing its advantages as low-cost additional cell in improving performance of Si-based PV, instead parasitically deteriorating performance of the Si PV. Therefore, improving the stability of PSCs to match that of Si PV could be vital for a 2T tandem design and visualizing a 4T tandem device where degraded PSCs can be removed and replaced with ease would be more favourable.

*PSCs/PSCs Tandem Devices.* All-perovskite tandem device also attracted attention due to lower cost-to-performance ratio as well as high flexibility and semi-transparency. Previous literatures showed that all-perovskite tandem device based on lead and tin-lead hybrid perovskite as top and bottom sub-cell, respectively, was able to achieve $V_{OC}$ of ~1.8 V with PCE exceeding ~24%.[183-185] All-perovskite tandem device mostly employed tin-based perovskite as its low-energy gap sub-cell to absorb light with longer wavelength, which is out of reach for the lead-based perovskite (**Figure 2d**).[186-189] Even though durability improvement for tin-based perovskite was previously reported (to be further discussed in **subsection 4.3**), poorer durability of tin-based halide perovskite could lead to premature performance degradation of the tandem device. One major precaution in fabricating all-perovskite tandem device is the need to prevent dissolution of first perovskite layer during subsequent deposition of second perovskite layer. Three different deposition techniques for the second perovskite were envisaged; (i) using a different solvent system for the second perovskite film that would not dissolve the first perovskite film, (ii) a solvent-less approach (such as thermal deposition) for the second perovskite film, and (iii) deploying good barrier between the first and the second perovskite films.[190] The third technique was most widely used, often resulted in a small increase in the shunt resistance. Considering the wastage of solvent during annealing process, a solvent-less approach could be a better choice in achieving tandem device without tunnel recombination layer. Even though such architecture has not been demonstrated on all-perovskite tandem device, a tunnel recombination layer-free tandem device was previously demonstrated on PSCs/Si tandem cells, with a PCE of 21%,[191-194] which could play a pivotal role in further reducing both fabrication cost as well as parasitic absorption in 2-terminal tandem devices.

*PSCs/storage hybrid devices.* Similar to other PVs, power output from PSCs is intermittent and depending heavily on the weather condition as well as the intensity of solar

illumination. As an effort to stabilize the power output, PSCs was coupled with supercapacitors where the photogenerated charges were stored and released based on the power output of the PSCs.[195-197] Given the intrinsic instability of halide perovskite, moisture ingress into the halide perovskite need to be inhibited, either through deploying solid-state electrolyte or utilizing tunnelling layers (conductive layers deposited between the PSCs and supercapacitor sub-cells). Solid-state electrolyte has lower charge transport kinetics,[198-201] whereas tunnelling layers increased the internal shunt resistance of the device.[202-204] An effective technique to mechanically separate both sub-cells while ensuring electronic connectivity is required. Liu et al. devised carbon nanotube (CNT) as a bridge between PSCs and supercapacitor, reporting an overall efficiency of 0.8%, where the hydrophobicity of carbon based materials inhibited ingress of moisture into the PSCs sub-cells.[195] The CNT also offer excellent charge transfer between the photovoltaic and capacitor due to its high electrical conductivity. A two terminal photocapacitor based on carbon modified PEDOT as HTL as well as electrode for capacitor was also reported, showing overall efficiency of 7%.[205] Such device significantly cut down the manufacturing cost by combining the HTM, tunnelling layers, and capacitor electrode into one single material. The main drawback of supercapacitor is its low energy density where the power output of PSCs can only be stabilized for ~10 minutes of low illumination intensity. Replacing supercapacitor with metal ion hybrid capacitors (MI-hSC) offers another alternative for energy density enhancement (longer stabilization duration) without deteriorating the power density (instantaneous stabilization response).[206-208]

### *2.2.2. Flexible devices*

Capability to be fabricated into flexible devices allows the PSCs to be manufactured using high volume roll-to-roll production methods. Different from their rigid counterpart, flexible PSCs (fPSCs) have higher portability, which can be deployed as portable energy generators.

Compared to polymer and thin-film photovoltaics, PSCs offer better photovoltaic performance at a much lower cost.[14,209-210] Progress in flexible PSCs panel is remarkable, with PCE as high as 18% and now approaching 20% achieved.[211-216] Modules on plastic substrates, where series connected cells were fully monolithically patterned by laser ablation, have reach efficiencies in the ~10-15% range depending on size and device architecture.[215,217-219] Nevertheless, fPSCs have always resulted in lower PCE compared to their FTO-glass counterpart, basically due to three reasons: (i) high performing PSCs require heat treatment of $TiO_2$ to 400-500$^oC$, which is too high for flexible substrate such as PET,[220-222] (ii) different wetting and transparency vs sheet resistance properties,[223-225] and (iii) higher roughness in ITO-PET substrate compared to ITO-glass resulted in incomplete coverage of ETL or HTL, inducing degradation and current leakage.[214,226-227] Yang et al. replaced $TiO_2$ with $SnO_2$ (fabrication temperature ~150$^oC$), showing outstanding PCE of 17%; a further development with PCE ~16% in large area module would trigger market possibilities.[228-229] A one-step co-deposition of $Al_2O_3$/perovskite film was also demonstrated by dissolving alumina nanoparticles in perovskite solution, followed by sintering at low temperature.[230-231] Even though only PCE of ~7% was achieved, performance improvement was suggested via optimization of HTL thickness. Recently, carbon materials based ETL was suggested due to its low-cost nature as well as low temperature processing process, with a PCE of ~15%.[232] The hydrophobic nature of carbon materials also aided to reduce ingress of moisture, improving the stability of the PSCs. Besides, flexible carbon materials, such as graphene, also offer capability to function optimally when twist as well as retaining photovoltaic performance under numerous cycles of bending. In term of current collector, Meng et al. studied a combination of PET substrate embedded with Ag-mesh and covered with high-conductivity transparent polymer as anode for the fPSCs, demonstrated flexible device with 14% efficiency and >95% efficiency retention for 5000 hours under bending.[13,233] Such anode offered better conductivity (~3 ohm/sq compared to ~10 ohm/sq for ITO), improved flexibility, better weight-to-performance ratio, and lower cost. Continuous

development of fPSCs into fibrous PSCs thread/yarn, which can be knit into wearable products, were foreseen for future development of wearable electronics.[234-236] Such wearable PSCs technology must withstand substantial bending, twisting, stretching, and folding while retaining its PCE in line with recent recommendation of Tebyetekerwa et al. on flexible charge storage devices.[237] Unfortunately, techniques to turn flexible PSCs into yarns/threads would add additional cost to the overall cost of wearable PSCs, which will be further discussed in **Section 2.3**. As a result, the market for wearable PSCs is niche, most likely to focus on military and space programs where cost is not a limiting factor. It is undeniable that wearable PSCs is still in its infancy and commercializing this technology would reduce the cost and make it more mainstream. Further developing fPSCs onto adhesive tape could be favourable in terms of commercialization, where the degraded PSCs can be easily removed and transported for further processing.

*2.2.3. Transparent photovoltaics*

In the year 2019, Ubiquitous Energy Inc. introduced its leading transparent solar window (ClearView Power) with PCE ~9.8% and transparency of 38.3%, with further effort to achieve transparency as high as 80%.[238] The company then initiated a co-development with NSG Group, a global glass manufacturer, to integrate ClearView Power into architectural window glass, moving the technology from laboratory to industry.[239] Other than Ubiquitous Energy Inc., ClearVue$^{PV}$ corporate also has involved actively in the development of BIPV technology and has close collaboration with the government of Hebei Province, Mainland China as the exclusive BIPV supplier.[240-241] Thus far, commercialized glass window is developed from Si PV (through down-sizing into strips for high window transparency), dye-sensitized or organic PVs (although with low PCE). In this scenario, halide perovskites stand up as high performing transparent active materials, offering large promise for integrating into glass windows. A

thinner active layer is required for higher transparency but it limits the photocurrent density.[242-244] Yuan et al. devised a method to improve the transparency of PSCs via energy gap manipulation where partial substitution of iodide with bromide improved the transparency but reduced the photovoltaic performance (from 27 %T, PCE 12.1% to 41 %T, PCE 8.8%).[242] However, manipulating the energy gap of perovskite does not offer neutral coloured windows but only shifted the colour from brownish to orange. Eperon et al. then reported that constraining the growth of perovskite into island-like structure allowed transparent neutral colour appearance without any reduction in thickness and offered PCE ~6.4%.[245] They selectively wetted the conductive substrate, leading to island-like PSCs growth at the scale small enough to appear continuous to the human eyes, allowing light to pass through the uncoated area. They further demonstrated that such device can be coloured by incorporating dyes in the HTL layer, without affecting the performance of the PSCs. Similar architectures are proposed for DSSCs also but mainly for minimising the lateral charge diffusion through the charge transport layer thereby increasing PCE.[246] Colour incorporation was also demonstrated via applying dielectric mirrors, which is often used in skyscrapers to filter out incident illumination.[247] Surprisingly, 21% improvement in photocurrent was observed when placing the dielectric mirror behind the PSCs.[248] The dielectric mirror also functioned as a reflector, reflecting part of the transmitted light back to the PSCs and boosted the photocurrent. Transparent photovoltaics are favourable for the integration of PV into building windows without affecting the aesthetic of the building as well as the top sub-cells of tandem PVs with low parasitic absorption.

*2.2.4. Photovoltaics for indoor environments*

The interest in perovskite solar cells for indoor applications has picked up rapidly in the last few years after the first results published on both p-i-n and n-i-p configurations.[249-250]

PCEs larger than those under standard test conditions (STC), i.e. of over 25%, were reported under light emitted by compact fluorescent and LED lamps used for illuminating indoor environments. The light spectra from these sources are concentrated in the visible range (400-700 nm) as well as their irradiance is ~3 orders of magnitude lower than that of light at STC. Indoor Perovskite Photovoltaic (IPV) in fact can become an enabling technology in the development of autonomous wireless sensors, low-power consumer electronics, and the internet-of-things (IoT) ecosystem. Installation of these products in the coming years are expected to be phenomenal; powering them from straylight is indeed a zero-emission (low-carbon) approach. The market for IPV is growing at a cumulative annual rate of 70% and is expected to reach 1 billion USD in 2024.[251] Indoor illumination is, in most cases, in the 100 to 500 lx range, with homes and corridors typically ~200 lx whereas office spaces have it in the 400–500 lx range. By different optimization routes, including increasing the quality of electron and hole transport layers as well as their interfaces, [252-254] defect passivation,[255-256] and composition engineering of halide perovskites,[257-258] PCEs in the ~27% to over 30% have been achieved (~ 36% at illumination intensity of 1000 lx). This makes PSCs as the PV technology of the highest reported PCEs under indoor lighting. Lead-free perovskite-inspired materials such as $Cs_3Sb_2Cl_xI_{9-x}$ have shown PCEs of around 4% indoors, a four-fold increase with respect to their (low) PCE under 1 sun illumination which constitutes a promising initial result.[259] Furthermore, PCEs of 13% on PET films[219] and 22% on flexible ultra-thin glass[221] have been obtained, making the latter the highest PCE for a flexible PV technology to date. To power a multitude of products, sensors and surfaces, the possibility of using thin flexible substrates for PV cells will enable more seamless integration even on curved objects found everywhere in buildings and homes. As an application example, perovskite devices have been demonstrated to increase the communication range of wireless temperature sensor by a factor of seven.[260] Overall, the niche but fast-growing market of indoor PVs, can go hand-in-hand with that of autonomous wireless sensor networks and the IoT. Typically, electronic products have much

shorter lifetimes than "the over 20-year products lifetimes" expected for outdoor solar installation. However, operating indoors expose the PSCs to less environmental stresses (illumination, temperature, UV, etc.), making the IPV one of the more attractive entry markets for this new PV technology.

### 2.3. Cost of PSCs

Cost of PSCs is the major component in commercializing the technology, directly affecting customer interest. A report by U.S. Energy Information Administration in February 2020 showed that the Levelized Cost of Electricity (LCOE; average cost of generated energy throughout the lifetime of the generator) for PV is roughly three times higher than coal.[261] Therefore, for PSCs to attract public interest, its LCOE need to be lowered than those of silicon PV or petroleum. In 2011, US Department of Energy initiated "Sunshot Initiative", setting goal for the LCOE of PV to only 6 US cents/kWh to improve its competitiveness with other form of energy. Cost estimation by Cai et al. on two different PSCs modules reported a LCOE of 3.5-4.9 US cents/kWh, three times lower than that of Si PV and surmounted the target of 6 US cents/kWh.[262] Li et al. further extended the cost modelling on tandem devices, reporting an estimated LCOE of 5.50, 4.34, 5.22, and 4.22 US cents/kWh for solo Si PV, solo PSCs, PSCs/Si pair and PSCs/PSCs pair, respectively.[263] Other than Si PV, thin film PV, such as CIGS, was also studied to tandem with PSCs as tabulated in **Table 2**. However, no cost estimation on PSCs/CIGS tandem photovoltaic was been reported previously and no direct comparison with PSCs and Si PV can be made here. Few literatures had concluded that the LCOE of thin film PV, especially CIGS, is slightly higher or identical with that of Si PV.[264-265] Therefore, Si PV, as the most mature with lowest LCOE PV technology, is used as the benchmark for cost comparison between PSCs and other PV technologies with efficiency ≥20%. Both cost estimation concluded that lowering material cost is the key to reduce LCOE of PSCs than Si

PV (half of the cost is on the precursors for perovskite synthesis).[266-267] It is noteworthy that silicon is widely abundant, but the cost of silicon ingot is a lot higher than halide perovskite due to its manufacturing and processing techniques.[268] Undoubtedly, less abundant elements such as bismuth, indium (in double perovskite) etc. will increase the material cost of the PSCs. Current research on 2-dimensional perovskites, where bulkier organic molecules are utilized as cation A, could involve complex material synthesizing process thereby increasing the material cost of the PSCs. Even though low LCOE of PSCs was previously reported, the cost estimation is only a future projection based on PSCs with 20% efficiency and durability of 15 years.[263,266]

Currently, PCE of PSCs has reached ~25% for laboratory scale and ~22.3% for large-scale (1 $cm^2$),[269] approaching the PCE ~20% requirement during cost estimation. However, the longest durability reported for PSCs was ~10,000 hours under constant illumination.[38] To make the scenario worse, such durability is obtained by synthesizing 2D/3D hybrid perovskite, which only offer PCE of 12.9%. These facts clearly indicated that current achievement of PSCs does not meet the projection requirement and no cost estimation was published based on current achievement of PSCs. According to the equation generated by Li et al.,[263] both the total module cost (TMC) as well as LCOE can be estimated using equation 2 and 3.

$$TMC = \frac{1}{\eta \times P_O}(MC + OH + WACC) \tag{2}$$

$$LCOE = \frac{\sum_{t=0}^{T} C_t/(1+r)^t}{\sum_{t=0}^{T} E_t/(1+r)^t} \tag{3}$$

where $\eta$ is the PCE of the modules, $P_O$ is the irradiance power density (1,000 $W/m^2$), $MC$ is the manufacturing cost, $OH$ is the overhead cost, $WACC$ is the rate of profit of the upstream company, $T$ and $t$ are the lifetime and the age of PSCs, $C_t$ and $E_t$ are the net cost and energy production on year $t$, and $r$ is the discount rate. The $OH$ and $WACC$ are assumed to be 15% and 14% of the $MC$, respectively. In accordance to equation 2, a reduction of PCE from 20% to

13.9% resulted in 1.5-fold increase of TMC and 1.5 times increase in LCOE. Shorter durability of PSCs (~3 years) further increased the LCOE by 3-fold compared to the 15 years estimation. Deducted from these estimations, the LCOE for PSCs with current achievement could be around 0.3-0.5 US dollar/kWh. Unfavourably, the PSCs at its current stage is not economically viable compared to the Si PV, mostly due to its low durability. Extensive efforts were poured into improving the performance of PSCs for attaining their Shockley-Queisser limit of 31%.[270] However, the durability of PSCs is seriously lagging behind than that of Si PV and required focused attention. In terms of areal cost, manufacturing cost of single-junction PSCs deposited using roll-to-roll production was estimated to be 29-37 US dollar/$m^2$.[271-272] In order to manufacture wearable PSCs, the flexible device need to be further processed into thread or yarn, which could add an additional 15-25% to the areal cost. Considering the cost of fabric for daily clothing to be 1.6-8.0 US dollar/$m^2$, wearable PSCs would be roughly 5-20 times more costly compared to ordinary fabric for clothing. It is, thereby, insensible to focus on developing wearable PSCs for the public due to the high cost, once again indicating that the market for wearable PSCs is niche, at the current stage of development.

**3. Stability: To be on par with Silicon PV**

Compared with other photovoltaic technologies, PSCs have, indeed, the lowest device stability primarily due to its structural instability and sensitivity towards external stimuli. The halide perovskites are not the only compounds that showed instability in the history of engineered materials; for example, the boron nitride synthesized during 1842 using molten boric acid and potassium cyanide[273] took over two centuries of research to stabilize them, especially when hot pressing of boron nitride was realized after 1960s.[274] Nevertheless, extensive research on PSCs over a decade had improved the stability of the PSCs from several minutes to a few thousand hours.[275-277] To identify the current stability status of PSCs, the

stability of laboratory scale PSCs tabulated in **Table 1** is separated into three categories, namely non-encapsulated device, encapsulated device, and device stored in inert atmosphere (**Figure 5a**). Highest reported stability for laboratory-scale devices is from the mesoporous carbon-based $(5\text{-AVA})_x MA_{1-x}PbI_3$ PSCs (PCE ~17%), with no performance degradation after 9000 hours of testing while encapsulated using hot melt films and glass.[278] However, in terms of precision, most of the reported PSCs showed 90% performance retention in the 1,000-1,500 hours range. This situation marked the immeasurable gaps between the currently achieved durability compared to the 15 years used in LCOE prediction. In order to visualize possible technique to prolong the service life of PSCs to 15 years or on par with Si PV, we discuss several degradation mechanisms in halide perovskite and their respective counteracting measures.

### 3.1. Degradation mechanisms of halide perovskite

#### *3.1.1. Ion migration*

Degradation of PSCs due to ion migration has been one of the main factors impeding large-scale commercialization of PSCs.[279-281] The migration of cation A and halide anion towards the ETL and HTL, respectively, is driven by the electric field induced within the halide perovskite upon illumination.[141,282-283] The role of organic cation (MA or FA) orientation in initializing ion migration cannot be ruled out. Even though such speculation was rebuked on the basis that long timescale (in nanosecond) is required for organic ions to re-orient compared to picosecond time scale in halide ions migration,[284-285] the ferroelectric field generated from the orientation of organic cation could be responsible for the ion migration at longer timescales.[286] Nonetheless, vacancies within the halide perovskite, mostly vacancies of cation A ($V_A^-$) and halide anion ($V_X^+$) are the main driving force for ion migration. First principles calculation showed that the migration activation energy ($E_{Ac}$) for $V_I^+$ (along octahedron edge), $V_{MA}^-$ (adjacent vacant site), and $V_{Pb}^{2-}$ (diagonally in <100> direction) are 0.58, 0.84, and 2.31 eV,

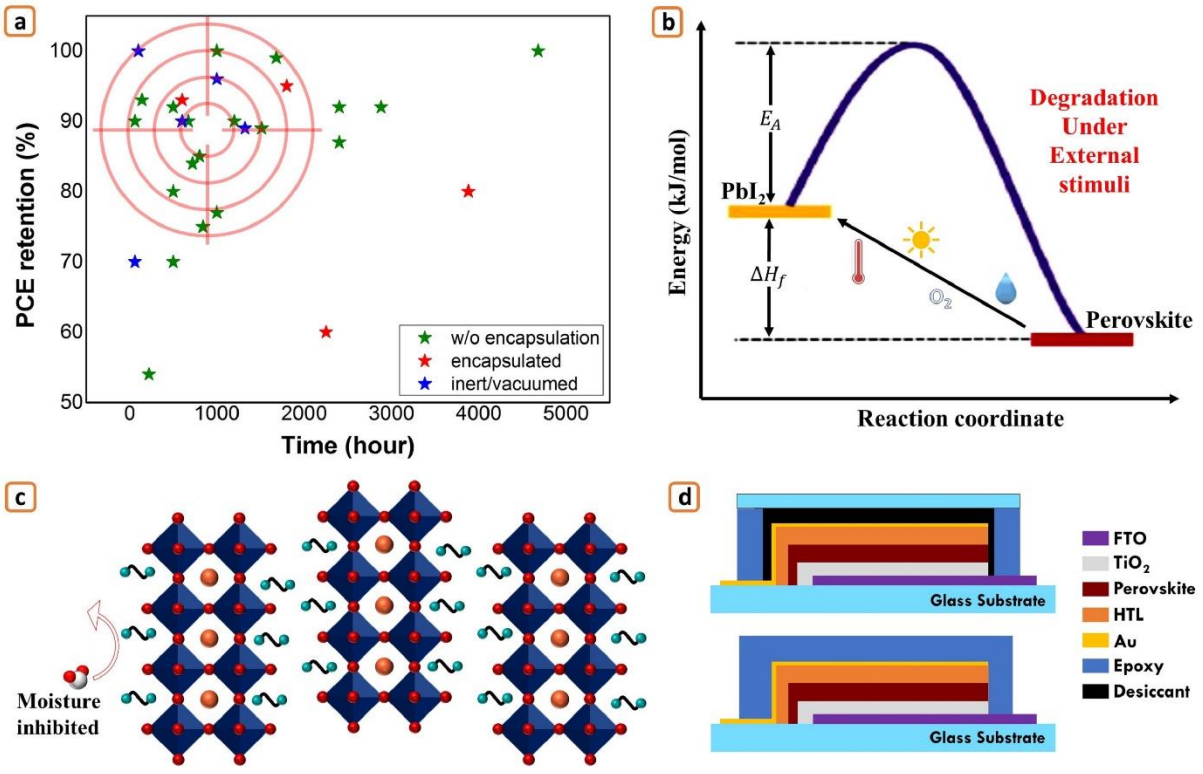


**Figure 5. Intrinsic instability and degradation of halide perovskite.** (a) The PCE retention vs testing duration curve of PSCs tabulated in table 1, clearly pointed out the urgency for stability improvement prior to commercialization. (b) The small enthalpy heat of formation for halide perovskite provides low barrier for degradation into $PbI_2$ phase, which can be easily overcome by external stimuli. Reproduced with permission.[287] Copyright 2017, RSC publications. (c) Bulkier and hydrophobic cation A molecules screen off the moisture ingression, improving resilience of halide perovskite toward moisture. (d) Device encapsulation. (top) Device with edge sealed and interior space filled with desiccant. (bottom) Device completely covered with UV-cured epoxy resin.

respectively.[288] Consistent results were also reported in another study, where an $E_{Ac}$ of 0.48 and 0.57/0.61 eV were calculated for $I^-$ and $MA^+/FA^+$ ion, respectively,[289] showing the ease in halide ion migration compared to that of cation A. Migration of halide ions into both metal electrode and HTL of PSCs was reported to degenerate their electronic conductivity by forming insulating metal halides,[290-291] and deoxidating spiro-OMeTAD HTL,[292-293] increasing shunt resistance followed by deteriorating photovoltaic performance. Besides, phase segregation in hybrid-halide perovskite was also reported due to the migration of halide ion under illumination, resulting in generation of energy trap states.[294-296] Few of the most frequently adopted techniques to overcome ion migration are utilizing inorganic HTL, composition engineering of halide perovskite, and defects passivation. Inorganic metal oxide HTL has been shown to resist

halide ions ingression into/through the HTL;[297-299] negligible concentration of iodide ions is detected at the HTL/metal electrode interface,[300-302] which can be attributed to the high density of the HTL films. However, the demonstration of HTL-free PSCs with PCE ~20% and acceptable durability (92% retention after 500h)[104] clearly indicate that chemically engineered halide perovskite plays vital role in inhibiting ion migration. Substituting larger sized cation A (formamidinium, FA) with smaller sized one (methylammonium, MA and cesium, Cs) was reported to improve the stability of perovskite.[303-304] FA-based perovskite has high tendency to transform into structures of lower symmetry (with poorer opto-electronic properties) at lower temperature,[305-306] where partial substitution of FA with MA or Cs tune the tolerance factor and stabilize the perovskite.[307-308] Alloying the hybrid-halide perovskite with chloride ions also inhibited halide ion migration, increasing $E_{Ac}$ for $V_X^+$ and successfully prevented phase segregation upon illumination.[309-312] In other words, smaller lattice parameter and crystal cell could be able to pinch the ions in place, imposing higher $E_{AC}$ for ion migration,[313-314] which was demonstrated through straining ($E_{Ac}$ for $V_X^+$ 0.29 eV) and compressing ($E_{Ac}$ for $V_X^+$ 0.53 eV) the PSCs devices.[315] Another route would be blocking the migration pathway of the ion vacancies. Substituting MA cation with large radii propane-1,3-diammonium cation (hydrophobic in nature) inhibited thermally induced ion migration,[316-317] where higher $E_{AC}$ was calculated for the migration of halide ions.[147,318] Defect passivation at the interface and grain boundaries of perovskite films also demonstrated significant improvement in both photovoltaic performance as well as durability of PSCs, where the J-V hysteresis was greatly reduced.[319-321] Passivating these defects not only reduced charge recombination by minimizing energy trap states but also decreased the driving force for ion migration as well. Readers are directed to a few extensive reviews for further study on defect passivation.[322-323]

*3.1.2. Humidity induced degradation*

Halide perovskites containing lead are extremely sensitive to moisture and form lead halide by-product once in contact with moisture. It was previously proposed that the organic cation A escapes from the crystal lattice during ingress of moisture due to the deprotonation of MA ions and formation $H_3O^+$ ions.[286] Later studies disputed such theory, stating that $H_3O^+$ is very unstable and transfers the proton back to MA ions in order to retain stability[324] and further investigation showed physisorption of $H_2O$ molecules on the surface of halide perovskite without any significant decomposition.[325] Instead, the chemisorption of hydroxyl ions ($OH^-$) played a vital role in perovskite decomposition.[325] Given the instability of $OH^-$ ions (high tendency to form $O_2$ and $H_2O$ molecules in atmosphere to regain stability), $OH^-$ is expected to originate from the photocatalytic water splitting reaction in metal oxide ETL under ultra-violet (UV) illumination.[326-328] Correlating both water splitting by MO and degradation of perovskite, the overall process can be simplified as (i) physisorption of $H_2O$ at the MO/perovskite interface, (ii) photocatalytic water splitting of $H_2O$, producing $OH^-$, (iii) electron extracted from perovskite by $OH^-$ as well as destabilization of MA cation, and lastly, (iv) collapse of crystal lattice and degradation of perovskite. Surprisingly, humidity has both pros and cons in the film quality as well as the photovoltaic performance of halide perovskite. Humidity played crucial role in perovskite film formation,[329-334] where rapid film-formation (at low humidity) was reported to form large discontinuity (grain boundaries) between films, favourable for ion migration.[335] Initial humidity exposure was reported to improve the film quality of perovskite, most likely due to partial solvation of organic cation, inducing "self-healing" which improved the crystallinity of the halide perovskite.[329] Larger crystallite size and better connectivity between the crystallites of halide perovskite was also reported when synthesized at higher humidity atmosphere.[336] In fact samples prepared under ambient conditions, can take benefit of the moisture during preparation, increasing the long term stability.[337] Nevertheless, long

humidity exposure of the fabricated device will eventually degrade the perovskite and, therefore, efforts to isolate halide perovskite from moisture is crucial in durability enhancement.

Formation of 2-dimensional (2D) perovskite has demonstrated superior endurance against humidity-induced degradation, mainly due to the hydrophobic character of the bulky cations employed in the fabrication (**Figure 5c**). When a much bulkier or long chain molecules (denoted as $A'$) were adopted as the cation A, transformation of 3D bulk perovskite ($ABX_3$) into 2-dimensional layered perovskite ($A'_2A_{n-1}B_nX_{3n+1}$) with the number of layer ($n$) decided by the $A/A'$ ratio was observed.[316-317,338-339] Few previously reported 2D halide perovskites-based PSCs are tabulated in **Table 1**. In fact, the 2D/3D hybrid perovskite is the current record holder for highest durability (~10,000 hours),[38] where part of the improvement could be attributed to the high hydrophobicity of carbon electrode; this topic requires further investigation to unveil the factors leading to the champion durability. Unfortunately, 2D halide perovskite offer inferior photovoltaic performance (~11% compared to >20% for the 3D perovskite), attributing to the long chain cation $A'$ adopted to obtain the 2D structure.[38,340] The layered $ABX_3$ structure constrained charge transport to 2-dimensional planes, where the $ABX_3$ plane readily orientated horizontally to the substrate due to interaction of cation $A'$ with ambient humidity during deposition.[341-342] Such orientation inhibiting vertical carrier diffusion by the insulating bulky cation A, leading to recombination prior to extraction by the ETL.[339,343] A vertically orientated 2D perovskite was then revised with an improved PCE of 12.5%, where deposition was carried out under finely tuned low humidity environment.[344-347] Replacing long chain cation $A'$ by counterpart with shorter chain has enhanced the PCE to ~20% while retaining superior durability.[348-350] Embedding halide perovskite within polymer matrix was reported to improve its hydrophobicity,[351-352] alongside with deteriorated electron diffusion due to insulating nature of most polymers, detrimental to photovoltaic performance. Surprisingly, better photovoltaic performance was reported in PVP-embedded perovskite

compared to its pure counterpart,[353-354] where the underlying mechanism to such improvement in photovoltaic performance for polymer-perovskite hybrid remain unravelled. Encapsulation, on the other hand, isolate halide perovskite from the ambient atmosphere, creating a controlled inner environment (**Figure 5d**).[355-356] With current device materials, degradation rates depend empirically via a sigmoid curve[357] on oxygen transmission rate (OTR) and water vapour transmission rate (WWTR) of the sealing system, which must be in the order of $10^{-4}$-$10^{-6}$ $cm^3/m^2 \cdot d \cdot atm$ and $10^{-3}$-$10^{-6}$ gm/d, respectively, in order to guarantee strong encapsulation performance.[358-359] It is thus important to improve not only the intrinsic stability of PSCs but also the effectiveness of encapsulating system hand in hand.[360-362] Degradation of halide perovskite during curing process of some encapsulant materials was reported,[363-364] urging the establishment of selection standards in choosing suitable encapsulant, which can be summarized as follows: (i) chemically inert with halide perovskite, (ii) solvent-less deposition or, if necessary, use a less damaging solvent system toward all the PSCs components, (iii) low curing temperature <150$^o$C, and (iv) low moisture ingression through the encapsulant. Based on these criteria, paraffin as solvent-less and low-temperature processing encapsulant was developed,[364] showing 90% retention of initial PCE after 1000 hours, owing to both the improve hydrophobicity and chemical inertness between parafilm and PSCs. Li et al. then demonstrated that the encapsulation of PSCs can be done by merely covering the deposited components with adhesive polyimide tape, recording PCE of ~19% with improved moisture and thermal resistance.[365] Encapsulation using glass substrate was also demonstrated by sandwiching PSCs between two glass substrates, edge sealed with highly elastic sealant and the inner space filled with desiccant to absorb moisture.[366-367] Even though the glass substrate offers additional impact protection, such encapsulation technique is not suitable for flexible device and will greatly increase the weight-to-performance ratio. Although glass is an exceptional barrier against ingress of moisture, the solutions for flexible cells are more complex since plastics are highly permeable. Development and application of mechanically flexible

transparent barriers made of oxide and/or organic-inorganic hybrid polymer multi-stack[368] has shown to be effective in improving lifetimes.[357,369] Nevertheless, further developments are required to improve the effectiveness of these solutions over large areas and drive cost reduction to assist the commercialization of fPSCs. A combination of device encapsulation together with molecular engineering on perovskite will further improve the stability of the materials.

*3.1.3. Temperature and light induced degradation*

Temperature and light induced degradation are often inter-related. Both degradation pathways can be regarded as the greatest complications among all the extrinsic factors leading to decomposition of PSCs. Given that the main source for both temperature and light induced degradation is the solar illumination, isolating PSCs from the degradation agent will deem the technology worthless. Therefore, understanding the degradation mechanism and devising proper ways to maintain stability under constant illumination are crucial. The solar panels are exposed to sun throughout the day and they could easily reach temperature as high as 80$^{o}$C depending on the season and the region.[366,370] The photovoltaic performance of PSCs drops with an increase in temperature where transformation of tetragonal perovskite into cubic structure was observed, forming an intermediary state which triggers the degradation of perovskite.[371-372] At high temperature ($t \geq 90^{o}$C), the organic moieties (MA or FA) is removed from the perovskite crystal structure as gaseous by-products.[371] The whole degradation process started with breaking of the relatively weak Pb-I bond, triggering the formation of trigonal $PbI_2$ and the release of gaseous organic moieties.[373] Such process was validated by the detection of $NH_3$, $CH_3I$, HCN, and $H_3C_3N_3$ gaseous by-products through temperature programmed desorption mass spectroscopy (TPD-MS) in vacuum at elevated temperature (150$^{o}$C to 300$^{o}$C),[374-375] suggesting that halide perovskites with organic moieties as the cation A are not susceptible to high temperature. The release of gaseous decomposition by-products at lower

temperature (140°C and 85°C) were also studied using Gas Chromatography-Mass Spectroscopy (GC-MS) to unveil the degradation pathway of halide perovskites.[376-377] At lower temperature (85°C), the organic moieties were degraded into $CH_3NH_2$ and HX (for $MAPbX_3$) or $CH_2(NH_2)NH$ and HX (for $FAPbX_3$) (reaction #4 and #5), which can be recrystallized into perovskite structure through Lewis acid and base reaction further cooling to room temperature. In this case, inhibiting the outgassing of these gaseous degradation by-products is crucial to ensure the recrystallization of the halide perovskite crystal, where polymer-glass blanket encapsulation techniques proved to be effective in suppressing such outgassing.[377] However, at elevated temperatures (≥ 140°C), several irreversible degradation processes occur, simplified in reaction #6-10:[377]

$$CH_3NH_3X\ (s) \rightarrow CH_3NH_2\ (g) + HX\ (g) \quad (4)$$

$$CH(NH_2)_2X\ (s) \rightarrow CH(NH_2)NH\ (g) + HX\ (g) \quad (5)$$

$$CH_3NH_3X\ (s) \xrightarrow{\Delta} CH_3X\ (g) + NH_3\ (g) \quad (6)$$

$$CH(NH_2)_2X\ (s) \xrightarrow{\Delta} HCN\ (g) + NH_3\ (g) + HX\ (g) \quad (7)$$

$$CH_3NH_3X\ (s) \xrightarrow{\Delta} CH_3X\ (g) + NH_3\ (g) \quad (8)$$

$$CH_3NH_2\ (g) + HX\ (g) \xrightarrow{\Delta} CH_3X\ (g) + NH_3\ (g) \quad (9)$$

$$3CH(NH_2)_2X\ (s) \xrightarrow{\Delta} H_3C_3N_3\ (g) + 3NH_3\ (g) + 3HX\ (g) \quad (10)$$

where X represents the halide ions (i.e. Cl, Br, or I). Formation of gaseous hydrogen cyanide and *sym*-triazine were observed in formamidinium lead halide perovskite, with their concentration highly dependent on the temperature, as simplified in reaction #7 and #10.[376] Both reactions are irreversible, leading to substantial deterioration in the performance of FA-based PSCs. However, FA-based PSCs do show better thermal stability compared to that of MA-based counterpart, a conclusion that can be drawn from higher thermal activation energy

for the former.[378] The inorganic $Cs^+$-based perovskite, on the other hand, showed 6-fold increase in the thermal activation energy compared to the FA-based counterpart, indicating superior thermal stability compared to its organic moieties.[376] Indeed, substituting organic moieties with inorganic $Cs^+$ shown to significantly improve the thermal stability of halide perovskite, with $CsPbCl_3$ demonstrating high thermal stability ($t_{degradation}$ > 500ºC).[379-380] As a result, mixed cation A halide perovskites (for example $Cs_{0.05}FA_{0.8}MA_{0.15}Pb(I_{0.85}Br_{0.15})_3$) were widely adopted in current research on perovskite solar cells. The content of inorganic $Cs^+$ was usually low in order to inhibit the formation of inactive yellow $CsPbI_3$ phase and the high FA content was adopted to enhance the thermal stability of the halide perovskite given the high resilience of FA against thermal degradation compared to MA.[381]

When illuminated, the degradation rate of halide perovskite is increased,[372] where lower thermal stability ($t_{degradation}$ ~75ºC) was reported compared to a control sample kept under dark condition ($t_{degradation}$ ~95ºC).[382] The halide bonding was reported to break under illumination, leading to sublimation of halide ions,[383] which could react with HTL or metal conduct, further deteriorating PSCs performance as discussed before. Upon illumination, an in-situ XRD analysis have demonstrated that the $MAPbI_3$ crystal structure decomposed to $PbI_2$ initially, where prolonged illumination further reduced $PbI_2$ to metallic Pb under vacuum or inert atmosphere.[384] In-situ XPS further confirmed the escape of gaseous $NH_3$, HI and $I_2$ by-products from the films, leaving behind hydro-carbonaceous species on the surface.[385-387] Besides, uniform expansion of halide perovskite unit cell was also observed when exposed to continuous light soaking,[388-389] which speed up the moisture penetration into the bulk of halide perovskite, followed by humidity-induced degradation. In contrast, Bastos et al. reported a 50% reduction in photocurrent and 15% reduction in both photovoltage and fill factor at the first 100 hours of illumination,[390-391] even though no changes were recorded in the optical absorbance and X-ray diffraction spectra of sample before and after light-soaking; visible light soaking

deteriorates the photovoltaic performance without degradation of halide perovskite. The halide perovskite could be shielded from moisture by the polymeric HTL; and therefore, no degradation was observed. Decline in photocurrent, on the other hand, can be related to the generation of meta-stable trap state triggered during illumination.[392-393] The origin of the meta-stable trap state is attributed to the generation of polaronic state enhanced by the cation orientation freezing, trapping the electron within the lattice cube.[392] Organic cation such as MA are non-centrosymmetric and its charge distribution depends heavily on its orientation, where substituting organic cation with centrosymmetric $Cs^+$ ion could eliminate the generation of polaronic states.[394] The deterioration of photocurrent can also be attributed to the loss of electrical conductivity of spiro-OMeTAD due to the redistribution of tBP ions (additive in spiro-OMeTAD) into the bulk halide perovskite, facilitated by Au electrode.[288,395-396] Sun et al. then devised a fluoranthene-cored dopant free-HTM, offering PCE of 19.3% and 90% performance retention after 500 hours of illumination (compared to 75% for spiro-OMeTAD based device),[397] concluding that photodegradation of PSCs can be overcome by utilizing either dopant-free HTL or encapsulated HTL-free devices. Bulky cations can also help to increase the thermal stability even in the case of using secondary ammonium cations.[340] Recovery of photocurrent to its original value was observed when the PSCs was stored in dark,[391] suggesting deterioration of photocurrent during daytime operation, followed by recovery in the night. However, the effects of such deterioration-recovery cycle on the long-term stability of PSCs remain unknown. Similar to the thermal degradation, prevention of gaseous degradation by-products outgassing from the device, which could be achieved through developing low-cost, roll-to-roll producible encapsulation techniques, played a crucial role in ensuring the continuity of such deterioration-recovery cycle.

*3.1.4. Stability of cation B oxidation state*

Replacing lead with either tin (Sn) or germanium (Ge) always resulted in both lower performance and stability. It is indisputable that lead-based perovskite, so far, offer higher performance, longer durability and longer carrier lifetime (nanoseconds compared to picoseconds of Sn analogues).[7,398-399] Sn and other group 14 elements have greater +4 oxidation tendency compared to +2 oxidation state. On the other hand, Pb stabilizes at +2 oxidation state as a result from the "Inert Pair Effect" due to its greater atomic mass.[176] With and without the presence of oxygen, $Sn^{2+}$ and $Ge^{2+}$ at the B-site of the perovskite lattice are oxidized into the more stable +4 oxidation state, forming $MO_2$ or $MX_4$ by-products,[400] confirmed through shifting of Sn 3d XPS binding energy during decomposition.[401] Under the condition that no by-product is formed, $Sn^{2+}$ and $Sn^{4+}$ transition transfer extra electrons into perovskite, resulting in higher carrier concentration and electrical conductivity similar to that observed in bismuth (III) doped lead-based perovskite.[402] However, in the case of $SnO_2$ and $SnI_4$ by-products formation the $Sn^{4+}$ impurities will lead to p-type doping of Sn-based perovskite through the formation of tin vacancies, which act as the electron trap states, explaining the poorer electron lifetime of tin-based perovskite compared to their lead-based counterpart.[88,403-405] We speculate similar changes in oxidation state could occur in Pb ion as well, where the "Inert Pair Effect" will cause the less stable $Pb^{4+}$ to convert back to $Pb^{2+}$, resulting in unlimited loop of $Pb^{2+} \leftrightarrow Pb^{4+}$ conversion. The doping ($Pb^{2+} \rightarrow Pb^{4+}$) and de-doping ($Pb^{4+} \rightarrow Pb^{2+}$) process altered the electronic environment and could explain the better electrical properties and stability compared to Sn and Ge analogues. However, no study was ever reported, and such idea remains a hypothesis. Undoubtedly, improving the stability and performance of tin-based perovskite is crucial in order to achieve lead-free perovskite with both long durability and high performance. The most straightforward technique is to inhibit or slow down the oxidation of $Sn^{2+}$ as an effort to stabilize the crystal lattice of tin-based halide perovskite, which will be further discussed in **subsection 4.1**.

### 3.2. Acquiring 20 years lifetimes

Together with all the techniques devised to counteract the degradation mechanism, it is undeniable that the durability of PSCs, despite constant increases, is still not fully satisfactory in the current stage of development. As discussed in **section 2.3**, the PCE and durability of PSCs need to be at least greater than 20% and 15 years, respectively, for it to compete with other PV technologies in term of LCOE. We first look into the intrinsic stability of perovskite crystal by comparing the enthalpy of formation ($\Delta H_F$) between halide and oxide perovskite. A $\Delta H_F$ of -4.82 kJ/mol was previously reported for $MAPbI_3$,[181] which is at least one order lower than their oxide counterpart, with $\Delta H_F$ = -70.06, -64.58, -107.64, and -57.31 kJ/mol for $LaCrO_3$, $LAFeO_3$, $LaCoO_3$, and $LaNiO_3$, respectively.[406] Deduced from the low $\Delta H_F$, halide perovskite can easily revert back to its precursor state once externally stimulated, for example by moisture which leads to humidity-induced degradation.[286] Therefore, increasing the $\Delta H_F$ of halide perovskite is crucial to improve its intrinsic stability and enhancing the durability of PSCs. Both 2D halide perovskite and double perovskite could be promising solutions. Significantly higher $\Delta H_F$ was previously reported for 2D perovskite (-58 kJ/mol)[339,407] as well as double perovskite (-60 to -90 kJ/mol)[408], with the latter expected to be the focus of research in PSCs. Improving the photovoltaic performance of oxide-based perovskite could provide other alternatives for achieving PSCs with stability on a par with Si PV. Compared to halide counterpart, oxide perovskites demonstrated superior durability where no structural changes were observed up to one year, given their high $\Delta H_F$.[406,409] However, the indirect gap and the relatively high bandgap do not make this system attractive for photovoltaic applications. Most of the oxide perovskite based PSCs, also known as ferroelectric oxide photovoltaic (FeOP), offered PCE < 1%, doubting their applicability to be developed into useful PSCs.[410-414] The poor photovoltaic performance of these FeOP could be attributed to their wide optical energy gap, resulting in narrower absorption range which leads to small photocurrents as well as poor band edge alignment at the interfaces.[412,414] The low photocurrent from oxide perovskite could also be

attributed to their heavier carrier effective mass and poor charge transportation, reflected in their low fill factor (<40%).[415-417] Even though PCE of 8.1% ($J_{SC}$ 20.6 mA/cm$^2$; $V_{OC}$ 0.84 V; FF 47%) was achieved through widening the absorption range by stacking several layers of finely tuned energy gap active materials,[416] poor fill factor still persist and extensive work required to reach the current status achieved by halide perovskites. The other concern is the huge $V_{OC}$-deficit in oxide perovskite ($V_{OC}$ ~0.79 V from $E_g$ ~1.6 eV) compared to its halide counterpart ($V_{OC}$ ~1.25 V from $E_g$ ~1.55 eV).[28,416] Higher values of $V_{OC}$ in FeOP were reported by increasing the photoactive layer thickness,[418] which also reduced photocurrent due to increasing charge recombination rates and considering the heavier carrier effective mass and low carrier diffusion coefficient.[419] Deduced from the previous reports, the fill-factor (FF) of the FeOP-based PV is very low (<40%), indicating that optimization of charge transfer is lacking in these devices. Optimization of charge transfer kinetics in solar cells positively affect both $V_{OC}$ and FF,[420] which will further improve the performance of FeOP-based PV. In terms of device manufacturing and film deposition, FeOP materials require high temperature sintering (>500$^o$C), which is not applicable to flexible substrates and may not be manufactured using roll-to-roll production. Back to halide perovskites, even though improving PCE through developing tandem device could drive down the LCOE, low durability is still a major obstacle. Taking solar farm as an example, current PSCs with average durability of 1.5 years (or 3 years from the highest record) would need to be replaced ~13 times (~7 times) to match that of Si PVs. In order to generate energy throughout the lifespan similar as Si PVs, the cost of PSCs installation will be >10 times higher due to sequential replacement. Fortunately, such situation only occurs according to the application of PSCs. In addition, stability reported for PSCs is continuously increasing since the first report and the numbers could be improved in the near future, and the improvement will be one of the factors determining the commercial viability of PSCs.

## 4. Safety: Towards lead-free perovskite

Toxicity of the element lead in the halide perovskites has been one of the major concerns towards industrializing PSCs, leading to extensive investigation on lead-free perovskites.[421-423] Currently, tin-based halide perovskites and double perovskites are extensively studied as the promising lead-free alternatives, with its durability improved to 2000 hours.[424] However, its low photovoltaic performance as well as stability compared to those of lead-based counterpart pose great doubts on its viability as the suitable replacement for lead-based perovskite. On the other hand, even though double perovskites do not show promising photovoltaic performance so far, its development in the future cannot be ruled out. In this section, the bottlenecks of lead-free perovskite materials in replacing lead-based analogue are discussed. A brief comparison for both PCE and stability among different halide perovskite is given in **Figure 6a**.

### 4.1. Mono-cation B lead-free perovskite

Some of the lead-free perovskites and their respective energy gap as well as photovoltaic performance are tabulated and compared in **Table 3**. The first element considered for lead replacement was tin, which occur at the same periodic group as lead (G14 element), offering energy gap of 1.3 eV for $MASnI_{3-x}Br_x$.[87,425-427] However, $MASnI_{3-x}Br_x$ showed extremely low stability (80% performance retention after 12h under $N_2$ condition) with an initial PCE of 5.73%.[87] Studies had also reported replacing lead with Germanium (Ge, G14 element), resulting in $MAGeI_3$ with energy gap of ~2.0 eV and PCE of 0.57%, with low stability as well.[428-431] Currently, tin-based perovskite is considered as the main player among the lead-free analogues due to its superior performance (PCE >10%).[424,432-433] However, the stability of tin-based halide perovskite is still low, with several reviews published on possible techniques for stability improvement, including additives engineering,[434-437] ion substitution,[438-442] and

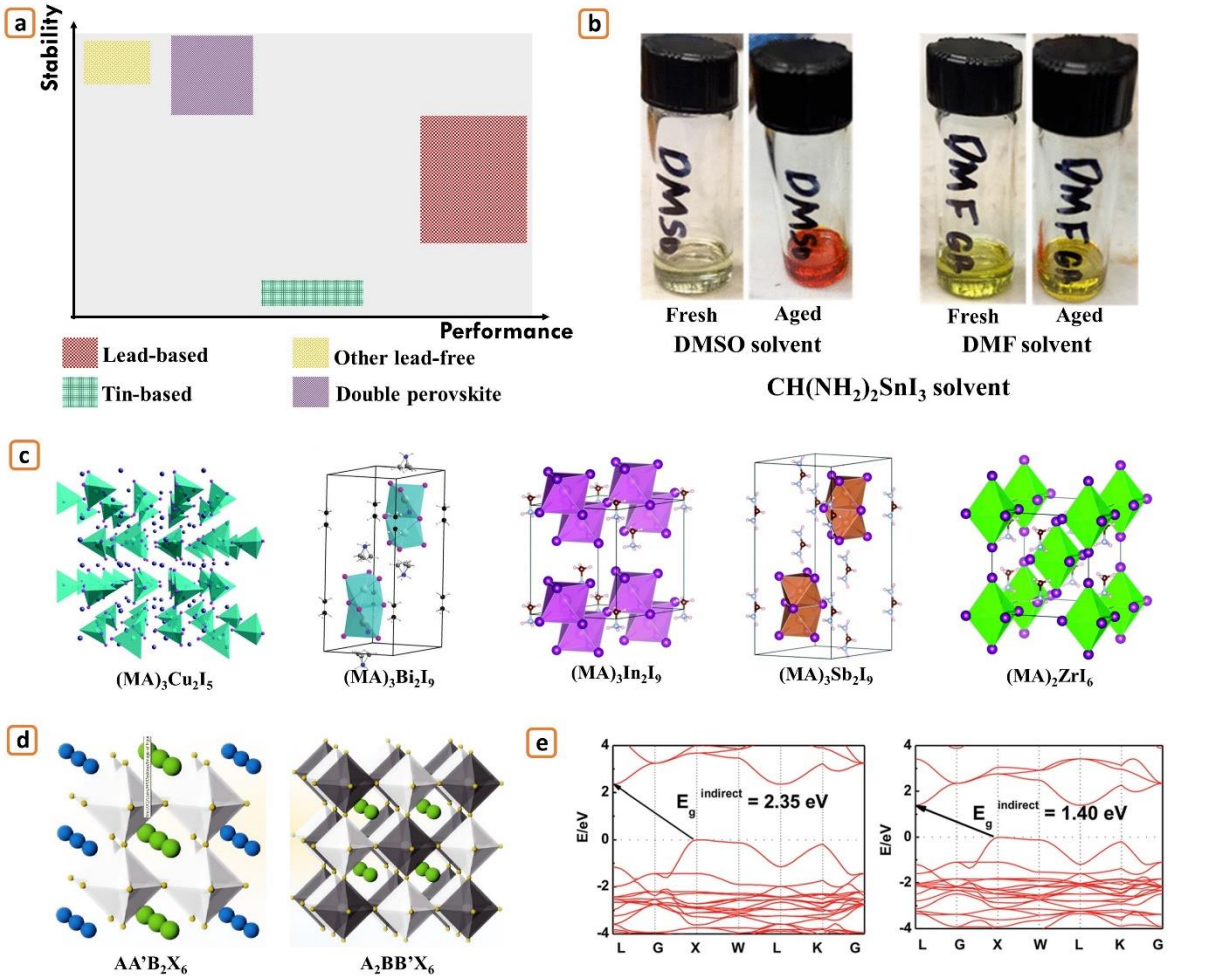


**Figure 6. Lead-free halide perovskite.** (a) Performance vs stability of different PSCs materials, showing tin-based perovskite has the highest commercial value compared to other lead-free counterparts. (b) Illustration of the formation of Sn vacancies in mixed Pb-Sn perovskite due to the presence of $Sn^{4+}$ in the precursor solution, indicating the importance of inhibiting premature $Sn^{4+}$ formation prior to deposition. Reproduced with permission.[445] Copyright 2020, ACS Publications. (c) The lack of 3D connects polyhedron network in most lead-free perovskite, leading to high binding energy for charge extraction. Reproduced with permission.[449] Copyright 2020, RSC publications. Reproduced with permission.[450] Copyright 2016, RSC publications. Reproduced with permission.[451] Copyright 2019, RSC publications. (d) (left) Cubic single perovskite $ABX_3$ where cation A is surrounded by a network of corner-sharing $BX_6$ octahedra. (right) Double perovskite $A_2BB'X_6$ where cation A is surrounded by an alternating network of $BX_6$ and $B'X_6$ octahedra. Reproduced with permission.[452] Copyright 2019, Elsevier. (e) Map of the elements that occupy the A, B, and/or X sites with the compounds characterized experimentally at ambient conditions. Reproduced with permission.[453] Copyright 2017, RSC.

2D structural manipulation.[443-444] The low stability of tin-based perovskite revolved around the high tendency of tin to be oxidized into $Sn^{4+}$ (as discussed in **subsection 3.1**).[424] Stopping the oxidation of $Sn^{2+}$ could involve carefully controlled environment, such as inert environment throughout the production line, which increase the production cost. Besides, the oxidation of

$Sn^{2+}$ was reported to occur prior to deposition, with DMSO acting as the oxidizing agent (**Figure 6b**).[445-446] Unless oxidation of $Sn^{2+}$ can be inhibited during fabrication, further improvement in the performance of tin-based perovskite could be strenuous. Partially substituting tin with other stable elements could result in better stability, with crystal structure alike the double perovskite counterparts.[447-448] A hybrid tin-lead based perovskite was previously demonstrated, with a narrow optical absorption onset at 1060 nm, the narrowest bandgap reported on perovskite material.[81,454] Such material system suggested that partially substituting Sn with transition metal of +2 oxidation state could stabilize the crystal structure.. In terms of photovoltaic performance, the poor PCE achieved in $ASnX_3$ could be due to poorer charge transport compared to $APbX_3$ counterpart, where molecular engineering only boosts the PCE of tin-based perovskite to ~10%.[455-456] Through redesigning the ETL, a PCE of ~12.4% was achieved for tin-based halide perovskite,[86,457-459] indicating the need for complete overhaul on the device design for tin-based halide perovskite.

Elements other than that of group 14 elements were also investigated to replace lead, few are illustrated in **Figure 6c**. Cu-based perovskite ($C_6H_4NH_2CuBr_2I$) exhibit extraordinary hydrophobicity, improving its stability to an extent that no change in crystal structure was observed after 4 hours of immersion in water.[460-462] Surprisingly, an efficiency of ~21.76% ($V_{OC}$ ~1.1 V; $J_{SC}$ ~23.3 mA/cm$^2$; FF ~85%) in $MA_2CuCl_4$ perovskite was achieved through computation simulation; however, PCE of only ~2.4% ($V_{OC}$ ~0.56; $J_{SC}$ ~8.1 mA/cm$^2$; FF ~52%) was achieved experimentally.[463] Even though the reason behind such discrepancy was not discussed, the theoretical calculation showed promising results in Cu-based perovskites. Subsequent studies then showed that the low PCE of Cu-based halide perovskite was the result of low absorption coefficient and heavy holes carrier mass.[464] Recently, trivalent elements, such as bismuth ($Bi^{3+}$) and antimony ($Sb^{3+}$) were also utilized for lead-free perovskite.[465-469] However, low photovoltaic performance was recorded for both $Bi^{3+}$ and $Sb^{3+}$ analogues, as

tabulated in **Table 3**. Large $V_{OC}$-deficit was common among the newly discovered lead-free perovskite materials, which can be enhanced through improving material crystallinity as well as efficient surface trap passivation.[470-472] However, the low $J_{SC}$ could indicate poor carrier transport properties and could be a major hindrance in further improving the photovoltaic performance of these lead-free perovskites. Xiao et al. introduced the term "Electronic Dimensionality" to explain the relationship between the opto-electronic properties and the "Structural Dimensionality" of these lead-free perovskites.[473] The "Structural Dimensionality" of perovskite refers to the connection of $BX_6$ octahedron cage in the 3-dimensional space whereas the "Electronic Dimensionality" represents the freedom in the motion of charge carriers within the perovskite. In order to maintain charge neutrality, both Bi- and Sb-based perovskites are assembled into compounds with lower structural dimensionality.[474-475] The low structural dimensionality eventually leads to low electronic dimensionality where the motion of electron is confined, leading to poorer charge transport behaviour. Even though improved charge transport behaviour was reported in 1-dimensional structured metal oxide,[476-478] the confinement of carrier motion in specific direction in perovskite could result in higher charge recombination.[339,343-347]

### 4.2. Double cation B perovskite

Double perovskites utilize two metals of different oxidation state (+1 and +3) as hybrid cation B, resulting in $AM^{(I)}M^{(III)}X_6$ structure.[479-481] A general comparison of double perovskite is shown in **Figure 6d** and tabulated in **Table 4**. Both $M^{(I)}$ and $M^{(III)}$ have substantial effects on the characteristics of energy gap. Zhao et al. correlated the nature of energy gap in double perovskites through studying the lone-pair state of both cations B.[482] Generally, the double perovskites are categorized into three types; type 1 ($s^2+s^2$) where both cation B have a lone-pair state; type 2 ($s^0+s^2$) where only one of the cations B has a lone-pair state; type 3 ($s^0+s^0$) where

both cation B have no lone-pair state. Both type 1 and 3 double perovskites offered direct energy gap excitation whereas type 2 showed indirect. $Cs_2AgBiX_6$ was successfully synthesized, with indirect energy gap of 2.87 and 3.39 eV for X = Br and Cl, with long photoluminescence lifetime.[483-484] $Cs_2AgBiI_6$ was then synthesized via anion substitution mechanism using trimethylsilyl iodide (TMSI), reporting indirect energy gap of 1.75 eV.[485] Iodide anion was later showed to be unsuitable for some double perovskite materials due to its larger ionic radii which does not satisfy both Goldschmidt tolerance factor as well as octahedral factor.[486] Even though $Cs_2AgBiX_6$ double perovskite demonstrated narrow energy gap, the fabricated PSCs often resulted in poor photovoltaic performance and extremely low photocurrent. Long photoluminescence lifetime (660 ns) was reported for $Cs_2AgBiX_6$ (where X = Br or Cl) due to its indirect band gap.[484,487-489] However, poor electron diffusion coefficient (30 nm) was also observed in this material due to high density of electron traps, justifying the poor photocurrent.[488,490] The deep energy trap states attributed to the 0D electronic dimensionality arising from the separation of the $M^{(I)}X_6$ octahedra by the $B^{(III)}X_6$ octahedra.[473] This statement was further verified through simulation of 3D structural dimension $Cs_2SrPbI_6$, where opto-electronic properties to 0D $Cs_4PbI_6$ was observed,[491] concluding that the carrier in double perovskite is indeed confined electronically. Such confinement of carrier could explain the low photovoltaic performance in double perovskites and also indicate that double perovskites could not be as effective as the lead- or tin-based perovskite. In term of durability, the high enthalpy of formation $\Delta H_F$ (-600 to -900 eV) for $(MA)_2KB^{(III)}X_9$ ($B^{III}$ = Gd, Y, or Bi) halide perovskite[408] indicated that double perovskite could be the lead-free candidate in achieving PSCs with durability on par with silicon PV. However, stability analyses through studying the changes on crystal structure and photoluminescence over time,[492-493] thus far, do not offer clear indication on the maximum stability extend of double perovskite. Besides, as summarized in **Table 4**, most of the studies investigated the intrinsic properties of double perovskite only, where only few were eventually developed and tested as PSCs.[494-496] Few factors could be

hindering the double perovskite from receiving equal attention as their lead-based counterpart; (i) most double perovskites were discovered through computational calculations due to difficulties in their synthesis, (ii) most double perovskites were from type 2 and 3, where photocurrent are limited by deep energy trap states, (iii) the usage of rare and expensive elements in producing double perovskites. Given the indirect energy gap nature for most of the double perovskites, we believe that employing the device architectures adopted in direct energy gap lead-based halide perovskite could be inappropriate. Photoactive material with direct energy gap offers high photon absorption even at low thickness, a direct opposite to that of indirect energy gap material. Therefore, it would be more appropriate for double perovskite to adopt device design and technology innovation pathway similar to that of Si PV, where silicon is an indirect energy gap semiconductor. It is undeniable that development of double perovskite is still in its early stage with unpredictable outcome.

## 5. Scalability: Module production

Compared to non-renewable sources, such as natural gas, fossil fuel, etc., solar cells release less greenhouse gases during operation, where significant reduction in the carbon footprint among coal-fired (975.2 g $CO_2$-eq/kWh) and silicon PV-based (36.75 g $CO_2$-eq/kWh) power plants can be observed. [497-498] However, carbon footprint can still be significant during the silicon PV manufacturing processes, mostly originating from the preparation of pure silicon ingot as well as chemicals used for wafer etching. The production of metallurgical-grade silicon from mined quartz inside huge furnaces release tremendous amount of carbon dioxide and sulphur dioxide, amounting to ~20-40 g $CO_2$-eq/kWh[268,498] which saw a significant improvement compared to roughly 143 and 409 g $CO_2$-eq/kWh in the year 1992 and 1986, respectively.[499-500] Such improvement was argued not due to improved manufacturing processes but attributed to the increasing cumulative installed silicon PV, from 1 $MW_P$ (1975)

to 180 $GW_P$ (2014).[268] The purification of metallurgical-grade silicon into polysilicon involved corrosive chemicals such as hydrochloric acid and hydrofluoric acid,[501] with four-fold amount of toxic silicon tetrachloride by-product in respect to polysilicon produced. Although current technology allows recycling of silicon tetrachloride back into polysilicon with the help of expensive machinery, news regarding the irresponsible dumping of toxic silicon tetrachloride are common, causing lands to be infertile.[502] Compared to silicon-based system, fabrication of PSCs require neither acidic solution nor extreme heat, so a lowering of carbon footprint and more environmental-friendly manufacturing is expected. Even so, solution deposition of perovskite involves volatile organic compounds, such as dimethylformamide (DMF) and dimethyl sulfoxide (DMSO), which could be harmful for both human health as well as aquatic environments. A green PSCs production flow, with low toxic waste as well as low carbon footprint, would be crucial for sustainable PSCs manufacturing. While looking for suitable large-scale production techniques for PSCs, following features should be considered: (i) low wastage, (ii) low-cost capital, (iii) good quality and reproducibility, (iv) mass producibility, and (v) amount of volatile organic compounds released during fabrication. Few reviews correlating the deposition techniques and photovoltaic performance of PSCs have been published previously.[503-505] Therefore, we will only briefly touch on four main deposition techniques, namely physical vapor deposition (PVD), chemical vapor deposition (CVD), solution-based coating, and solution-based printing. With the expectation that PSCs/Si PV tandem been the main commercialized product, techniques with capability to be integrated into Si PV manufacturing line as well as roll-to-roll production would be favourable. Details of these techniques are summarized in **Table 5**.

### 5.1. Deposition techniques

*5.1.1. Physical vapor deposition (PVD)*

Owing to the success of PVD in semiconductor and metal network industries for producing high-quality thin films (e.g., thin film photovoltaics) and corrosion and abrasive resistance coatings, the technique is studied as an economical and environmental-friendly alternative to solution deposition methods, where the usage of any volatile organic compounds could be eliminated. PVD can be achieved through evaporation from either single-source (depositing MAI and $PbI_2$ at the same time) or dual-source (depositing MAI and $PbI_2$ separately). The precursors were evaporated through either direct or induction heating, where the vaporized ions transferred and deposited on the substrate placed directly above the evaporation source. A combination between PVD and solution-based deposition was demonstrated previously, where $PbI_2$ framework was vapor deposited, followed by spin-coating of MAI solution, showing high quality perovskite layer with excellent coverage.[506-510] The process can be reversed where substrate with inorganic framework deposited is subjected to the vaporized cation A-halide powder (by heating) inside a closed chamber. Tafazoli et al. demonstrated that second stage vapor assisted deposition of MAI precursors, after two-step spin-coating deposition, could improve the morphology of the perovskite film (flat and full coverage) while converting any residual $PbI_2$ framework into perovskite phase.[511] Indeed, compared to solution deposition, perovskite with better coverage and stoichiometry from vapor deposition was also reported elsewhere.[512-513] For industrial scale production, large panel (with $PbI_2$ framework deposited) can pass through a conveyor belt into a large chamber filled with MAI vapor, removing the requirement of dipping or spin-coating. This advantage basically resulted in a cleaner deposition method as well as allowing large area deposition of PSCs compared to the spin-coating procedure. During PVD, the vaporized source is deposited on ‘cold’ substrate, making the process applicable to flexible substrate as well. However, vapor deposition usually take hours for completion, which would largely reduce the industrial productivity. Unintentional

impurities as well as other gaseous element could be deposited during PVD and will affect PSCs photovoltaic performance, which call for a controlled atmosphere to ensure high quality and contamination-free perovskite deposition. Besides, the high temperature and vacuum conditions has safety implications, coupled with relatively slow deposition rate of PVD make it less-attractive for cost effective production (further discussed in **subsection 5.2**).

*5.1.2. Chemical vapor deposition (CVD)*

Chemical vapor deposition (CVD) is considered as a matured technology for large area thin film fabrication,[514-518] which offers better film quality compared to PVD technique in producing high quality inorganic thin films. Perovskite films with small roughness (~50 nm) and large grain size (up to microscale), beneficial for high performance of PSCs, have been successfully fabricated using CVD.[519-520] Thus far, PCE ~15.6% was reported for $FAPbI_3$ based device, where 9.5% and 9% efficiency were reported in device of area ~8.8 and ~12 $cm^2$, respectively,[521] suggesting high suitability of CVD in large area PSCs fabrication. For CVD to be more economical in PSCs production, low pressure CVD process in coating $MAPbI_3$ layer was revised, showing a PCE of 12.73% while fabricated under high humidity (~60%) condition.[522] Patterning of perovskite film on conductive substrate was demonstrated using CVD through masking the $PbI_2$ framework throughout the deposition process, showing that isolated cells can be deposited over a large substrate.[523] Despite the promising results obtained from CVD techniques, solution-based deposition attracted more attention as they required less energy during deposition. However, compared to solution-based deposition, film deposited using vapor deposition (both PVD and CVD) showed better film quality and coverage, but with poorer photovoltaic performance. This contradiction could be attributed to higher shunt resistance at the interfaces between different components.[524] Besides, no literature had previously reported deposition of polymeric charge transport materials using both PVD and

CVD, indicating that both techniques can only be used to deposit non-polymeric materials. Furthermore, reaction time of CVD need to be precisely controlled where insufficient time could lead to unconverted $PbX_2$ framework and prolonged time would cause accumulation of MAX precursors. The latter accumulation would act as the decomposition nucleus, detrimental to stability and photovoltaic performance of PSCs. The manufacturing cost using CVD is quite high as well, unsuitable for a new start-up company with lower production capability.

*5.1.3. Solution coating*

Solution coating is one of the most effective methods to deposit thin layers of materials dissolved in a solvent over a large surface area. Compared to other methods available this is one of the most economic options that offer scalability. Depending on the nature of the solution to be deposited and the nature of the substrates, different methods of laydown are available. Some of the most commonly used ones are blade coating, curtain coating, slot die coating, roller coating and spray coating. Spin coating is not counted as industrial, because it is used in the laboratory and not really scalable. Blade coating and curtain coating are generally used for continuous coating and is common in manufacturing lines of flexible substrates. Slot dies coating and roller coating also can be used for similar applications. However, the process does not have to be continuous. Spray coating is versatile and has the advantage over the above-mentioned methods that the substrates can be 3 dimensional and is non-contact method. In all the coating methods various factors like choice of appropriate solvent, viscosity of solution, homogeneity of solution, temperature, speed of coating process and evaporation of solvent are critical and need to be controlled carefully for high quality and consistency of coated product. For PSCs, blade coating, slot die coating and spray coating may be used for both ETL and HTL. Reports have shown that blade coating technique (**Figure 7a**) is capable of producing PSCs with high photovoltaic performance (~20%).[104,525] Blade coated ETL and HTL also offer possibility of fully coated PSCs with good stability in air.[526-527] Using dimethylsulfoxide

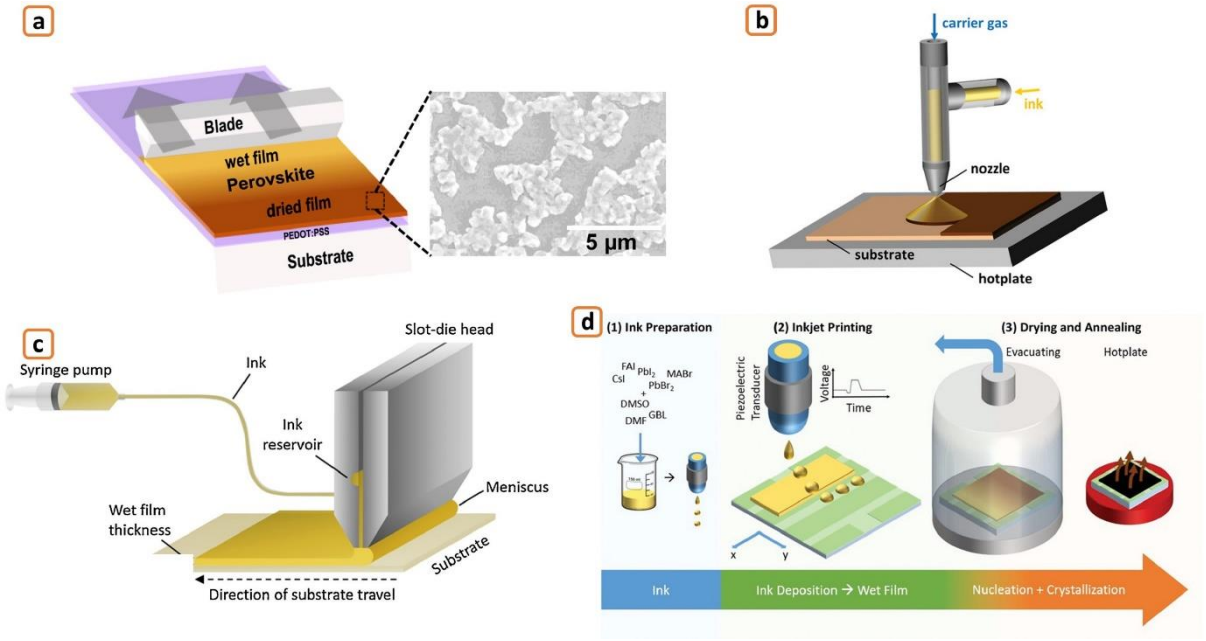


**Figure 7. Possible large-scale deposition techniques.** (a) Blade-coating. Reproduced with permission.[540] Copyright 2016, Elsevier. (b) Spray-coating/Spray-pyrolysis. Reproduced with permission.[541] Copyright 2019, Wiley. (c) Slot-die coating. Reproduced with permission.[542] Copyright 2020, Elsevier. (d) Inkjet-printing. Reproduced with permission.[543] Copyright 2020, Wiley.

(DMSO) as solvent to slow down the crystallization, halide perovskite film with large grain size can be blade-coated,[528-532] where uniform thickness can be obtained by adjusting the precursors' concentration toward solvent solubility limit.[533] Embedding surfactant-like monoammonium zinc porphyrin (ZnP) also greatly improve the crystallinity of perovskite, resulting in large area PSCs (~1.96 $cm^2$) with PCE of ~18% due to ability of ZnP to passivate defects.[534] During blade-coating, coating parameters such as temperature, speed, and air drying could significantly affect the crystallinity, thickness and morphology of the perovskite films as well.[535-536] Both solution formulation as well as coating parameters need to be controlled to the precisely in order to achieve highly uniform coating. However, long exposure of coating solution to the ambient environment could lead to premature degradation of perovskite.

Spray coating/spray pyrolysis (**Figure 7b**) also offer high film quality over large area substrates,[537-539] where process parameter such as the temperature of the substrate, gaseous carrier, spraying time, and post annealing need to be optimized. Large grain size perovskite similar to that obtained from solution deposition was previously reported in spray coating,

together with high repeatability in producing large area and high quality perovskite film.[544-545] Coupled with optical curing (where halide perovskite was exposed to high-density infrared light at a short period of time), fPSCs with PCE of 8.1% were realized via spray coating.[546-547] Thus far, spray coating is widely studied to prepare polymer solar cells,[548-549] but its involvement in PSCs is still lacking. Deducting from the successful application of spray coating in polymer solar cells, the situation for PSCs could be similar. One of the main issues that requires further attention with spray coating would be the generation of solvent emission during deposition processes, which may be hazardous to humans and the environment. Therefore, the volatile organic compounds content in the perovskite precursor solution needs to be lowered to ensure lower release of volatile organic compounds during spraying.

Slot-die coating was revised and extensively studied as the promising scale-up, roll-to-roll production coating method for PSCs (**Figure 7c**).[550-552] For slot-die coating, the material ink flow through the inner space of the blade and deposited on the substrate, greatly reducing the exposure of materials to ambient atmosphere prior to deposition.[553-554] One of the main issues with slot-die coating is the morphology inconsistency of the deposited film that can generate defects which are detrimental to the performance of PSCs. As the results, the solution viscosity, flow rate of the solution, coating thickness and coating speed (also known as web-speed) need to be carefully controlled.[542] Controlling the crystallization rate of slot-die coated perovskite film would be vital to achieve high photovoltaic performance. Several methods were previously reported and reviewed, such as the application of cold air-knife, pre-heating of substrate, near-infrared radiation post-annealing, air drying etc.[542,555-557] Surprisingly, slot-die coated PSCs have shown PCE as high as ~18%, similar to its spin-coated counterpart, demonstrating its viability in up-scaling PSCs production.[558] Although it is possible to conveniently deposit films in rectangular stripe format with slot-die coating, it can be beneficial, and becomes necessary with blade and spray coating, to pattern the layers deposited by coating techniques over the entire substrate after deposition. The prime industrially application

technique for carrying out this patterning is represented by raster scanning laser system which are able to ablate layers very rapidly and precisely.[559-560] Lasers are used to fully scribe, in three separate processes (P1, P2, P3), the electrode and multilayer stacks that make up the device architecture on both glass and plastic substrate.[219,561] Perovskite modules with monolithically series-connected solar cells over large areas with geometrical aperture ratios greater than 90% have been manufactured with this method.[562-564]

*5.1.4. Inkjet printing*

Among all printing techniques, inkjet-printing is considered a more favourable method for industrial scale production as the process is contactless, with high material utilization rate, compatible with both batch and roll-to-roll processes, as well as being able to deposit the inks in any patterns (**Figure 7d**).[565-566] Various types of piezo printheads are available with droplet volume ranging from 2.5 pL to up to a nL enabling very low to very high ink laydown capabilities. There are modern printheads available with jetting frequencies above 40kHz enabling fast printing and productivity. However, inkjet printing challenges are plenty, starting with low solution viscosity requirement, substrate wetting, printing reliability and deposition accuracy. During printing, wettability of the ink is one of the major considerations where poor ink wettability will lead to poor adhesion as well as film peeling off from the substrate. The wettability of perovskite ink can be improved by merely doping bromide and chloride ions, without deploying any additives that could increase the resistance of perovskite film.[34] Choice of the right solvent for ink formulation is critical to provide jetting reliability, solvent evaporation and optimal crystallization of the perovskite.[567] Li et al. employed γ-butyrolactone ($t_{boiling}$ ~200$^{o}$C) and applied in-situ heat treatment during printing, followed by post-heat treatment (100$^{o}$C for 10 minutes in $N_2$ atmosphere) to speed up the crystallization process.[568] Their work reported that the crystallinity of perovskite increased with increasing substrate temperature (25-50$^{o}$C) where further increment in temperature will lead to generation of pin-

hole, detrimental to the performance of PSCs. Large area inkjet-printed PSCs (~4.0 $cm^2$) with PCE of 13.3% was also demonstrated (17% for 0.04 $cm^2$).[569] Inkjet-printing can be used in mass production with its capability to be fully automated, high material utilization rate and high-speed large area printing. However, the PCE of inkjet-printed PSCs is still far from their spin-coated analogues (~17% compared to 24%) and the throughput of manufacturing needs to be compared to that of slot-die coated counterparts. Further investigation on solvent engineering as well as control on printing parameters and condition is required to further improve the performance of inkjet-printed PSCs.

### 5.2. Merits and de-merits of different deposition techniques

To identify the compatibility of each deposition techniques for mass production of large-area PSCs, (i) low wastage, (ii) low-cost capital, (iii) good quality and reproducibility, (iv) mass producibility, and (v) amount of volatile organic compounds released during fabrication, were considered and summarized in **Table 6** and **Figure 8**. Even though the spin-coating technique is not suitable for large-scale production, it is included as a benchmark for comparison. In line with the development of IR 4.0, where automation and physical-cyber interaction become the focus of industrialization, we define mass production as the capability of a product to be manufactured continuously, without the interference from a technician, in large quantities without affecting the quality of the products. Under this definition, mass-production such that roll-to-roll production required the product to be rollable, specifically on flexible substrate. To grasp the productivity of each technique, we estimate the deposition speed, also known as web-speed, based on previous reported literature. Thus far, spray-coating has the highest web-speed of 9.0 m/min,[570] followed by slot-die coating and physical vapor deposition (5.0 and 4.8 m/min, respectively).[571-572] Web-speed for both spin-coating and chemical vapor deposition cannot be estimated due to their incapability for roll-to-roll production, as well as lack of deposition information in literature. Even though high web-speed is more favourable due to its capability

to manufacture more PSCs at a given time, increasing web-speed was reported to deteriorate the photovoltaic performance due to poorer film quality.[573] Therefore, optimum web-speed without severe deterioration on film quality is included in **Table 6**. Large-scale production is not only reflected on the capability to mass produce (in large quantity) but also in large size (larger active area for the case of PSCs). In an effort to preserve the photovoltaic performance while scaling-up the area of PSCs, the PCE loss/area need to be reduced as much as possible. **Table 6** summarizes the highest achievable efficiency for different active area that can be realized from respective deposition techniques. The values were collected based on few criteria:

(i) Only the surface area for pristine cells is considered. The area of the module consists of a combination of few pristine cells is not considered.

(ii) Only planar and inverted device architectures are considered for better data analysis, given the fact that they have almost identical photovoltaic performance as well as widespread adoption in PSCs research.

(iii) The highest recorded efficiency for respective active area is collected individually to show the highest possible efficiency that can be achieved by each deposition method.

From our estimation, with current achieved deposition techniques, an increase in PSCs area from 1 $cm^2$ to 10 $cm^2$ will leads to a drop in PCE ranging from 1.3% (spray-coating) to 5.1% (blade coating), where further increase to 50 $cm^2$ caused 6.5%. Thus far, factors leading to such PCE loss remain unknown (results from DSSCs suggest that lateral diffusion of charge carriers increases with increase in device area, which eventually lead to electron energy loss, charge recombination and efficiency loss on scaling up)[246] where proper solution to achieve low PCE loss/area would eventually allow the direct manufacturing of large sized module with high photovoltaic performance. Wastage from the manufacturing process is always a focus point due to its undivided role in determining the final production cost. Here we focus on the wastage of perovskite precursor solution as they occupy a significant portion of the total cost.

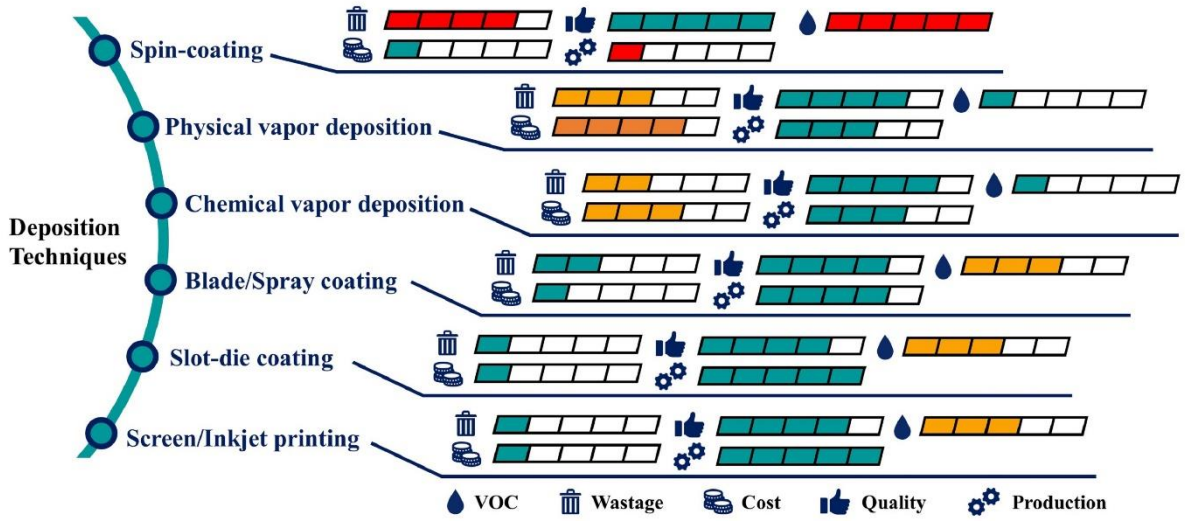


**Figure 8. Suitability of deposition techniques for large-scale production.** The deposition techniques were compared in terms of (i) amount of volatile organic compounds emitted, (ii) wastage of precursors, (iii) overall capital cost for production, (iv) quality of the deposited films, and (v) production capability, also known as web-speed, of the deposition.

The life cycle assessments also show that the lead content of PSCs is not the main source of environmental impact; the organic wastes due to film deposition is more polluting.[574-577] Throughout the deposition of perovskite, the wastage of volatile organic compounds is estimated by considering their amount used during preparation of the precursor solution. Both physical and chemical vapor deposition has the lowest total wastage due to their direct deposition from solid precursors, where volatile organic compounds are not required. We estimated slightly higher wastage in chemical vapor deposition by considering that some vaporized precursors could be carried away by the inert gas prior to deposition. The estimated total wastage for slot-die coating and inkjet-printing are the lowest among solution-based techniques, attributing the higher material utilization rate and precursor concentration within the ink, which reduced the wastage of volatile organic compounds. While comparing the wastage of precursor as well as volatile organic compounds, we observe that most of the wastage originated from the volatile organic compounds. Indeed, stability of the PSCs is one of the important factors for practical application. However, current investigation on deposition techniques focused on improving the web-speed, reducing wastage, and lowering the PCE

loss/area of large area PSCs. Even though stability of the fabricated PSCs were reported on few occasions by comparing these deposition techniques with their spin-coating counterpart, different testing conditions (i.e. encapsulated/unencapsulated, inert/ambient atmosphere, dark/constant illumination, etc.) were adopted, which does not provide a comprehensive assessment to be done on the stability of PSCs deposited using different deposition methods. Given the fact that other factors, such as device architecture (hydrophobic HTL or carbon electrode), chemical composition (hybrid-halide or 2D/3D perovskite), encapsulation, etc, played a much influential role in determining the stability of halide perovskite than the deposition techniques (considering all the deposition techniques were carried out under clean room environment), stability was not considered as the criterion for deposition techniques selection. Deducing from all these estimations, slot-die coating stands out among the other techniques. Its capability for high-speed roll-to-roll production, acceptable PCE loss/area, lower wastage, as well as high photovoltaic performance would allow the fabrication of high-quality PSCs in large quantities. In term of device patterning, inkjet-printing could be the best alternative. With the current silicon PV production line based on 150-160 mm wafer, undoubtedly PSCs/Si tandem PV could be produced at such sizes as well. Given the low active area adopted in current investigation, 6.5 mm for 2T[578-579] and 25 mm for 4T[174,180] devices, reducing the PCE loss when active area is scaled-up would be the most urgent complication to be overcome in all deposition techniques.

**6. Sustainability: Social responsibility**

Even though few lead-free perovskites have been pointed out as suitable candidate, lead-based PSCs are still the main choice due to their superiority in photovoltaic performance and durability. The concerns on lead toxicity both during manufacturing and after decomposition should not be taken lightly. Extraction process of lead from galena (lead ores) produces

greenhouse gases as well as toxic fumes, which is extremely hard to contain and harmful to the human health.[580-582] Upon disposal, lead element from PSCs could seep into soil, which is reported to be one of the most important routes to human lead exposure.[583] Nevertheless, one should compare sustainability, not to metal-free perovskites films but to lead alternatives such as tin. If tin-based (or with other metals) PSCs do not reach similar efficiencies, then the sustainability of these alternatives come into question even compared to those with lead. Furthermore, the preparation and annealing of the precursor solution has more impact on environment during the manufacturing of PSCs compared to the content of lead.[575] Nevertheless, it is always beneficial to reduce the toxicity of perovskite device manufacturing. One avenue is to use secondary sources of lead instead of mining. In such case, lead can be easily extracted from the disposed lead-acid battery, which is more environmental-friendly and reduces the risk of lead leakage from the disposed battery. Previous studies have reported a PCE ~9.37% for PSCs fabricated using lead recycled from the disposed battery, in par with ~9.73% from the commercial precursor.[584] Such demonstration are one of the examples emphasizing the importance of developing 6Rs (Reuse, Reduce, Recycle, Recover, Redesign, Remanufacture) as well as circular economy throughout the lifespan of PSCs, ranging from manufacturing toward disposal (**Figure 9a**).[585-586] A mature 6Rs and circular economy will greatly reduce negative impact of PSCs on the environment, making it a more sustainable energy technology.

### 6.1. Incorporating circular economy

In developed countries, such as United State, Germany, Japan, etc, policies have been established to enforce responsibility in companies to manage their products at the end of the service life either through proper disposal or recycling. Given the dire situation of household and electronic waste pile, it is necessary that most countries need to follow suit and waste

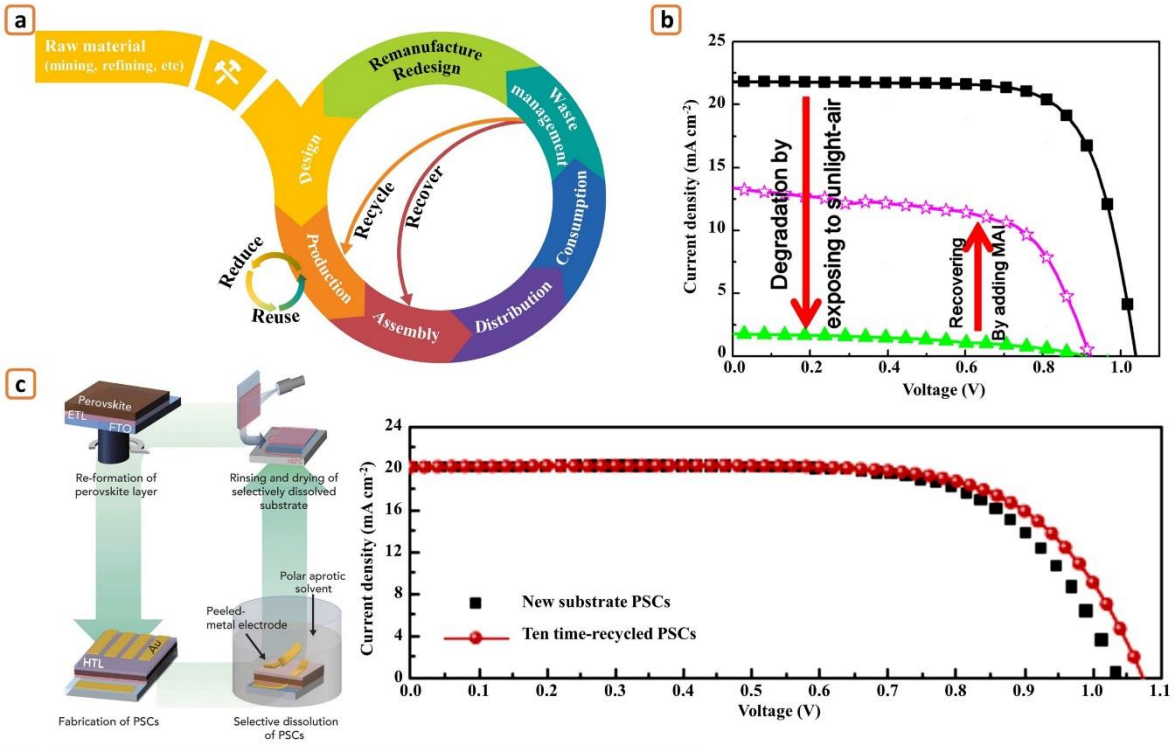


**Figure 9. Waste management for PSCs technology.** (a) Circular economy for PSCs where the degraded PSCs were recovered, recycled, remanufactured, and redesign so that their value replenished as little as possible. Excess precursors during production could be reduced or reused to further reduce wastage. (b) Recovery of $MAPbI_3$ perovskite through MAI solution treatment, offering complete recovery of crystal structure and partial recovery of photovoltaic performance. Reproduced with permission.[181] Copyright 2017, Elsevier. (c) Promising recycling of FTO-glass substrate which is claimed to significantly reduce the cost of PSCs fabrication. Reproduced with permission.[39] Copyright 2016, Nature.

management will become a necessary part of the business model for most of the manufacturing companies, including PSCs industries. Circular economy, defined as a close looped system where an end-of-use-product is reprocessed (reduced, recycled, reused, remanufactured, redesigned, and recovered) so that their value replenished as much as possible, has been viewed as the most appropriate methods in waste management while ensuring environmental sustainability. Various techniques for circular economy implementation in PSCs have been reported.[587-588] Yakiangngam et al. demonstrated the reuse of the leftover $PbI_2$ during fabrication, showing similar photovoltaic performance compared to PSCs prepared using fresh $PbI_2$ (PCE ~4%).[589] Such technique would also reduce wastage generated during fabrication, especially for spin-coating process where wastage can be as high as 90%.[590] However, taking

into consideration that spin-coating is not available for large-area production, the above demonstration has little effect in commercialization of PSCs. Efforts should be focused on reducing the release of volatile organic solvent during the deposition stage for coating and printing techniques. Techniques to recycle each component of PSCs were investigated as well, especially conductive glass, hole-transport material, and metal electrode which occupied over half the total cost in material cost.[591-592] Transparent conductive glass (TCG) was repeatedly recycled by immersing the full device in single polar aprotic solvent (DMF, DMSO, etc), where t other components were removed.[39] Surprisingly, when the new PSCs was fabricated on the recycled TCG, similar performance was observed even after ten cycles of TCG recycling (**Figure 9c**). Augustine et al. then recycled the TCG with the use of KOH solution instead of polar aprotic solvent, demonstrate similar photovoltaic performance compared to the pristine TCG.[591] Even though the recycled TCO could reduce the fabrication cost, the removed components cannot be reused. Therefore, appropriate technique to strip individual PSC components is crucial for them to be recycled, which is claimed to reduce the risk of lead contamination as well as the fabrication cost.[40] The gold electrode was removed either by using adhesive tape or filtered after dissolving the organic components in ethyl acetate. The latter procedure allows the reuse of gold electrode. The spiro-OMeTAD was removed via chlorobenzene immersion and perovskite film was broken down into MAI and $PbI_2$ framework by brief immersion in water. The $PbI_2$ framework can be removed by brief immersion in DMF, where extended immersion would result in $TiO_2$ removal. Such technique allows the reuse of $PbI_2$ and TCG several times without any significant photovoltaic performance deterioration (PCE ~14-15%) compared to the PSC fabricated using fresh $PbI_2$ and TCG.[592]

Recovery of degraded halide perovskite was demonstrated through MAI solution treatment, where the crystal phase of perovskite was restored after treatment (**Figure 9b**).[181,593] However, severe photovoltaic performance degradation after recovery was observed, which can

be attributed to the modified perovskite/HTL interface that leads to higher recombination rates. We speculate that the MAI solution treatment most likely increases the ratio of halide salt in perovskite, where the accumulation of halide ions will enlarge grain boundary and promoting ion migration, detrimental to the performance. It was then reported that the initial perovskite precursors used for deposition played a vital role in subsequent recovery process.[594] While comparing $MAPbI_3$ deposited using lead acetate, $Pb(Ac)_2$ and lead chloride, $PbCl_2$, the former showed improved crystallinity in $PbI_2$ phase after degradation where the opposite was observed in the latter. The high crystallinity in $PbI_2$ phase from acetate-based precursor eventually showed better recovery results compared to chloride-based counterpart. Unfortunately, MAI treatment required the stripping of metal electrode and hole transport material, which is not favourable in terms of wastage minimization, especially when considerable amount of volatile organic compounds is involved. Investigation by Carolus et al on the potential-induced degradation on PSCs suggested another recovery route without dismantling the device.[595] The performance of PSCs severely degraded when potential difference of 1000 V was applied perpendicular to the short-circuited device through aluminium plate placed underneath. Surprisingly, when the applied potential was reversed, the photovoltaic performance recovered ~90% of its initial value. Even though such technique was not tested on completely degraded PSCs, it does hold certain possibility. With these efforts, operation lifespan of PSCs can be prolonged by continuously reprocessing the degraded device. The capability to recover and remanufacture degraded PSCs do show remarkable importance in prolonging total durability of lead-based PSCs, where the PSCs can be recovered until a point where it is no longer recoverable. Unfortunately, studies on reprocessing PSCs at this stage only focused on lead-based perovskite. Similar investigation on lead-free and double perovskite, as well as flexible or wearable PSCs is required as well for future PSCs where lead-free perovskite could play an even vital role. Efforts on recovering degraded PSCs without device disassemble is most likely to be the mainstream because it requires less procedure and chemicals. With tandem cells

playing important role in future high performance photovoltaic, studies are required to understand the recovering or recycling process of tandem cells. Successful lengthening lifetimes of PSCs to ~20 years through recovers, comparable to that of silicon PV sub-cell, would place PSCs/silicon tandem cell in a favourable position to replace silicon solar cells as major player photovoltaic market. Recycling PSCs will produce a significant reduction of the environmental impacts of PSCs.[574]

### 6.2. Incorporating artificial intelligence

Artificial intelligence (AI) is most likely be the mainstream solution provider in future society, with digital devices being able to make decision without human interference. Factories are expected to have AI integrated into their production line, which is expected to lower the production cost and time. Therefore, incorporating AI in PSCs technology will be another milestone for commercializing PSCs. Here, we discuss the integration of AI and blockchain technology into PSCs technology by: (i) building virtual laboratory, and (ii) automated circular economy. Virtual laboratory is a concept where experiment can be carried out through computer simulation, which is more environmental-friendly compared to traditional method involving chemicals and trial-and-error experimentation.[596] One of the major issues with trial-and-error experimentation in PSCs is the involvement of large quantity of volatile organic compounds, such as dimethylformamide (DMF), dimethyl sulfoxide (DMSO), etc, in perovskite synthesis. According to material safety data sheet (MSDS) provided by Fisher Scientific, DMF harms both respiratory and reproductive organs. Unorganized disposal of DMF or DMSO would harm the aquatic environment as well as polluting source of drinking water. Using traditional trial-and-error method to screen out a suitable single solvent to replace harmful volatile organic compound would involve usage and disposal of other harmful solvents as well as wastage in research funding, which can be avoided through building and utilizing virtual laboratory.

Unfortunately, a complete and reliable virtual laboratory is currently unavailable not only for PSCs but for other technologies as well. Fortunately, the progress in materials theories (DFT, Monte-Carlo, etc) would allow simulation of materials of target properties,[597-601] although experimental validation could not be avoided. Currently, these simulation software were used mainly to determine new perovskite materials with suitable opto-electronic properties as well as explaining intrinsic factors that lead to specific behaviour of PSCs.[409,602-603] Underlying mechanism investigated through some in-situ techniques in halide perovskite PSCs during operation could be unravelled in great details using simulation, giving detailed insight on how to further improve both the PSCs performance as well as durability.[604] It is apparent that simulation will be a vital element in future research and could augment traditional experiment in material discovery. However, even though large materials property database has been created and updated regularly,[605-606] a complete reliable virtual laboratory is still far from reality and further development is still required in this field. Beside from virtual laboratory, AI can be incorporated into the circular economy to keep track of all the installed PSCs devices. The fabricated PSCs products can be given a code and sensors which can monitor the performance of the PSCs products and upload all the information to a combined cloud database integrated with blockchain technology. The blockchain technology offers easy access for user to store and track information on the previous performance and maintenance record on PSCs panel, which will help to organize the 6R efforts. This information can then be accessed using artificial intelligence (AI) to sort out which products required maintenance, recovery, and disposal automatically without the intervention of technicians, which will reduce both time and cost. Without such incorporation in the waste management system, most of the degraded PSCs would likely end up in landfill, thereby requiring extra efforts to sort them out for recovery or recycling.

**7. Storage: Solving PV's intermittency**

Photovoltaics cannot work alone as they are intermittent; therefore, and a good energy storage system is required for a reliable photovoltaic ecosystem. As a result, photovoltaics including PSCs need to be coupled with other energy source for higher reliability as well for undisrupted energy supply. Electric grid is utilized to counteract the intermittency of renewable energy (especially photovoltaic and wind energy). However, a large portion of the energy in electric grid is derived from non-renewable source (with the value differing according to respective nation), defying the motive for complete decarbonization of electric grid. Fuel cell and battery power stations were introduced to store renewable energy and further decarbonize the electric grid. However, the high installation and maintenance cost of both fuel cell and battery power stations could inevitably increase the generated electric cost of photovoltaic as well. Therefore, the role of other energy sources cannot be disregarded as they could indirectly affect public interests in adopting photovoltaic (including PSCs) as their primary energy source. In this section, three main alternatives in overcoming the intermittency of PSCs as well as other photovoltaics technology, namely national electricity grid (NEG), fuel cells, and secondary battery are briefly discussed (**Figure 10a**). Here, we focused on individual consumers where PV system is purchased for personnel household usage given the fact that application of PSCs does not only confined in solar farm.

NEG is the main choice to connect to for PV installation, given that no extra spending such as battery is required on storage system. In brief, the energy demand and supply are balanced by extracting or channelling electricity into the NEG. The extra energy (channelled into the NEG) is said to be "sold" to energy suppliers whereas the shortage in energy (extracting from the NEG) is fulfilled through "buying" from the energy suppliers. This buying-selling energy process offers two benefits: (i) electricity bill is lowered by selling extra energy to the government, and (ii) household generating and channelling renewable energy into the grid

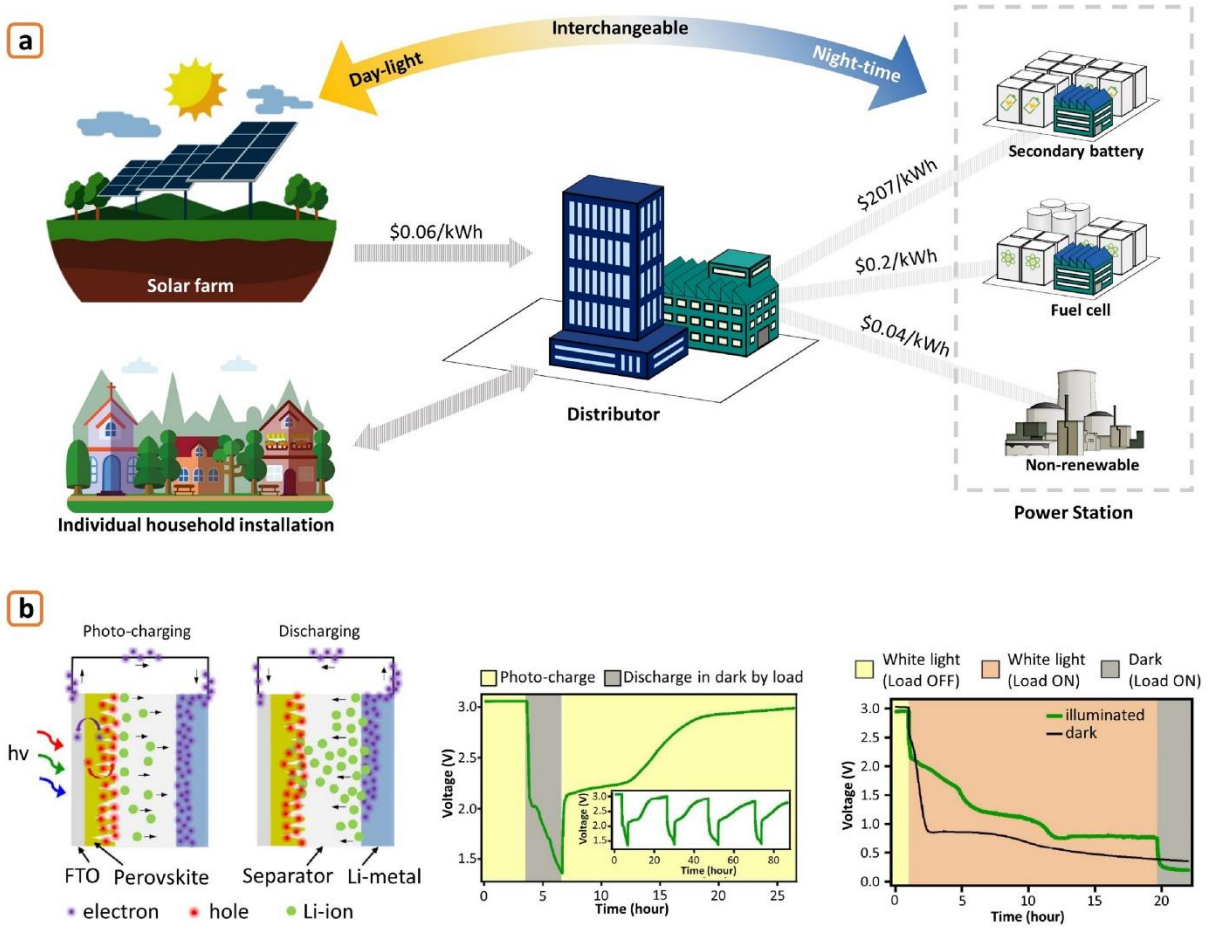


**Figure 10. Solving intermittency of PV technologies.** (a) Connecting PV system to the National Electricity Grid (NEG) would allow the shortage of PV during night-time to be covered by other energy source. "Selling and Buying" approach could be adopted between individual household and centralized energy distributor with the approval of government policies. (b) Self-rechargeable battery where the secondary battery can be charged upon illumination. Reproduced with permission.[607] Copyright 2018, ACS Publications.

further reduce the demand on non-renewable source such as coal power plant during daylight. However, the involvement of selling and buying electricity will require government policy regulation and approval for NEG to be used as storage legally as well as a smart electricity network system able to manage the PV-connected and conventional systems all over the grid efficiently. The only drawback would be the dependencies on non-renewable sources to supply the household demand on electricity during night-time. In other words, non-renewable energy generation cut during daytime could be eventually overridden by overproduction during night-time. In order to reduce the dependency on non-renewable source in covering the energy demand during night-time, large-scale energy storage system, fuel cells or secondary batteries,

was constructed as an effort to decarbonize the NEG. Stationary lithium-ion battery power station are constructed by companies, such as APB Corporation (Japan) and Tesla Inc. (USA) whereas South Korea has recently built the largest fuel cell power station in Seosan, Seoul (South Korea) in August 2019, producing energy of 50 MWh and is expected to be expanded to 1GWh by 2030.[608] Due to the maturity of secondary lithium-ion battery, which had shown widespread utilization in electric vehicle (EV), battery power station is recognized as the best storage medium for smart grid. However, the high LCOE of battery (~$200/kWh) would drive the total LCOE of PV system higher, prompting public to choose traditional non-renewable energy due to steady power output and low cost of electricity. Fortunately, given the current performance status of PSCs, applications such as indoor PVs for IoT or flexible portable electronics would be the main focus for commercialization where huge energy storage power station is not required. With the continuous improvement on the durability of PSCs, there is possibility that PSCs-based solar farm would be established after another decade of dedicated research. Therefore, the issue of PSCs intermittency and proper storage medium need to be considered as well.

Beside from been known as green technology, PV is also viewed as promising energy source for rural or remote places where there is no access to the NEG and other storage alternatives are required. One would be storing the photo-energy as potential energy, where water is pumped into an elevated reservoir and then released to generate electricity, analogue to a dam. However, such technique involved moving mechanical parts that are subjected to wear, fatigue, or corrosion, which require routine maintenance and replacement. For stand-alone system (PV system unconnected to NEG), fuel cells have been considered. LogicEnergy (a collaboration between American and Germany companies) introduced "PureCell® Model 400" fuel cells, which utilized natural gases supplied through natural gas pipeline system as the fuel.[609] The 8.3 × 2.5 × 3.0 $m^3$ model is capable of delivering ~400 kWh of energy where the

generated heat during power generation can be redirected for heating purpose, resulting in energy efficiency as high as 90%. However, without the access to NEG, these places would not have access to the national gas pipeline system as well. Even though a photocatalysis/PSCs tandem devices can be developed where metal oxides (such as $TiO_2$) utilize UV radiation for water splitting,[610-614] the amount of fuel produced (oxygen and hydrogen gases) would be insufficient. On the other hand, even though secondary batteries could store photo-energy effectively in such scenario, it is too costly to store than generate energy. Ideas were proposed to adopt photoactive materials as the electrode of the batteries, resulting in a self-recharging battery as shown in **Figure 10b**.[607,615-617] When the photoactive material was illuminated, the extraction of electron will positively charge the electrode, inducing de-lithiation where lithium ion diffused to opposite electrode. In other words, the battery was charged merely by illumination. Even though the battery showed low cycling stability to the poor stability of halide perovskite in organic solvent, further effort as discussed in **Section 3** could be adopted to improve the stability of the halide perovskite. Compared to other photoactive materials, halide perovskite, in fact, is the most suitable photoactive electrode materials given its high photovoltaic performance at a much lower cost, ensuring that high efficiency self-charging battery can be developed at a much lower price. A self-rechargeable battery would find widespread market, including electric vehicle, Internet-of-Things, etc., and could be the next breakthrough in both PSCs and battery technologies, which deserves research attention and development in order to reach a new height.

## 8. Outlook: Lowering commercialization barrier

Current achievements of PSCs, mainly in terms of stability, are not enough to compete with major player of photovoltaic (Si PV as well as CdTe, CIGS thin film); however, the field is progressing very fast and an application-driven development is expected to secure a place in

photovoltaic market for PSCs. A technology roadmap of PSCs in the next 15-20 years is presented in **Figure 11**. To ensure a smooth transition from laboratory to industry, standard testing protocol need to be established to close the gap between the results reported for laboratory-scale (aperture area ~0.1 $cm^2$) and large-scale (aperture area >100 × 100 $cm^2$).[618] Even though PCE as high as 25% have been reported, most of the PSCs function at PCE ≤20%, similarly in the case of PSCs durability. For better durability comparison between different research groups and testing at near real-time operation conditions, stability testing protocol in-line with that of silicon PVs and specifically developed for PSCs was previously suggested elsewhere.[619-621] Standard testing protocol for both PCE and durability of the modules would be crucial to prevent overestimation on the readiness of PSCs to be commercialized. The suitability of PSCs to be commercialized should not depend solely on its champion PCE as well as stability because these readings cannot be achieved easily. Therefore, planning to commercialize PSC should be done in a cautiously optimistic manner. The most fast-forward platform to introduce PSCs into the PV market would be adopting the production line of Si PV to manufacture PSCs/Si tandem PV, as stated by some important industrial players in the field.[622] Due to the low durability of PSCs, the application of PSCs/Si tandem PV would most likely be focused on short-lived electronic devices instead of solar farms. As discussed in **Section 2**, a more favourable way would be mechanically attaching flexible PSCs on Si PV in the form of 4-terminal tandem PV, which allow easy removal of degraded PSCs for further reprocessing. Therefore, we do expect construction of independent roll-to-roll production facilities for PSCs where manufacturing of flexible PSCs would be scaled-up using either slot-die coating or inkjet-printing deposition. Such deposition techniques, especially inkjet-printing, allowed the integration of PSCs as an electronic compartment in Internet-of-Things (IoT) products, resulting in self-powered electronic applications. The degradation of commercialized PSCs products will initiate the establishment of proper waste management protocol and circular economy facilities as an effort to enhance the sustainability of the PSCs technology. However,

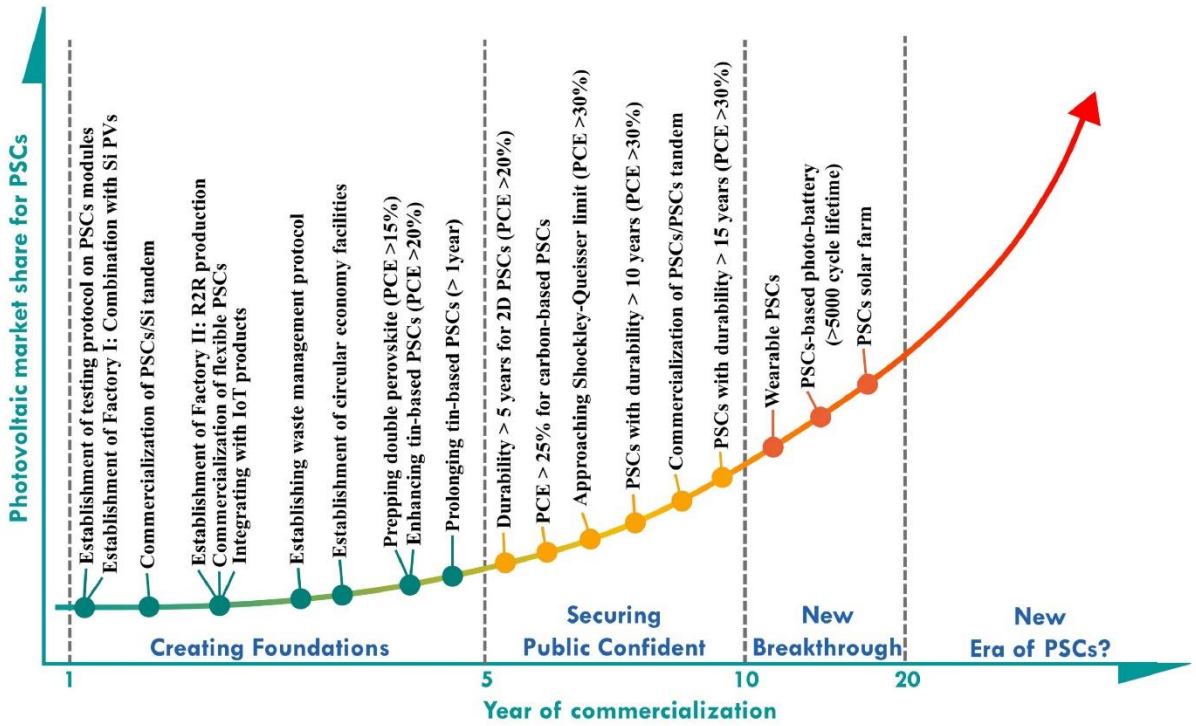


**Figure 11. Roadmap for commercialization of PSCs.** Successful commercialization of PSCs could be achieved through different stages/phases. First and foremost, foundation need to be created where establishment of testing protocol and production facilities are foreseen. Secondly, improving both performance and durability of PSCs would be crucial to secure public confident on the technology. Then, new breakthrough in PSCs technology would boost the competitiveness of PSCs with Si PV. Finally, PSCs could enter a new era where monopolizing PV market could be possible. However, the so call "new era" is too far to be foreseen.

in order to establish efficient circular economy model for PSCs, techniques to recover PSCs without device disassembly and recycling of each component without disposing huge amount of organic solvents need to be revised. Techniques on recovering and recycling degraded PSCs reported previously are not adequate to manage the waste after commercialization. Improvement in the performance and durability of halide perovskite could be anticipated. Given the promising stability of double perovskites and low-ecotoxicity of tin-based perovskites, extended researches could possibly enhance their efficiency to 15% and 20%, respectively, assuming the utilization of suitable ETL and HTL. Instead of adopting device architectures illustrated in **Figure 3**, a new architecture which highly resemble that of Si PV would be revised for double perovskite as discussed in **Section 4.2**. An improvement in the durability of the tin-based halide perovskite to 1 years is also anticipated through synthesizing 2D tin-based

perovskite and proper encapsulation. However, the maximum stability extends need to be identified, most likely through computation, to estimate the durability of tin-based PSCs.

With continued research efforts on various fronts, the commercialization of PSCs would enter a second phase, where ensuring the public that PSCs would be one of their best choices for green energy beside the existing Si PV. In order to secure public confidence on PSCs, improving both PCE and durability of PSCs on par to Si PV would be crucial. Even though IoT application allows the deployment of PSCs with durability <3 years, durability on par to Si PV is still required for PSC to achieve low LCOE and be deployed as solar farm. Efforts would be focused on improving the durability of 2D perovskite with efficiency of >20%. Deducted from discussion from **Section 2 and 3**, we estimate high durability PSCs to be developed from 2D perovskite with mesoporous carbon-based PSCs. Future efforts required to improve the PCE of mesoporous carbon-based PSCs device from 15%to >20%, on par with other device architecture, resulting in PSCs with high PCE as well as durability. The next step would be challenging the Shockley-Queisser limit, pushing PCE of PSCs toward 30% as an effort to improve the competitiveness through further lowering the LCOE. Continuous effort on improving the stability of halide perovskite would eventually push the durability of PSCs beyond 10 years through (i) improving the PCE of double perovskite, or (ii) polymer-embedded 2D perovskite in mesoporous carbon-based device. We anticipate a continuous enhancement of durability beyond 15 years as an effort to rival that of Si PVs. However, with PCE approaching 30% and durability of 10 years, the LCOE of PSCs would be much lower that Si PV to an extend that further enhancement in durability of PSCs no longer be the focus of development. Instead of further improving PCE and durability of PSCs, research would be switched toward exploring new breakthrough in term of applications. After a decade of comprehensive research and development, the cost of PSCs would be low enough for the wearable or breathable PSCs to be available to the public. The superior durability of halide perovskite would also allow the

manufacturing of self-rechargeable battery with stability greater than 5000 cycles. PSCs-based solar farm can also be anticipated with PSCs reaching 10 years durability, offering photo-energy at a record low cost. For the coming decades, development of PSC would be focused around improving the efficiency of large-area cells (reducing PCE loss/area) in order to match the production line of current Si PV with wafer size ranging from 150 to 200 mm. Transformation of traditional printing industries into PSC's fabrication line is envisioned as an effort to reduce the capital cost. Deployment of PSC in wireless, portable, and less energy demanding electronics, such as wireless headphones, smartwatch, etc, would act as the low barrier point for PSC to enter the PV market.

## 9. Conclusions

For the past ten years, extensive research activities have pushed PSCs to new heights, with photovoltaic performance almost equivalent to that of silicon solar cells. Previous investigations have successfully improved the durability with numerous methods, reducing lead toxicity either by developing lead-free and double perovskite or re-processing degraded PSCs as well as lowering PSCs production cost by adopting solution deposition techniques. However, these achievements are far from enough for PSCs to be successfully commercialized. Through brief comparison of previous reports, the commercialization plan for PSCs is too optimistic. Therefore, 5S criteria, namely Stability, Safety, Scalability, Sustainability, and Storage, were discussed respectively to identify the missing link for successful commercialization of PSCs. We observe that adopting 2D perovskite, double perovskite, and mesoporous carbon-based device architecture would be the most effective way to enhance the durability of PSCs. However, given the indirect energy gap nature of most double perovskite, new device architecture that highly resemble that of Si PV need to be revised for effective charge extraction and high photovoltaic performance in double perovskite-based PSCs. Therefore, considering

the growing global population for the coming decade, we identified three initial application markets, namely portable and indoor flexible PSCs, transparent building-integrated and automotive-integrated photovoltaic as the starting point for commercializing PSCs. PSCs are still far from their pinnacle, where continuous efforts are required to further improve this technology for its deployment in other applications, such as wearable or breathable applications, self-rechargeable battery, as well as solar farms.

**Acknowledgements**

The authors would like to thank the Ministry of Higher Education for providing financial support under Fundamental Research Grant Scheme (FRGS) No. FRGS/1/2019/STG07/UMP/01/1 (University reference RDU1901165) and Universiti Malaysia Pahang for laboratory facilities. J.K. Ling acknowledges the financial funding by Post-graduate Research Scheme (PGRS) by University Malaysia Pahang through UMP.05.02/26.10/03/03/PGRS2003123. I. Mora-Sero acknowledges financial funding by Ministry of Science and Innovation of Spain under Project STABLE PID2019-107314RB-I00 and the European Research Council (ERC) via Consolidator Grant (724424, No-LIMIT). TM. Brown acknowledges funding from the Italian Ministry of University and Research (MIUR) through the PRIN2017 BOOSTER (project no. 2017YXX8AZ).

**Conflict of interest**

The authors declare that they have no known competing financial interests or personal relationships that could have appeared to influence the work reported in this paper.

**Table 1. Comparison between different device architecture**: meso-structured (MSSCs), n-i-p (planar), p-i-n (inverted), electron transport layer (ETL)-free, as well as hole transport layer (HTL)-free. Brief details on improvement and condition for stability measurement for respective report were superscripted. Take note that the stability tabulated here was determined from the retention of PCE, which is usually doubled compared to the stabilized power output. The photovoltaic performance for the improved device were given in the bracket.

| Device | Perovskite | Structure | Photovoltaic performance | | | | Stability | ref |
|---|---|---|---|---|---|---|---|---|
| | | | $V_{OC}$ (V) | $J_{SC}$ (mA/cm$^2$) | FF | PCE (%) | | |
| MSSCs$^{a\beta}$ | $FAMAPbI_{3-X-Y}Br_XCl_Y$ | FTO/c-$TiO_2$/m-$TiO_2$/Perovskite/Spiro/Au | 0.97 **(1.02)** | 23.6 **(24.0)** | 59.9 **(66.2)** | 13.7 **(16.3)** | | [623] |
| MSSCs$^{b\gamma}$ | $(CsPbI_3)_{0.05}(FAPbI_3)_{0.95}(MAPbBr_3)_{0.05}$ | FTO/c-$TiO_2$/m-$TiO_2$/Perovskite/Spiro/Au | 1.09 **(1.14)** | 22.8 **(23.4)** | 73.1 **(77.4)** | 18.2 **(20.8)** | 90%; 1200h$^{a,b}$ | [624] |
| MSSCs$^{b\delta}$ | $(FAPbI_3)_{0.875}(MAPbBr_3)_{0.125}(CsPbI_3)_{0.1}$ | FTO/c-$TiO_2$/m-$TiO_2$/Perovskite/Spiro/Au | 1.07 **(1.14)** | 24.1 **(24.3)** | 79.4 **(80.3)** | 20.5 **(22.1)** | 77%; 1000h$^{a,b}$ | [625] |
| MSSCs$^{b\beta}$ | $(FAPbI_3)_{0.85}(MAPbBr_3)_{0.15}$ | FTO/c-$TiO_2$/m-$TiO_2$/Perovskite/Spiro/Au | - **(1.16)** | - **(23.2)** | - **(79.0)** | 18.7 **(20.5)** | | [626] |
| MSSCs$^{b\gamma\delta}$ | $FAPbI_3$ | FTO/c-$TiO_2$/m-$TiO_2$/Perovskite/PTAA-TBP/Au | - **(1.10)** | - **(25.0)** | - **(80.3)** | - **(22.1)** | 94%; 400h$^{a}$ | [100] |
| MSSCs$^{b\phi}$ | $BA_{0.1}MA_{0.9}PbI_3$ | ITO/$NiO_x$/Perovskite/PCBM/ZrO | - **(1.06)** | - **(22.7)** | - **(72.5)** | - **(17.5)** | 75%; 840h$^{a,b}$ | [627] |
| MSSCs$^{b\phi}$ | 2D/3D 3%-$(AVAI)_2PbI_4/MAPbI_3$ | FTO/c-$TiO_2$/m-$TiO_2$/Perovskite/Spiro/Au | 1.05 **(1.03)** | 21.5 **(18.8)** | 70.3 **(75.5)** | 16.0 **(14.6)** | 60%; 300h$^{e}$ | [38] |
| MSSCs$^{b\phi}$ | 2D/3D (8%-ThMA)$_2(MA_XFA_{1-X})_{n-1}Pb_nI_{3n+1}$ | ITO/$SnO_2$/Perovskite/Spiro/$MoO_3$/Ag | 1.09 **(1.16)** | 22.3 **(22.4)** | 78.8 **(81.0)** | 19.2 **(21.5)** | 99%; 1680h$^{a,b}$ | [348] |
| MSSCs$^{bc\beta\phi}$ | 2D (5-AVA)$_2PbI_4$/3D $(FAPbI_3)_{0.88}(CsPbBr_3)_{0.12}$ | FTO/c-$TiO_2$/m-$TiO_2$/Perovskite/CuSCN/Au | 0.99 **(1.02)** | 21.1 **(20.6)** | 66.0 **(67.0)** | 13.7 **(13.5)** | 89%; 1512h$^{b,d,g}$ | [628] |
| MSSCs$^{b\alpha\phi}$ | 2D/3D $(CEA_2PbI_4)_X[(Cs_{0.1}FA_{0.9})Pb(I_{0.9}Br_{0.1})_3]_{1-X}$ | FTO/c-$TiO_2$/m-$TiO_2$/Perovskite/Spiro/Au | 1.08 **(1.10)** | 22.9 **(22.8)** | 77.0 **(79.0)** | 19.0 **(20.1)** | 92%; 2400h$^{a,b,d}$ | [349] |
| MSSCs$^{b\alpha\phi}$ | 2D/3D $(BEA_2PbI_4)_X[(Cs_{0.1}FA_{0.9})Pb(I_{0.9}Br_{0.1})_3]_{1-X}$ | FTO/c-$TiO_2$/m-$TiO_2$/Perovskite/Spiro/Au | 1.08 **(1.11)** | 22.9 **(21.5)** | 77.0 **(79.5)** | 19.0 **(19.8)** | 87%; 2400h$^{a,b,d}$ | [349] |
| MSSCs$^{b\phi}$ | $(TFEA)_2(FA_{0.825}MA_{0.15}Cs_{0.025})_{29}Pb_{30}(I_{0.85}Br_{0.15})_{91}$ | FTO/c-$TiO_2$/m-$TiO_2$/Perovskite/Spiro/Au | 1.06 **(1.10)** | 22.6 **(21.2)** | 80.8 **(78.3)** | 19.2 **(18.2)** | 90%; 672h$^{a,b}$ | [629] |
| MSSCs$^{b\phi}$ | $MAPbI_3$ | FTO/c-$TiO_2$/m-$TiO_2$/Perovskite/Spiro/Au | 1.05 **(1.03)** | 21.5 **(18.8)** | 70.3 **(75.5)** | 16.0 **(14.6)** | 50%; 300h$^{c}$ | [38] |
| Planar$^{a\beta}$ | $FA_{0.95}Cs_{0.05}PbI_3$ | FTO/EDTA-$SnO_2$/Perovskite/Spiro/Au | 1.10 **(1.11)** | 22.8 **(24.6)** | 75.5 **(79.2)** | 18.9 **(21.6)** | 92%; 2880h$^{a,b}$ | [101] |
| Planar$^{b\varepsilon}$ | $(FA_{0.83}MA_{0.17})_{0.95}Cs_{0.05}PbI_{0.9}Br_{0.1})_3$ | FTO/NiO/Perovskite/PCBM/BCP/Cr/$Cr_2O_3$/Au | 1.02 **(1.08)** | 23.2 **(23.8)** | 79.0 **(81.0)** | 18.5 **(19.8)** | 95%; 1800h$^{c,h}$ | [630] |
| Planar$^{c\lambda}$ | $CsPbI_2Br$ | FTO/$TiO_2$-Cl/Perovskite/PDCBT/$MoO_x$/Au | - **(1.24)** | - **(15.5)** | 80.0 **(85.2)** | 15.5 **(16.4)** | 96%; 1000h$^{e,h}$ | [631] |
| Planar$^{b\gamma}$ | $(FAPbI_3)_{0.85}(MAPbBr_3)_{0.15}$ | $In_2O_3$:H/PTAA/Perovskite/PCBM/ZnO/ZnO:Al | 1.10 **(1.10)** | 22.3 **(23.2)** | 78.3 **(78.6)** | 19.2 **(20.1)** | >70%; 60h$^{a,h,k}$ | [632] |
| Planar$^{b\gamma}$ | $FA_{0.85}MA_{0.15}PbI_{2.55}Br_{0.45}$ | ITO/PTAA/Perovskite/PCBM/BCP/In | - **(1.10)** | - **(23.2)** | - **(78.6)** | - **(20.1)** | 90%; 60h$^{a,b}$ | [633] |
| Planar$^{c\alpha}$ | $CsFAMAPbI_{3-X}Br_X$ | ITO/$SnO_2$/Perovskite/Spiro/Au | 1.07 **(1.10)** | 21.8 **(22.8)** | 73.0 **(72.4)** | 17.1 **(18.1)** | 85%; 800h$^{a,b}$ | [634] |
| Planar$^{b\gamma}$ | $MAPbI_{3-X}(SGN)_X$ | FTO/c-$TiO_2$/Perovskite/Spiro/Ag | 1.03 **(1.05)** | 18.5 **(21.2)** | 68.0 **(75.0)** | 13.0 **(16.6)** | 84%; 720h$^{a,b}$ | [635] |
| Planar$^{b\gamma}$ | $MAPbI_3$ | FTO/c-$TiO_2$/Perovskite/Spiro/Ag | 1.02 **(1.06)** | 20.8 **(22.6)** | 73.0 **(78.4)** | 15.7 **(18.8)** | 90%; 400h$^{a}$ | [636] |
| Planar$^{a\beta}$ | $MAPbI_3$ | FTO/c-$TiO_2$/ZnO/Perovskite/Spiro/$MoO_3$/Ag | - **(0.95)** | - **(20.3)** | - **(63.0)** | - **(12.2)** | | [637] |
| Planar$^{c\varepsilon}$ | $CsFAMAPbI_{3-X}Br_X$ | FTO/C-$TiO_2$/Perovskite/Spiro/Au | 1.10 **(1.15)** | 23.7 **(23.9)** | 74.7 **(78.4)** | 19.5 **(21.5)** | 100%; 600h$^{a}$ | [638] |
| Planar$^{a\beta}$ | $(FAPbI_3)_{0.85}(MAPbBr_3)_{0.15}$ | FTO/$SnO_2$/Zwitterion/Perovskite/Spiro/Au | 1.10 **(1.16)** | 23.0 **(23.6)** | 77.6 **(78.4)** | 19.6 **(21.4)** | 93%; 140h$^{a,b,h}$ | [639] |
| Planar$^{c\alpha\varepsilon}$ | $(FAPbI_3)_{0.85}(MAPbBr_3)_{0.15}$ | ITO/$SnO_2$/Perovskite/rGO-Spiro/Au | 1.10 **(1.11)** | 22.6 **(23.1)** | 70.0 **(71.0)** | 17.3 **(18.1)** | 75%; 500h$^{a,d}$ | [640] |
| Planar$^{b\varepsilon}$ | 3D/2D $MAPbI_3$-$(BA)_2(MA)_{n-1}Pb_nI_{3n+1}$ | FTO/c-$TiO_2$/Perovskite/Spito/Au | 0.31 **(1.03)** | 14.0 **(20.1)** | 29.2 **(63.6)** | 1.3 **(13.2)** | 71%; 1200h$^{a,f}$ | [641] |
| Planar$^{b\gamma\delta}$ | Quasi-2D $PEA_2Cs_{n-1}Pb_nI_{3n+1}$ | ITO/$SnO_2$/Perovskite/Spiro/Au | 1.10 **(1.07)** | 14.3 **(16.6)** | 70.0 **(70.0)** | 11.0 **(12.4)** | 94%; 960h$^{a}$ | [642] |
| Planar$^{b\phi}$ | 2D $(BA)_2(MA)_3Pb_4I_{13}$ | FTO/PEDOT:PSS/Perovskite/PCBM/Al | - **(1.01)** | - **(16.8)** | - **(74.1)** | - **(12.5)** | 60%; 2250h$^{a,c}$ | [643] |
| Planar$^{b\phi}$ | 2D/3D $BA_{0.05}(FA_{0.83}Cs_{0.17})_{0.91}Pb(I_{0.6}Br_{0.4})_3$ | FTO/$SnO_2$/$SnO_2$@N-DPBI/Perovskite/Spiro/Au | 1.14 **(1.14)** | 19.8 **(22.7)** | 75.0 **(80.0)** | 16.9 **(20.6)** | 80%; 3880h$^{a,c}$ | [644] |
| Planar$^{b\gamma\delta}$ | Quasi-2D $PEAI_{n-1}Pb_nI_{3n+1}$ (n=60) | FTO/c-$TiO_2$/Perovskite/Spiro/Au | - **(1.09)** | - **(19.1)** | - **(73.7)** | - **(15.4)** | 85%; 336h$^{a}$ | [407] |
| Inverted$^{b\beta\delta}$ | $Cs_{0.05}(FA_{0.92}MA_{0.08})_{0.95}Pb(I_{0.92}Br_{0.08})_3$ | ITO/PTAA/Perovskite/$C_{60}$/BCP/Cu | 1.06 **(1.17)** | 24.2 **(24.1)** | 80.0 **(81.6)** | 20.5 **(23.0)** | 100%; 1000h$^{a}$ | [102] |
| Inverted$^{c\beta}$ | $CsPbI_{0.05}[(FAPbI_3)_{0.89}(MAPbBr_3)_{0.11}]_{0.95}$ | ITO/PTAA/Perovskite/$C_{60}$/Cu | 1.09 **(1.16)** | 21.7 **(23.2)** | 77.9 **(80.4)** | 18.4 **(21.6)** | | [645] |
| Inverted | $FA_{0.83}Cs_{0.17}Pb(I_{0.6}Br_{0.4})_3$ | ITO/PEDOT:PSS/Perovskite/$C_{60}$/BCP/Ag | - **(0.85)** | - **(28.5)** | - **(72.5)** | - **(17.6)** | | [646] |
| Inverted$^{b\gamma}$ | $FA_{0.85}MA_{0.15}PbI_{2.55}Br_{0.45}$ | FTO/$TiO_2$/Perovskite/PTAA/Ag | - **(1.10)** | - **(22.3)** | - **(78.3)** | - **(19.2)** | | [633] |
| Inverted$^{b\gamma}$ | $MAPbI_3$ | ITO/PTAA/PEN/Perovskite/$C_{60}$/CIL/Cu | 1.10 **(1.11)** | 20.9 **(20.9)** | 79.0 **(77.0)** | 18.2 **(17.7)** | 80%; 1000h | [647] |
| Inverted$^{b\alpha}$ | $MAPbI_3$ | ITO/NiO/Perovskite/ICBA:PCBM/Al | 1.03 **(1.05)** | 20.4 **(20.5)** | 79.0 **(80.0)** | 16.7 **(17.3)** | 100%; 4680h$^{a,b}$ | [648] |
| Inverted$^{b\delta}$ | $FASnI_3$ | ITO/PEDOT:PSS/Perovskite/$C_{60}$/BCP/Ag | 0.49 **(0.60)** | 20.9 **(21.1)** | 55.3 **(75.1)** | 4.1 **(9.5)** | 93%; 600h$^{a,c}$ | [649] |
| Inverted$^{b\gamma}$ | $MAPbI_3$ | FTO/Poly/TPD/Perovskite/$C_{60}$/BCP/Ag | 1.04 **(1.10)** | 21.3 **(22.4)** | 77.2 **(77.6)** | 17.1 **(19.1)** | | [650] |
| Inverted$^{b\delta}$ | $Cs_{0.05}FA_{0.70}MA_{0.25}PbI_3$ | ITO/PTAA/Perovskite/$C_{60}$/BCP/Cu | 1.08 **(1.16)** | 22.0 **(22.0)** | 77.5 **(82.0)** | 18.4 **(21.5)** | | [651] |

| | | | | | | | | |
|---|---|---|---|---|---|---|---|---|
| Inverted$^{b\delta}$ | 2D-$PEA_2SnI$/3D-$FASnI_3$ | ITO/$NiO_x$/Perovskite/$C_{60}$/BCP/Ag | 0.58 **(0.61)** | 22.1 **(22.0)** | 65.2 **(70.1)** | 8.3 **(9.4)** | 90%; 600h$^{b,e}$ | [652] |
| Inverted$^{b\delta}$ | 2D-$BA_2PbI_4$/3D-$MAPbI_3$ | ITO/PTAA/Perovskite/PCBM/$C_{60}$/BCP/Cu | 1.08 **(1.11)** | 22.2 **(22.5)** | 74.0 **(78.0)** | 17.1 **(18.9)** | 97%; 100h$^{b,h}$ | [653] |
| Inverted$^{b\alpha\phi}$ | 2D-$CA_2PbI_4$/3D-$MAPbI_XCl_{3-X}$ | ITO/PEDOT:PSS/Perovskite/PCBM/LiF/Ag | 0.92 **(0.92)** | 18.5 **(19.3)** | 76.6 **(77.3)** | 13.1 **(13.9)** | 54%; 220h$^{a,b}$ | [654] |
| ETL-free | $MAPbI_{3-X}Cl_X$ | FTO/Perovskite/Spiro/Au | 0.96 **(1.06)** | 17.9 **(19.8)** | 45.0 **(67.0)** | 7.8 **(14.1)** | >70%; 500h$^{a,b}$ | [151] |
| ETL-free$^{b\delta}$ | $FAMAPbI_{3-X}Br_X$ | FTO/Perovskite/Spiro/Au | 1.02 **(1.17)** | 22.5 **(23.2)** | 62.4 **(73.9)** | 14.4 **(20.1)** | 90%; 400h$^{a}$ | [105] |
| ETL-free$^{TCO\varepsilon}$ | $(FAPbI_3)_{1-X}(MAPbBr_3)_X$ | NTO/Perovskite/Spiro/Au | 0.85 **(1.08)** | 20.6 **(19.1)** | 43.0 **(61.0)** | 7.6 **(12.5)** | | [655] |
| ETL-free$^{TCO\beta\varepsilon}$ | $MAPbI_3$ | FTO/BIPH-H/Perovskite/Spiro/Au | 0.98 **(1.08)** | 15.3 **(22.4)** | 60.2 **(71.4)** | 9.0 **(17.3)** | 80%; 500h$^{a,b}$ | [656] |
| HTL-free$^{TCO\varepsilon}$ | $FA_{0.75}Cs_{0.25}Sn_{0.4}Pb_{0.6}I_3$ | ITO/Perovskite/$C_{60}$/$SnO_2$/IZO | 0.72 **(0.72)** | 30.8 **(30.2)** | 75.0 **(69.8)** | 16.6 **(16.4)** | 100%; 1000h$^{a,b,h}$ | [657] |
| HTL-free$^{b\alpha\beta}$ | $(5\text{-}AVA)_X(PEA)_X(MA)_{1-X}PbI_{3+X}$ | FTO/c-$TiO_2$/m-$TiO_2$/m-$ZrO_2$/Perovskite | - **(0.88)** | - **(15.8)** | - **(49.0)** | - **(6.72)** | 80%; 420h$^{a}$ | [658] |
| HTL-free$^{d\alpha}$ | $Cs_{0.05}MA_{0.16}FA_{0.79}Pb(I_{0.84}Br_{0.16})_3$ | FTO/$TiO_2$/Perovskite/Carbon | 0.96 **(1.03)** | 20.2 **(22.2)** | 58.0 **(65.0)** | 11.9 **(14.9)** | 95%; 1000h$^{a}$ | [659] |
| HTL-free$^{b\beta\varepsilon}$ | $MAPbI_3$ | ITO/Perovskite/$C_{60}$/BCP/Cu | 1.00 **(1.10)** | 19.7 **(22.7)** | 56.0 **(81.0)** | 11.0 **(20.2)** | 92%; 500h$^{a,b}$ | [104] |
| HTL-free$^{b\beta\delta}$ | $MAPbI_{3-X}Cl_X$ | ITO/Perovskite/$C_{60}$/BCP/Ag | 1.00 **(1.11)** | 20.5 **(21.7)** | 47.6 **(77.6)** | 8.9 **(18.6)** | 89%; 1320h$^{d,e}$ | [660] |
| HTL-free$^{b\gamma\varepsilon}$ | $MAPbI_3$ | ITO/Perovskite/PCBM/Ag | 0.88 **(1.01)** | 16.6 **(22.9)** | 44.1 **(70.8)** | 6.4 **(16.4)** | 70%; 500h$^{a,b}$ | [661] |

- Stability testing condition: [a]in ambient air; [b]without encapsulation; [c]with encapsulation; [d]stored in dark; [e]stored in inert gas environment; [f]high humidity >70%; [g]low humidity <20%; [h]heated at temperature >75 °C; [k]vacuumed atmosphere.
- Device component improvement: [a]ETL; [b]Perovskite; [c]HTL; [d]counter electrode; $\alpha$hydrophobicity improvement; $\beta$interface modification; $\gamma$crystallinity improvement; $\delta$surface passivation; $\varepsilon$charge transport modification; $\lambda$lattice stress relaxation; $\phi$ dimension reduction.

**Table 2. Photovoltaic performance of tandem photovoltaic devices.** Comparison of some reported tandem photovoltaics, consisting perovskite/Si, perovskite/thin film, all perovskite, organic/organic, as well as perovskite/DSSCs tandem architecture.

| Top cell | | | | Bottom cell | | | | Tandem cell | | | | | |
|---|---|---|---|---|---|---|---|---|---|---|---|---|---|
| Material | $V_{OC}$ (V) | PCE (%) | Conducting layer (top) | Material | $V_{OC}$ (V) | PCE (%) | Conducting layer (bottom) | Type | $V_{OC}$ (V) | $J_{SC}$ (mA/cm$^2$) | FF | PCE (%) | ref |
| $Cs_{0.1}MA_{0.9}Pb(I_{0.9}Br_{0.1})_3$ | 1.17 | 20.1 | PDMS/Ag/ITO/$SnO_2$/$C_{60}$ | c-Si | | | PTAA/ITO/a-Si:H | s-2T | 1.82 | 19.2 | 75.3 | 26.2 | [578] |
| $Cs_{0.15}(FA_{0.83}MA_{0.17})_{0.85}Pb(I_{0.7}Br_{0.3})_3$ | 1.19 | 18.6 | Cu/$MgF_2$/IZO/$SnO_2$/$C_{60}$/ICBA | c-Si | | | PTAA/ITO/a-Si:H | s-2T | 1.80 | 17.8 | 79.4 | 25.4 | [579] |
| $FA_{0.75}Cs_{0.25}Pb(I_{0.8}Br_{0.2})_3$ | 1.05 | 15.8 | $MgF_2$/ITO/$SnO_2$/$C_{60}$ | c-Si | | | PTAA/ITO/a-Si:H | s-2T | 1.77 | 18.4 | 77.0 | 25.0 | [662] |
| $Cs_{0.17}FA_{0.83}Pb(Br_{0.17}I_{0.83})_3$ | 0.98 | 14.5 | Ag/LiF/ITO/$SnO_2$/ZTO/$C_{60}$/LiF | c-Si | | | NiO/ITO/a-Si:H | s-2T | 1.65 | 18.1 | 79.0 | 23.6 | [663] |
| $Cs_{0.05}(MA_{0.17}FA_{0.83})Pb_{1.1}(I_{0.83}Br_{0.17})_3$ | 1.11 | 18.4 | LiF/IZO/$SnO_2$/$C_{60}$ | c-Si | | | PTAA/ITO/nc-$SiO_X$:H/a-Si:H | s-2T | 1.76 | 18.5 | 78.3 | 25.4 | [664] |
| $Cs_xFA_{1-x}Pb(I,Br)_3$ | 1.04 | 11.4 | Ag/IZO/$SnO_2$/$C_{60}$/LiF | c-Si | 0.72 | 22.6 | Spiro-TTB/nc-$SiO_X$:H/a-Si:H | s-2T | 1.79 | 19.5 | 73.1 | 25.2 | [665] |
| $Cs_{0.05}(FA_{0.83}MA_{0.17})_{0.95}Pb(I_{0.82}Br_{0.18})_3$ | 1.10 | 18.4 | ARC/ITO/Buffer/$PC_{61}BM$:BCP | c-Si | 0.72 | 20.5 | Poly-TPD/ITO/nc-$SiO_X$:H/a-Si:H | s-2T | 1.79 | 19.0 | 74.6 | 25.4 | [179] |
| $Cs_{0.05}(MA_{0.17}FA_{0.83})Pb_{1.1}(I_{0.83}Br_{0.17})_3$ | 1.09 | 16.7 | LiF/IZO/$SnO_2$/$C_{60}$ | CIGS | 0.65 | 16.3 | PTAA/$NiO_X$/ZnO/CdS | s-2T | 1.58 | 18.0 | 76.0 | 21.6 | [666] |
| $MAPbI_3$ | 0.48 | 5.06 | ITO/bis-$C_{60}$/$C_{60}$ | CuInS,Se | 0.51 | 13.0 | Cu:$NiO_X$/ITO/CdS/ZnO | s-2T | 1.36 | 15.5 | 88.0 | 18.5 | [667] |
| $MAPbI_{2.4}Br_{0.6}$ | 0.48 | 5.49 | ITO/bis-$C_{60}$/$C_{60}$ | CuInS,Se | 0.51 | 13.0 | Cu:$NiO_X$/ITO/CdS/ZnO | s-2T | 1.39 | 13.0 | 93.4 | 16.9 | [667] |
| $DMA_{0.1}FA_{0.6}Cs_{0.3}PbI_{2.4}Br_{0.6}$ | 1.15 | 19.0 | Au/$C_{60}$/BCP | $FA_{0.75}Cs_{0.25}Sn_{0.5}Pb_{0.5}I_3$ | 0.69 | 16.5 | PEDOT:PSS/AZO/IZO/LiF/$C_{60}$/PEIE | s-2T | 1.88 | 16.0 | 77.0 | 23.1 | [190] |
| $DMA_{0.1}FA_{0.6}Cs_{0.3}PbI_{2.4}Br_{0.6}$ | 1.15 | 19.0 | Au/$C_{60}$/BCP | $FA_{0.75}Cs_{0.25}Sn_{0.5}Pb_{0.5}I_3$ | 0.69 | 16.5 | PEDOT:PSS/AZO/IZO/LiF/$C_{60}$/PEIE | f-2T | 1.82 | 15.6 | 75.0 | 21.3 | [190] |
| $(FA_{0.8}Cs_{0.2}Pb(I_{0.7}Br_{0.3})_3$ | 1.14 | 14.0 | Ag/$C_{60}$/BCP | $(FASnI_3)_{0.6}(MAPbI_3)_{0.4}$ | 0.84 | 18.1 | PEDOT:PSS/Ag/$MoO_X$/ITO/$C_{60}$/BCP | s-2T | 1.92 | 14.1 | 78.1 | 21.0 | [668] |
| $FA_{0.8}Cs_{0.2}Pb(I_{0.6}Br_{0.4})_3$ | 1.22 | 16.5 | Cu/$C_{60}$/BCP | $FA_{0.7}MA_{0.3}Pb_{0.5}Sn_{0.5}I_3$ | 0.83 | 21.1 | PEDOT:PSS/ALLD-$SnO_2$/Au/$C_{60}$ | s-2T | 1.97 | 15.6 | 81.0 | 24.8 | [183] |
| $FA_{0.6}Cs_{0.4}Pb(I_{0.7}Br_{0.3})_3$ | 1.14 | 14.6 | ITO/PTAA | $FA_{0.75}Cs_{0.25}Sn_{0.5}Pb_{0.5}I_3$ | 0.76 | 15.6 | $C_{60}$/$SnO_2$/ITO/PEDOT:PSS | s-2T | 1.81 | 14.8 | 70.0 | 19.1 | [669] |
| $FA_{0.8}Cs_{0.2}Pb(I_{0.7}Br_{0.3})_3$ | 1.09 | 14.9 | ITO/PTAA | $(FASnI_3)_{0.6}(MAPbI_3)_{0.4}$ | | | $C_{60}$/BCP/Ag/$MoO_3$/ITO/PEDOT:PSS | s-2T | 1.91 | 14.1 | 78.5 | 21.0 | [670] |
| $Cs_{0.1}(FA_{0.6}MA_{0.4})_{0.9}Pb(I_{0.6}Br_{0.4})_3$ | 1.22 | 14.9 | ITO/PTAA | SN6IC-4F | 0.77 | 12.5 | PCBM/BCP/Ag/M-PEDOT/PBDB-T | f-2T | 1.85 | 11.5 | 71.0 | 15.1 | [671] |
| $Cs_{0.05}FA_{0.81}MA_{0.14}PbI_{2.55}Br_{0.45}$ | 1.12 | 19.4 | $MgF_2$/IZO/$MoO_3$/Spiro/Per/$SnO_2$/IZrO | c-Si | | | Ag/$In_2O_3$:H/a-Si:H/n-Si/a-Si:H/ITO/Ag | s-4T | | | | 28.2 | [174] |
| $MAPbI_3$ | 1.08 | 12.2 | Al:ZnO/ZnO/$C_{60}$/Per/Spiro/$MoO_3$/ITO | CIGS | 0.69 | 17.7 | | f-4T | | | | 18.2 | [672] |
| $MAPbI_3$ | 1.06 | 14.0 | IZO/PEIE/$C_{60}$/Per/Spiro/$MoO_X$/IZO | CIGS | 0.69 | 18.9 | | f-4T | | | | 19.6 | [673] |
| $MAPbI_3$ | 1.03 | 12.7 | FTO/$TiO_2$/Per/AgNW/LiF | CIGS | 0.71 | 17.0 | | s-4T | | | | 18.6 | [180] |
| $MAPbI_3$ | 1.01 | 16.1 | FTO/$TiO_2$/Per/Spiro/$MoO_3$/ZnO:Al/$MgF_2$ | CIGS | 0.69 | 18.4 | ZnO/ZnO:Al/CdS/CIGS/Mo | s-4T | | | | 19.5 | [674] |
| $MAPbI_3$ | 1.10 | 14.1 | FTO/ZnO/PCBM/Per/Spiro/$MoO_3$/ITO | CIGS | 0.70 | 18.3 | | s-4T | | | | 20.5 | [675] |
| $Cs_{0.05}Rb_{0.05}FA_{0.765}MA_{0.135}PbI_{2.55}Br_{0.45}$ | 1.14 | 18.4 | ITO/$TiO_2$/Per/Spiro/$MoO_X$/IZO/$MgF_2$ | CIGS | 0.66 | 16.5 | AZO/ZnO/CdS/CIGSe/Mo | s-4T | | | | 23.9 | [676] |
| $MAPbI_3$ | 0.61 | 5.22 | ITO/bis-$C_{60}$/$C_{60}$/Per/Cu:$NiO_X$/ITO | CIGS | 0.64 | 14.3 | $MgF_2$/ITO/CdS/ZnO/CIGS/Mo | s-4T | | | | 18.8 | [667] |
| $MAPbI_{2.4}Br_{0.6}$ | 0.61 | 5.90 | ITO/bis-$C_{60}$/$C_{60}$/Per/Cu:$NiO_X$/ITO | CIGS | 0.64 | 14.3 | $MgF_2$/ITO/CdS/ZnO/CIGS/Mo | s-4T | | | | 17.7 | [667] |
| $MAPbI_3$ | 0.48 | 5.06 | ITO/bis-$C_{60}$/$C_{60}$/Per/Cu:$NiO_X$/ITO | CuInS,Se | 0.51 | 13.0 | $MgF_2$/ITO/CdS/ZnO/CuInS,Se/Mo | s-4T | | | | 18.7 | [667] |
| $MAPbI_{2.4}Br_{0.6}$ | 0.48 | 5.49 | ITO/bis-$C_{60}$/$C_{60}$/Per/Cu:$NiO_X$/ITO | CuInS,Se | 0.51 | 13.0 | $MgF_2$/ITO/CdS/ZnO/CuInS,Se/Mo | s-4T | | | | 16.8 | [667] |
| $Cs_{0.05}FA_{0.8}MA_{0.15}PbI_{2.55}Br_{0.45}$ | 1.12 | 18.5 | IZO/$C_{60}$/$SnO_2$/ZTO/Per/PTAA/ITO | $(FASnI_3)_{0.6}(MAPbI_3)_{0.4}$ | 0.83 | 20.2 | Ag/$C_{60}$/BCP/Per/PEDOT:PSS/ITO | s-4T | | | | 24.7 | [677] |
| $FA_{0.8}Cs_{0.2}Pb(I_{0.7}Br_{0.3})_3$ | 1.20 | 15.7 | FTO/$SnO_2$/$C_{60}$/Per/Spiro/$MoO_X$ | $(FASnI_3)_{0.6}(MAPbI_3)_{0.4}$ | 0.85 | 17.5 | ITO/PEDOT:PSS/Per/$C_{60}$/BCP/Ag | s-4T | | | | 23.1 | [53] |
| PTB7-Th:O6T-4F:$PC_{71}BM$ | 0.76 | 13.6 | $MoO_X$/Ag | BDTID-Cl:$PC_{71}BM$ | 0.95 | 10.5 | PEDOT:PSS/ZnO/PEIE | s-2T | 1.63 | 12.9 | 72.0 | 15.1 | [678] |
| PTB7-Th:$PC_{71}BM$ | 0.77 | 9.49 | Ag/$MoO_3$ | PTB7-Th:$PC_{71}BM$ | 0.77 | 0.5 | CQD:PEI/M-PEDOT:PSS | s-2T | 1.58 | 11.5 | 66.8 | 12.1 | [679] |
| PTB7-Th:$PC_{71}BM$ | 0.91 | 8.76 | Al/ETL-1 | SM:$PC_{71}BM$ | 0.80 | 8.5 | n-PEDOT:PSS/np-ZnO | s-2T | 1.68 | 10.3 | 64.3 | 11.2 | [680] |
| PDPP4T-2F:$PC_{71}BM$ | 0.79 | 8.24 | Al/$MoO_3$ | PBDD4T-2F:$PC_{61}BM$ | 0.90 | 8.3 | PFN/Ag/$MoO_3$ | s-2T | 1.68 | 11.3 | 61.3 | 11.6 | [681] |
| N719 dye | 0.81 | 11.6 | FTO/ms-$TiO_2$/dye/Iodolyte AN-50/Pt | $MAPbI_3$ | 0.62 | 2.2 | Pt/Iodolyte AN-50/Per/ms-$TiO_2$/FTO | s-3T | 0.76 | 28.7 | 53.4 | 11.6 | [682] |
| N719 dye | 0.82 | 11.6 | FTO/ms-$TiO_2$/dye/Iodolyte AN-50/Pt | N719 dye | 0.78 | 4.6 | Pt/Iodolyte AN-50/dye/ms-$TiO_2$/FTO | s-3T | 0.80 | 31.4 | 58.1 | 14.5 | [682] |
| $MAPbI_3$ | 1.04 | 14.2 | Ag/ITO/PCBM/ZnO | c-Si | 0.59 | 6.8 | NiO/ITO/a-Si:H | s-3T | 1.65 | 18.5 | 78.0 | 23.8 | [172] |
| $Cs_{0.05}(FA_{0.83}MA_{0.17})_{0.95}Pb(I_{0.83}Br_{0.17})_3$ | 1.19 | 19.8 | LiF/IZO/$MoO_3$/Spiro | c-Si | 0.73 | 23.1 | $SnO_2$/ITO/a-Si:H | s-3T | | | | 17.1 | [46] |
| AlInP/GaInP/AlGaInP/AlGaAs | | | Metal/ZnS/$MgF_2$ | c-Si | | | TCO/TCA/TCO/poly-Si | s-3T | 2.05 | 14.9 | 86.2 | 26.4 | [173] |

The "s" and "f" in the type of tandem represent solid and flexible, respectively.

**Table 3. Photovoltaic performance of lead-free perovskite.** Few elements, such as $Sn^{2+}$, $Ge^{2+}$, $Cu^{+}$, $Bi^{3+}$, $Sb^{3+}$, etc, were utilized to substitute $Pb^{2+}$. Among these lead-free perovskite, tin-based counterpart demonstrated the best photovoltaic performance, together with continuous effort in durability improvement.

| Perovskite | Crystal phase | $E_g$ (eV) | VBM(CBM) | PCE (%) | $V_{OC}$ (V) | $J_{SC}$ (mA/cm) | FF | Stability | ref |
|---|---|---|---|---|---|---|---|---|---|
| $MASnI_3$ | P4mn | 1.3[D] | -5.47(-4.17) | 5.2 | 0.68 | 16.6 | 48.0 | 80%; 12h[c,e] | [87] |
| $MASnBr_3$ | P4mn | 2.2[D] | -5.54(-3.39) | 4.3 | 0.88 | 7.9 | 59.0 | 80%; 12h[c,e] | [87] |
| $GA_{0.2}FA_{0.78}SnI_3$-1% $EDAI_2$ | Amm2 | 1.5[D] | -5.20(-3.70) | 8.5 | 0.56 | 20.8 | 72.6 | 230%; 2000h[e] | [424] |
| 0.2% CDTA-$FASnI_3$ | Amm2 | 1.4[D] | | 10.2 | 0.63 | 21.2 | 74.7 | 90%; 1000h[c] | [432,683] |
| $FASnI_3$ | ACAM | 1.4[D] | | 6.5 | 0.55 | 18.1 | 64.7 | 23%; 48h[b,e] | [684-685] |
| $(PEA)_2FA_8Sn_9I_{28}$ | 2D | 1.4[D] | | 5.1 | 0.58 | 14.2 | 62.1 | 96%; 100h[b,e] | [685] |
| $FASnI_3$-PVP | ACAM | 1.4[D] | | 8.9 | 0.63 | 20.4 | 69.3 | 100%; 400h[c,e] | [684] |
| $BA_2MA_3Sn_4I_{13}$ | 2D | 1.4[D] | -4.76(-3.29) | 2.5 | 0.23 | 24.1 | 45.7 | 90%;720h[c] | [686] |
| $BA_2MA_2Sn_3I_{1-}$ | 2D | 1.5[D] | -4.76(-3.21) | 1.9 | 0.38 | 8.9 | 57.1 | 90%;720h[c] | [686] |
| $CsGe_{0.5}Sn_{0.5}I_3$ | *Pnma* | 1.5[D] | -5.40(-3.90) | 7.1 | 0.63 | 18.6 | 60.6 | 91%; 100h[b] | [687] |
| $MAGeI_{2.7}Br_{0.3}$ | *R3m* | 2.1[D] | | 0.7 | 0.46 | 3.1 | 48.0 | | [429] |
| $MAGeI_3$ | *R3m* | 2.0[D] | -5.20(-3.20) | 0.2 | 0.15 | 4.0 | 30.0 | | [428] |
| $FAGeI_3$ | *R3m* | 2.3[D] | -5.50(-3.20) | | | | | | [428] |
| $CsGeI_3$ | *R3m* | 1.6[D] | -5.10(-3.45) | 0.1 | 0.07 | 5.7 | 27.0 | | [428] |
| $(MA)_2CuCl_{0.5}Br_{3.5}$ | ACAM | 2.8[D] | -4.98(-2.12) | 0.002 | 0.29 | 0.002 | 28.0 | | [464] |
| $(MA)_2CuCl_2Br_2$ | ACAM | 1.1[D] | -4.98(-3.88) | 1.0 | 0.58 | 3.4 | 50.0 | | [463] |
| $(MA)_2CuCl_2I_2$ | ACAM | 2.0[D] | -5.61(-3.61) | 1.8 | 0.55 | 6.8 | 47.0 | | [463] |
| $(MA)_2CuCl_4$ | P121/A1 | 2.4-3.1[D] | -5.84(-3.44) | 2.4 | 0.56 | 8.1 | 52.0 | | [463-464] |
| $(MA)_3Bi_2I_9$ | $P6_3/mm$ | 2.0[D] | -5.63(-3.63) | 0.1 | 0.72 | 0.5 | 31.8 | | [688] |
| $Cs_3Bi_2I_9$ | $P6_3/mm$ | 2.2[D] | | 1.1 | 0.85 | 2.2 | 60.0 | 100%; 720h[d,g] | [689] |
| $CsBi_3I_{10}$ | | 1.7[D] | | 0.4 | 0.31 | 3.4 | 38.0 | 100%,17h | [690] |
| $(MA)_3Sb_2I_9$ | $P6_3/mm$ | 2.1[D] | -5.45(-3.35) | 1.1 | 0.64 | 3.8 | 45.5 | 15%; 720h[c,d,e] | [468,691] |
| $Cs_3Sb_2I_9$ | $P6_3/mm$ | 2.3[D] | -5.60(-3.30) | 0.8 | 0.60 | 2.9 | 48.1 | 90%;720h[c,d,e] | [468] |
| $Rb_3Sb_2I_9$ | P1*c*1 | 2.2[D] | -5.54(-3.30) | 0.7 | 0.55 | 2.1 | 57.0 | | [692] |

- Energy gap: [D]direct energy gap; [ID]indirect energy gap.
- Stability testing condition: [a]in ambient air; [b]without encapsulation; [c]with encapsulation; [d]stored in dark; [e]stored in inert gas environment; [f]high humidity >70%; [g]low humidity <20%; [h]heated at temperature >75 [o]C; [k]vacuumed atmosphere.

**Table 4. List of few double perovskite reported previously.** Most of the compounds was simulated and synthesized to investigate their intrinsic properties where only few were tested for their photovoltaic performance.

| Perovskite | Crystal phase | Bonding state | $E_g$ (eV) | Synthesis route | Remarks | ref |
|---|---|---|---|---|---|---|
| $(MA)_2TlBiBr_6$ | *Fm3m* | $s^2+s^2$ | $2.2^{D}$ | Hydrothermal; Solid state grinding | | [693-694] |
| $Cs_2TlBiI_6$ | *Fm3m* | $s^2+s^2$ | $1.4^{D}$ | | *Simulation* 1.05(0.23) | [695] |
| $(MA)_2KGdCl_6$ | *R3m* | $s^2+s^2$ | $4.9^{D}$ | Solution deposition | | [408] |
| $(MA)_2KYCl_6$ | *R3m* | $s^2+s^2$ | $5.1^{D}$ | Solution deposition | | [408] |
| $(MA)_2KBiCl_6$ | *R3m* | $s^0+s^2$ | $3.0^{ID}$ | Hydrothermal | | [408,696] |
| $(MA)_2AgBiI_6$ | *Fm3m* | $s^0+s^2$ | $2.0^{ID}$ | Hydrothermal; solid state grinding | XRD show no degradation for 4 months | [492,494,697] |
| $(MA)_2AgBiBr_6$ | *Fm3m* | $s^0+s^2$ | $2.0^{ID}$ | Hydrothermal | | [494,697] |
| $Cs_2NaBiI_6$ | $P6_3/mm$ | $s^0+s^2$ | $1.7^{iD}$ | | PCE 0.4%; $V_{OC}$ 0.5 V; $J_{SC}$ 2.0 mA/cm; FF 44.0% | [698] |
| $Cs_2AgBiI_6$ | *Fm3m* | $s^0+s^2$ | $1.8^{ID}$ | Anion exchange protocol | | [480] |
| $Cs_2AgBiBr_6$ | *Fm3m* | $s^0+s^2$ | $1.9^{ID}$ | Reflux; Solution deposition | PCE 2.5%; $V_{OC}$ 1.0 V; $J_{SC}$ 4.5 mA/cm; FF 55.1% | [479,483,699-700] |
| $Cs_2AgBiBr_6$/dye | *Fm3m* | $s^0+s^2$ | $1.9^{ID}$ | Reflux; Solution deposition | PCE 2.8%; $V_{OC}$ 1.1V; $J_{SC}$ 5.1 mA/cm; FF 52.4% | [479,483,699-700] |
| $Cs_2AgBiCl_6$ | *Fm3m* | $s^0+s^2$ | $2.0^{ID}$ | Solid state grinding; Reflux | | [479,483] |
| $(MA)_2AgSbI_6$ | *R3m* | $s^0+s^2$ | $1.9^{ID}$ | Solid-state grinding | | [480] |
| $Cs_2AgSbCl_6$ | - | $s^0+s^2$ | $2.7^{ID}$ | Hydrothermal | | [701-702] |
| $Cs_2AgSbBr_6$ | *Fm3m* | $s^0+s^2$ | $1.9^{ID}$ | Solid state grinding | | [694] |
| $Cs_3CuSbCl_6$ | - | $s^0+s^2$ | $1.0^{D}$ | Precipitation | 0.32(0.16) | [703] |
| $(MA)_2CuBiI_6$ | - | $s^0+s^2$ | $1.7^{ID}$ | Hydrothermal | XRD show no degradation for 30 days (dark) | [492] |
| $Cs_2CuBiI_6$ | *Fm3m* | $s^0+s^2$ | $1.3^{(ID)}$ | | *Simulation* | [479] |
| $Cs_2CuBiBr_6$ | *Fm3m* | $s^0+s^2$ | $1.9^{(ID)}$ | | *Simulation* | [479] |
| $Cs_2CuBiCl_6$ | *Fm3m* | $s^0+s^2$ | $2.0^{(ID)}$ | | *Simulation* | [479] |
| $Cs_2AuBiI_6$ | *Fm3m* | $s^0+s^2$ | $1.6^{(ID)}$ | | *Simulation* | [479] |
| $Cs_2AuBiBr_6$ | *Fm3m* | $s^0+s^2$ | $1.1^{(ID)}$ | | *Simulation* | [479] |
| $Cs_2AuBiCl_6$ | *Fm3m* | $s^0+s^2$ | $0.5^{(ID)}$ | | *Simulation* | [479] |
| $Cs_2Au^{I}Au^{III}I_6$ | *I4/mcm* | $s^0+s^0$ | $1.6^{(D)}$ | Precipitation | | [704] |
| $Cs_2Au^{I}Au^{III}Br_6$ | *I4/mcm* | $s^0+s^0$ | $1.3^{(D)}$ | Precipitation | | [705] |
| $Cs_2Au^{I}Au^{III}Cl_6$ | *I4/mcm* | $s^0+s^0$ | $2.0^{(D)}$ | Precipitation | | [705] |
| $Cs_2NaInCl_6$ | *Fm3m* | $s^0+s^0$ | $4.6^{D}$ | Reflux | PL show no degradation for 1 months (amb) | [493] |
| $Cs_2AgInBr_6$ | *Fm3m* | $s^0+s^0$ | $1.5^{D}$ | Solvothermal | | [706-707] |
| $Cs_2AgInCl_6$ | *Fm3m* | $s^0+s^0$ | $3.3^{D}$ | Reflux | | [708] |
| $Rb_2AgInBr_6$ | *Fm3m* | $s^0+s^0$ | $1.5^{D}$ | | *Simulation* | [706] |
| $Rb_2AgInCl_6$ | *Fm3m* | $s^0+s^0$ | $2.5^{D}$ | | *Simulation* | [706] |
| $Rb_2CuInBr_6$ | *Fm3m* | $s^0+s^0$ | $0.6^{D}$ | | *Simulation* | [706] |
| $Rb_2CuInCl_6$ | *Fm3m* | $s^0+s^0$ | $1.4^{D}$ | | *Simulation* | [706] |

- Bonding state: $s^2+s^2$ both cation B(I and III) has a lone-pair state; $s^0+s^2$ one of the cation B (I or III) has a lone-pair state; $s^0+s^0$ both cation B (I and III) has no lone-pair state.
- Energy gap: $^{D}$direct energy gap; $^{ID}$indirect energy gap; $^{(D)(ID)}$nature of energy gap speculated from bonding state.

**Table 5. Deposition techniques for PSCs.** Different perovskite deposition techniques and their effect on film morphology as well as the resulting photovoltaic performance.

| Deposition techniques | Perovskite | Solvent system | Remarks | Device architecture | Photovoltaic performance | | | | ref |
|---|---|---|---|---|---|---|---|---|---|
| | | | | | PCE (%) | $V_{OC}$ (V) | $J_{SC}$ (mA/cm) | FF (%) | |
| One-step Solution Deposition | $MAPbI_3$ | DMF+DMSO(50:1/v:v)$^{SC}$ | ~0.2 µm grain; $R_{ms}$ = 29.9 nm | MSSCs | 17.8 | 1.07 | 22.6 | 74.0 | [709] |
| | $MAPbI_3$ | DMF+DMSO(10:1/v:v)$^{SC}$ | ~1.8 µm grain; $R_{ms}$ = 5.9 nm | MSSCs | 17.5 | 1.05 | 22.8 | 73.1 | [710] |
| | $MAPbI_3$ | DMF+DMSO(9:1/wt:wt)$^{SC}$ | ~0.28 µm grain; $R_{ms}$ < 3 nm | Planar | 11.4 | 1.08 | 16.4 | 64.0 | [711] |
| | $MAPbI_3$ | DMSO$^{SC}$ | ~0.25 µm grain | MSSCs | 13.8 | 1.01 | 20.3 | 72.0 | [712] |
| | $MAPbI_3$ | DMF+DMSO(1.5:8.5/V:V)$^{SC}$ | ~0.5 µm grain; no pinhole observed | MSSCs | 14.7 | 1.02 | 21.2 | 73.0 | [712] |
| | $MAPbI_{3-X}Cl_X$ | DMF+1% DIO $^{SC}$ | 2-fold increment in crystallinity | Inverted | 11.8 | 0.92 | 15.6 | 71.0 | [713] |
| | $MAPbICl_2$ | DMF $^{SC}$ | Pinhole-free, dense film | MSSCs | 19.3 | 1.13 | 22.8 | 75.0 | [714] |
| Two-step Solution Deposition | $MAPbI_3$ | DMF$^{SC}$/Isopropanol$^{SC}$ | ~1 µm grain | Inverted | 18.2 | 1.02 | 22.9 | 77.6 | [715] |
| | $MAPbI_3$ | DMF$^{SC}$/2-propanol$^{SC}$ | ~0.25 µm grain | MSSCs | 13.9 | 1.02 | 21.5 | 63.4 | [716] |
| | $MAPbI_3$ | DMF$^{SC}$/Isopropanol$^{D}$ | Stronger optical absorption | MSSCs | 10.8 | 1.07 | 17.3 | 59.0 | [717] |
| | $MAPbI_3$ | DMF+DMSO(9:1/v:v)$^{SC}$/isopropanol$^{D}$ | 1.0 µm crystal, full coverage | MSSCs | 11.5 | 0.96 | 18.3 | 66.0 | [718] |
| | $MAPbI_3$ | DMF+DMSO(9:1/v:v)$^{SC}$/isopropanol$^{SK}$ | 200-400 nm crystal, few pinholes observe | MSSCs | 9.6 | 0.86 | 17.7 | 63.0 | [718] |
| | $MAPbI_3$ | DMF$^{SC}$/2-propanol$^{SC}$ | Reduced pinhole compared to one-step | Inverted | 15.4 | 0.99 | 19.6 | 79.3 | [719] |
| | $MAPbI_3$ | DMF+NMP$^{SC}$/2-propanol$^{AS}$ | Pinhole-free, dense film | MSSCs | 14.3 | 1.03 | 19.9 | 69.9 | [720] |
| | $MAPbI_3$ | DMF$^{SC}$/Isopropanol$^{SK}$ | Rough film with poor coverage | MSSCs | 9.3 | 0.93 | 18.2 | 55.0 | [512] |
| Physical Vapor Depostion | $MAPbI_{3-X}Cl_X$ | DMF+DMSO(4:1/v:v)$^{SC}$/2-propanol$^{SC}$/VASP | Continuous, flat and full coverage | MSSCs | 8.4 | 0.85 | 18.5 | 53.0 | [511] |
| | $MAPbI_{3-X}Cl_X$ | DMF+DMSO(4:1/v:v)$^{SC}$/2-propanol$^{D}$/VASP | Continuous, flat and full coverage | MSSCs | 7.4 | 0.82 | 19.1 | 46.0 | [511] |
| | $MAPbI_{3-X}Cl_X$ | DMF+DMSO(4:1/v:v)$^{SC}$/VASP | Continuous, flat and full coverage | MSSCs | 7.1 | 0.67 | 19.9 | 52.0 | [511] |
| | $MAPbI_3$ | DMF$^{SC}$/VASP | Dense, flat film with complete coverage | MSSCs | 13.5 | 0.96 | 21.3 | 66.0 | [512] |
| | $MAPbI_{3-X}(SCN)_X$ | DMF$^{SC}$/VASP | Large crystal, flat surface will no pinhole | MSSCs | 12.7 | 1.02 | 17.1 | 72.7 | [721] |
| | $MAPbI_3$ | DMF$^{SC}$/VASP | Microscale grain, $R_{ms}$ = 23.2 nm, 100% coverage | Planar | 12.1 | 0.92 | 19.8 | 66.3 | [519] |
| | $MAPbI_3$ | S-Thermal/2-propanol$^{SC}$ | Complete coverage | Planar | 17.9 | 1.11 | 21.0 | 76.6 | [506] |
| | $MAPbI_{3-X}Cl_X$ | D-Thermal | Dense, uniform film | Planar | 15.4 | 1.07 | 17.6 | 58.0 | [722] |
| Chemical Vapor Deposition | $Cs_{0.1}FA_{0.9}PbI_{2.9}Br_{0.1}$ | D-Thermal/CVD | Microscale grain, dense film coverage | Planar | 13.3 | 0.90 | 20.2 | 67.0 | [723] |
| | $MAPbI_3$ | Two-stage CVD | 0.4 µm grain, $R_{ms}$ = 19 nm | HTL-free | 7.9 | 0.91 | 15.5 | 56.0 | [724] |
| | $MAPbI_3$ | Two-stage CVD | | Planar | 15.6 | 1.06 | 21.7 | 68.0 | [521] |
| | $MAPbI_3$ | VASP/CVD | Dense and pinhole-free film | Planar | 15.4 | 0.97 | 21.2 | 75.0 | [725] |
| | $MAPbI_3$ | Two-stage CVD | Dense and pinhole-free film | MSSCs | 18.9 | 1.06 | 22.1 | 80.0 | [726] |
| Solution-based coating | $FAMACsPbI_{2.55}Br_{0.45}$ | Blade coating (DMF) | Smooth and pinhole-free film | Planar | 18.2 | 1.09 | 22.5 | 74.2 | [727] |
| | $MAPbI_3$ | Blade coating (DMF) | 0.8-1.7 µm grain | HTL-free | 20.2 | 1.10 | 22.7 | 81.0 | [104] |
| | $MAPbI_3$ | Blade coating (DMF) | < 10 µm grain, pinhole-free film | Planar | 17.5 | 1.08 | 22.3 | 74.2 | [535] |
| | $MAPbI_3$ | Blade coating (GBL:DMSO 3:1 v:v) | | MSSCs | 18.0 | 1.04 | 22.9 | 77.0 | [533] |
| | $MAPbI_{3-X}Cl_X$ | Slot-die coating (NMP:DMF 9:8 v:v) | ~1 µm grain, dense and pinhole-free film | Planar | 18.0 | 1.10 | 21.5 | 76.0 | [558] |
| | $Cs_{0.15}FA_{0.85}PbI_{2-X}Br_X$ | Slot-die coating (DMSO:2BE) | Pinhole-free film | ETL-free | 15.2 | 1.03 | 20.7 | 71.5 | [728] |
| | $MAPbI_{3-X}Cl_X$ | Slot-die coating (DMF) | Pinhole-free film | Inverted | 11.4 | 0.91 | 13.5 | 68.0 | [729] |
| Solution-based printing | $MAPbI_3$ | Inkjet-printing (DMSO:GBL 4:6 v:v) | ~0.5 µm grain, dense and pinhole-free film | Planar | 15.3 | 1.03 | 22.4 | 65.9 | [569] |
| | $CsFAMAPbBr_{3-X}I_X$ | Inkjet-printing (DMF:DMSO 4:1 v:v) | | Planar | 12.9 | 1.06 | 21.5 | 67.0 | [730] |
| | $CsFAMAPbBr_{3-X}I_X$ | Inkjet-printing | ~0.2 µm grain | Planar | 14.0 | 1.03 | 19.9 | 68.1 | [731] |

- Solvent abbreviation: DMF – N,N-dimethylfomamide; DMSO – dimethylsulfoxide; DMA – N,N-dimethylacetamide; NMP – N-methyl-2-pyrrolidone; DIO – 1,8-diiodooctane; 2BE – 2-butoxyethanol
- Deposition technique: $^{SC}$ Spin-coating; $^{D}$ Dipping; $^{SK}$ Soaking; $^{AS}$ Air-spray coating; (VASP) Vapor-assisted deposition; (S-Thermal) Single source thermal evaporation; (D-thermal) Dual source thermal evaporation; (CVD) Chemical vapor deposition

**Table 6. Comparison between different deposition techniques.** The active area of each device is given in a bolded-bracket besides their respective efficiency.

| Techniques | Mass production | Deposition speed (m/min) | PCE loss/area (%/cm²) | Wastage/deposition | | | Roll-to-roll production | Efficiency (%) * | | | Largest area reported (cm²) | ref |
|---|---|---|---|---|---|---|---|---|---|---|---|---|
| | | | | Precursors | VOC | Total | | Small (< 10 cm²) | Cell (≥ 10 cm²) | Module (≥ 100 cm²) | | |
| Spin-coating | ✕ | - | - | 50-70% | ✓ | 90-95% | ✕ | 18.0 **(0.16)** | 14.0 **(10.0)** | ✕ | 10.0 | [569,732-734] |
| Physical vapor deposition | ✓ | 2.4-4.8 | 0.16 | ~50% | ✕ | 50-55% | ✓ | 20.4 **(0.07)** | 15.8 **(64.0)** | ✕ | 400.0[#] | [572,735-739] |
| Chemical vapor deposition | ✓ | - | 0.17 | ~60% | ✕ | 60-70% | ✕ | 18.9 **(0.11)** | 13.4 **(25.0)** | ✕ | 100.0[#] | [732,736,740] |
| Blade-coating | ✓ | 0.7-2.4 | 0.51-0.68 | <10% | ✓ | 75-80% | ✓ | 20.3 **(7.50)** | 14.8 **(57.8)** | 13.3 **(100.0)** | 600.0[#] | [32,35,557,741-743] |
| Spray-coating | ✓ | 3.0-9.0 | 0.19 | 10-20% | ✓ | 85-90% | ✓ | 19.4 **(0.03)** | 14.2 **(56.3)** | - | 56.3 | [570,573,744] |
| Slot-die coating | ✓ | 3.0-5.0 | 0.13-0.54 | 5-10% | ✓ | 60-70% | ✓ | 18.0 **(0.16)** | 16.9 **(52.0)** | 11.8 **(149.5)** | 168.8 | [217,571,729,745-746] |
| Inkjet-printing | ✓ | 1.5-2.5 | 0.22 | 5-10% | ✓ | 55-56% | ✓ | 17.2 **(0.10)** | 12.3 **(10.0)** | 6.6 **(198.0)** | 198.0 | [113,569,739,742] |

[#] Reported values for the deposited coating without fabricated into functional PSCs device. The values were taken into consideration if the coating offered high quality films in term of grain size, crystallinity, low number of pinhole and high surface smoothness

* Highest reported value for each category to showcase the highest achievable efficiency for respective deposition techniques.

Received: ((will be filled in by the editorial staff))
Revised: ((will be filled in by the editorial staff))
Published online: ((will be filled in by the editorial staff))

References

[1] I. E. Agency, 2019.
[2] M. Shellenberger, If Solar Panels Are Clean, Why Do They Produce So Much Toxic Waste?, https://www.forbes.com/sites/michaelshellenberger/2018/05/23/if-solar-panels-are-so-clean-why-do-they-produce-so-much-toxic-waste/#3095bc8e121c, accessed.
[3] M. S. Chowdhury, K. S. Rahman, T. Chowdhury, N. Nuthammachot, K. Techato, M. Akhtaruzzaman, S. K. Tiong, K. Sopian, N. Amin, *Energy Strategy Reviews* **2020**, 27, 100431.
[4] A. Kojima, K. Teshima, Y. Shirai, T. Miyasaka, *Journal of the American Chemical Society* **2009**, 131, 6050.
[5] NREL, 2019.
[6] J. Y. Kim, J.-W. Lee, H. S. Jung, H. Shin, N.-G. Park, *Chemical Reviews* **2020**, 120, 7867.
[7] S. D. Stranks, G. E. Eperon, G. Grancini, C. Menelaou, M. J. P. Alcocer, T. Leijtens, L. M. Herz, A. Petrozza, H. J. Snaith, *Science* **2013**, 342, 341.
[8] F. Zhang, B. Yang, Y. Li, W. Deng, R. He, *Journal of Materials Chemistry C* **2017**, 5, 8431.
[9] W. Ning, F. Wang, B. Wu, J. Lu, Z. Yan, X. Liu, Y. Tao, J.-M. Liu, W. Huang, M. Fahlman, L. Hultman, T. C. Sum, F. Gao, *Advanced Materials* **2018**, 30, 1706246.
[10] F. Li, C. Ma, H. Wang, W. Hu, W. Yu, A. D. Sheikh, T. Wu, *Nature Communications* **2015**, 6, 8238.
[11] G. Giorgi, K. Yamashita, *Journal of Materials Chemistry A* **2015**, 3, 8981.
[12] N. D. Canicoba, N. Zagni, F. Liu, G. McCuistian, K. Fernando, H. Bellezza, B. Traoré, R. Rogel, H. Tsai, L. Le Brizoual, W. Nie, J. J. Crochet, S. Tretiak, C. Katan, J. Even, M. G. Kanatzidis, B. W. Alphenaar, J.-C. Blancon, M. A. Alam, A. D. Mohite, *ACS Materials Letters* **2019**, 1, 633.
[13] Y. Li, L. Meng, Y. Yang, G. Xu, Z. Hong, Q. Chen, J. You, G. Li, Y. Yang, Y. Li, *Nature Communications* **2016**, 7, 10214.
[14] F. Di Giacomo, A. Fakharuddin, R. Jose, T. M. Brown, *Energy & Environmental Science* **2016**, 9, 3007.
[15] Y. Kuang, Y. Ma, D. Zhang, Q. Wei, S. Wang, X. Yang, X. Hong, Y. Liu, *Nanoscale Research Letters* **2020**, 15, 213.
[16] A. Miyata, A. Mitioglu, P. Plochocka, O. Portugall, J. T.-W. Wang, S. D. Stranks, H. J. Snaith, R. J. Nicholas, *Nature Physics* **2015**, 11, 582.
[17] M. C. Gélvez-Rueda, M. B. Fridriksson, R. K. Dubey, W. F. Jager, W. van der Stam, F. C. Grozema, *Nature Communications* **2020**, 11, 1901.
[18] S. Rana, K. Awasthi, S. S. Bhosale, E. W.-G. Diau, N. Ohta, *The Journal of Physical Chemistry C* **2019**, 123, 19927.
[19] K. Galkowski, A. Mitioglu, A. Miyata, P. Plochocka, O. Portugall, G. E. Eperon, J. T.-W. Wang, T. Stergiopoulos, S. D. Stranks, H. J. Snaith, R. J. Nicholas, *Energy & Environmental Science* **2016**, 9, 962.
[20] Y. Jiang, X. Wang, A. Pan, *Advanced Materials* **2019**, 31, 1806671.
[21] F. Wang, S. Bai, W. Tress, A. Hagfeldt, F. Gao, *npj Flexible Electronics* **2018**, 2, 22.
[22] J. M. Ball, A. Petrozza, *Nature Energy* **2016**, 1, 16149.

[23] P. Zhao, B. J. Kim, H. S. Jung, *Materials Today Energy* **2018**, 7, 267.
[24] J. Qin, J. Zhang, Y. Bai, S. Ma, M. Wang, H. Xu, M. Loyd, Y. Zhan, X. Hou, B. Hu, *iScience* **2019**, 19, 378.
[25] M.-S. Lee, S. Sarwar, S. Park, U. Asmat, D. T. Thuy, C.-h. Han, S. Ahn, I. Jeong, S. Hong, *Sustainable Energy & Fuels* **2020**, 4, 3318.
[26] Y. Zhao, A. M. Nardes, K. Zhu, *Faraday Discussions* **2014**, 176, 301.
[27] N. Kitazawa, Y. Watanabe, Y. Nakamura, *Journal of Materials Science* **2002**, 37, 3585.
[28] C. Liu, Q. Zeng, B. Yang, *Advanced Materials Interfaces* **2019**, 6, 1901136.
[29] Z. Liu, L. Krückemeier, B. Krogmeier, B. Klingebiel, J. A. Márquez, S. Levcenko, S. Öz, S. Mathur, U. Rau, T. Unold, T. Kirchartz, *ACS Energy Letters* **2019**, 4, 110.
[30] Z. Guo, A. K. Jena, I. Takei, G. M. Kim, M. A. Kamarudin, Y. Sanehira, A. Ishii, Y. Numata, S. Hayase, T. Miyasaka, *Journal of the American Chemical Society* **2020**, DOI: 10.1021/jacs.0c02227.
[31] A. Dubey, N. Adhikari, S. Mabrouk, F. Wu, K. Chen, S. Yang, Q. Qiao, *Journal of Materials Chemistry A* **2018**, 6, 2406.
[32] H. Wu, C. Zhang, K. Ding, L. Wang, Y. Gao, J. Yang, *Organic Electronics* **2017**, 45, 302.
[33] N.-G. Park, K. Zhu, *Nature Reviews Materials* **2020**, 5, 333.
[34] A. Gheno, Y. Huang, J. Bouclé, B. Ratier, A. Rolland, J. Even, S. Vedraine, *Solar RRL* **2018**, 2, 1800191.
[35] A. Verma, D. Martineau, S. Abdolhosseinzadeh, J. Heier, F. Nüesch, *Materials Advances* **2020**, 1, 153.
[36] K. Hwang, Y.-S. Jung, Y.-J. Heo, F. H. Scholes, S. E. Watkins, J. Subbiah, D. J. Jones, D.-Y. Kim, D. Vak, *Advanced Materials* **2015**, 27, 1241.
[37] A. Al-Ashouri, E. Köhnen, B. Li, A. Magomedov, H. Hempel, P. Caprioglio, J. A. Márquez, A. B. Morales Vilches, E. Kasparavicius, J. A. Smith, N. Phung, D. Menzel, M. Grischek, L. Kegelmann, D. Skroblin, C. Gollwitzer, T. Malinauskas, M. Jošt, G. Matič, B. Rech, R. Schlatmann, M. Topič, L. Korte, A. Abate, B. Stannowski, D. Neher, M. Stolterfoht, T. Unold, V. Getautis, S. Albrecht, *Science* **2020**, 370, 1300.
[38] G. Grancini, C. Roldán-Carmona, I. Zimmermann, E. Mosconi, X. Lee, D. Martineau, S. Narbey, F. Oswald, F. De Angelis, M. Graetzel, M. K. Nazeeruddin, *Nature Communications* **2017**, 8, 15684.
[39] B. J. Kim, D. H. Kim, S. L. Kwon, S. Y. Park, Z. Li, K. Zhu, H. S. Jung, *Nature Communications* **2016**, 7, 11735.
[40] A. Binek, M. L. Petrus, N. Huber, H. Bristow, Y. Hu, T. Bein, P. Docampo, *ACS Applied Materials & Interfaces* **2016**, 8, 12881.
[41] Y. Jiang, L. Qiu, E. J. Juarez-Perez, L. K. Ono, Z. Hu, Z. Liu, Z. Wu, L. Meng, Q. Wang, Y. Qi, *Nature Energy* **2019**, 4, 585.
[42] C. Vaalma, D. Buchholz, M. Weil, S. Passerini, *Nature Reviews Materials* **2018**, 3, 18013.
[43] N. Delaporte, G. Lajoie, S. Collin-Martin, K. Zaghib, *Scientific Reports* **2020**, 10, 3812.
[44] M. Jaysankar, M. Filipič, B. Zielinski, R. Schmager, W. Song, W. Qiu, U. W. Paetzold, T. Aernouts, M. Debucquoy, R. Gehlhaar, J. Poortmans, *Energy & Environmental Science* **2018**, 11, 1489.
[45] P. S. C. Schulze, A. J. Bett, M. Bivour, P. Caprioglio, F. M. Gerspacher, Ö. Ş. Kabaklı, A. Richter, M. Stolterfoht, Q. Zhang, D. Neher, M. Hermle, H. Hillebrecht, S. W. Glunz, J. C. Goldschmidt, *Solar RRL* **2020**, 4, 2000152.
[46] P. Tockhorn, P. Wagner, L. Kegelmann, J.-C. Stang, M. Mews, S. Albrecht, L. Korte, *ACS Applied Energy Materials* **2020**, 3, 1381.
[47] S. M. Iftiquar, J. Jung, J. Yi, *Journal of Physics D: Applied Physics* **2017**, 50, 405501.

[48] J. H. Heo, D. S. Lee, D. H. Shin, S. H. Im, *Journal of Materials Chemistry A* **2019**, 7, 888.
[49] H. Xie, X. Yin, Y. Guo, J. Liu, W. Que, G. Wang, *physica status solidi (RRL) – Rapid Research Letters* **2019**, 13, 1800566.
[50] H. S. Jung, G. S. Han, N.-G. Park, M. J. Ko, *Joule* **2019**, 3, 1850.
[51] A. Rohatgi, K. Zhu, J. Tong, D. H. Kim, E. Reichmanis, B. Rounsaville, V. Prakash, Y. Ok, *IEEE Journal of Photovoltaics* **2020**, 10, 417.
[52] G. Coletti, S. L. Luxembourg, L. J. Geerligs, V. Rosca, A. R. Burgers, Y. Wu, L. Okel, M. Kloos, F. J. K. Danzl, M. Najafi, D. Zhang, I. Dogan, V. Zardetto, F. Di Giacomo, J. Kroon, T. Aernouts, J. Hüpkes, C. H. Burgess, M. Creatore, R. Andriessen, S. Veenstra, *ACS Energy Letters* **2020**, 5, 1676.
[53] D. Zhao, C. Wang, Z. Song, Y. Yu, C. Chen, X. Zhao, K. Zhu, Y. Yan, *ACS Energy Letters* **2018**, 3, 305.
[54] C. J. Bartel, C. Sutton, B. R. Goldsmith, R. Ouyang, C. B. Musgrave, L. M. Ghiringhelli, M. Scheffler, *Science Advances* **2019**, 5, eaav0693.
[55] M. A. Green, A. Ho-Baillie, H. J. Snaith, *Nature Photonics* **2014**, 8, 506.
[56] A. E. Fedorovskiy, N. A. Drigo, M. K. Nazeeruddin, *Small Methods* **2020**, 4, 1900426.
[57] W. Lee, J. W. Han, Y. Chen, Z. Cai, B. Yildiz, *Journal of the American Chemical Society* **2013**, 135, 7909.
[58] N. Soylu Koc, S. P. Altintas, N. Mahamdioua, C. Terzioglu, *Journal of Alloys and Compounds* **2019**, 797, 471.
[59] Y. Fu, M. P. Hautzinger, Z. Luo, F. Wang, D. Pan, M. M. Aristov, I. A. Guzei, A. Pan, X. Zhu, S. Jin, *ACS Central Science* **2019**, 5, 1377.
[60] R. E. Cohen, *Nature* **1992**, 358, 136.
[61] U. Kenji, *Science and Technology of Advanced Materials* **2015**, 16, 046001.
[62] Y.-M. You, W.-Q. Liao, D. Zhao, H.-Y. Ye, Y. Zhang, Q. Zhou, X. Niu, J. Wang, P.-F. Li, D.-W. Fu, Z. Wang, S. Gao, K. Yang, J.-M. Liu, J. Li, Y. Yan, R.-G. Xiong, *Science* **2017**, 357, 306.
[63] E. L. Unger, L. Kegelmann, K. Suchan, D. Sörell, L. Korte, S. Albrecht, *Journal of Materials Chemistry A* **2017**, 5, 11401.
[64] S. Adjokatse, H.-H. Fang, M. A. Loi, *Materials Today* **2017**, 20, 413.
[65] T. Lei, M. Lai, Q. Kong, D. Lu, W. Lee, L. Dou, V. Wu, Y. Yu, P. Yang, *Nano Letters* **2018**, 18, 3538.
[66] S. Aharon, B. E. Cohen, L. Etgar, *The Journal of Physical Chemistry C* **2014**, 118, 17160.
[67] T. C.-J. Yang, P. Fiala, Q. Jeangros, C. Ballif, *Joule* **2018**, 2, 1421.
[68] M. Karlsson, Z. Yi, S. Reichert, X. Luo, W. Lin, Z. Zhang, C. Bao, R. Zhang, S. Bai, G. Zheng, P. Teng, L. Duan, Y. Lu, K. Zheng, T. Pullerits, C. Deibel, W. Xu, R. Friend, F. Gao, *Nature Communications* **2021**, 12, 361.
[69] A. Suzuki, H. Okada, T. Oku, *AIP Conference Proceedings* **2016**, 1709, 020022.
[70] J. H. Noh, S. H. Im, J. H. Heo, T. N. Mandal, S. I. Seok, *Nano Letters* **2013**, 13, 1764.
[71] R. Dalven, *Physical Review B* **1973**, 8, 6033.
[72] S. Tombe, G. Adam, H. Heilbrunner, D. H. Apaydin, C. Ulbricht, N. S. Sariciftci, C. J. Arendse, E. Iwuoha, M. C. Scharber, *Journal of Materials Chemistry C* **2017**, 5, 1714.
[73] I. E. Castelli, T. Olsen, S. Datta, D. D. Landis, S. Dahl, K. S. Thygesen, K. W. Jacobsen, *Energy & Environmental Science* **2012**, 5, 5814.
[74] Y. Song, R. Yang, D. Li, W. T. Wu, Z. X. Guo, *Physical Review B* **1999**, 59, 14220.
[75] S. Colella, E. Mosconi, P. Fedeli, A. Listorti, F. Gazza, F. Orlandi, P. Ferro, T. Besagni, A. Rizzo, G. Calestani, G. Gigli, F. De Angelis, R. Mosca, *Chemistry of Materials* **2013**, 25, 4613.

[76] G. Nedelcu, L. Protesescu, S. Yakunin, M. I. Bodnarchuk, M. J. Grotevent, M. V. Kovalenko, *Nano Letters* **2015**, 15, 5635.
[77] L. Atourki, E. Vega, B. Marí, M. Mollar, H. Ait Ahsaine, K. Bouabid, A. Ihlal, *Applied Surface Science* **2016**, 390, 744.
[78] A. Senocrate, G. Y. Kim, M. Grätzel, J. Maier, *ACS Energy Letters* **2019**, 4, 2859.
[79] D. Sabba, H. K. Mulmudi, R. R. Prabhakar, T. Krishnamoorthy, T. Baikie, P. P. Boix, S. Mhaisalkar, N. Mathews, *The Journal of Physical Chemistry C* **2015**, 119, 1763.
[80] S. Gharibzadeh, B. Abdollahi Nejand, M. Jakoby, T. Abzieher, D. Hauschild, S. Moghadamzadeh, J. A. Schwenzer, P. Brenner, R. Schmager, A. A. Haghighirad, L. Weinhardt, U. Lemmer, B. S. Richards, I. A. Howard, U. W. Paetzold, *Advanced Energy Materials* **2019**, 9, 1803699.
[81] Y. Ogomi, A. Morita, S. Tsukamoto, T. Saitho, N. Fujikawa, Q. Shen, T. Toyoda, K. Yoshino, S. S. Pandey, T. Ma, S. Hayase, *The Journal of Physical Chemistry Letters* **2014**, 5, 1004.
[82] L. E. Mundt, J. Tong, A. F. Palmstrom, S. P. Dunfield, K. Zhu, J. J. Berry, L. T. Schelhas, E. L. Ratcliff, *ACS Energy Letters* **2020**, 5, 3344.
[83] S. Gu, R. Lin, Q. Han, Y. Gao, H. Tan, J. Zhu, *Advanced Materials* **2020**, 32, 1907392.
[84] K. Nishimura, M. A. Kamarudin, D. Hirotani, K. Hamada, Q. Shen, S. Iikubo, T. Minemoto, K. Yoshino, S. Hayase, *Nano Energy* **2020**, 74, 104858.
[85] B. Li, B. Chang, L. Pan, Z. Li, L. Fu, Z. He, L. Yin, *ACS Energy Letters* **2020**, 5, 3752.
[86] X. Jiang, F. Wang, Q. Wei, H. Li, Y. Shang, W. Zhou, C. Wang, P. Cheng, Q. Chen, L. Chen, Z. Ning, *Nature Communications* **2020**, 11, 1245.
[87] F. Hao, C. C. Stoumpos, D. H. Cao, R. P. H. Chang, M. G. Kanatzidis, *Nature Photonics* **2014**, 8, 489.
[88] N. K. Noel, S. D. Stranks, A. Abate, C. Wehrenfennig, S. Guarnera, A.-A. Haghighirad, A. Sadhanala, G. E. Eperon, S. K. Pathak, M. B. Johnston, A. Petrozza, L. M. Herz, H. J. Snaith, *Energy & Environmental Science* **2014**, 7, 3061.
[89] A. R. b. M. Yusoff, H. P. Kim, X. Li, J. Kim, J. Jang, M. K. Nazeeruddin, *Advanced Materials* **2017**, 29, 1602940.
[90] Y. Mei, C. Zhang, Z. V. Vardeny, O. D. Jurchescu, *MRS Communications* **2015**, 5, 297.
[91] G. Giorgi, J.-I. Fujisawa, H. Segawa, K. Yamashita, *The Journal of Physical Chemistry Letters* **2013**, 4, 4213.
[92] J. Peng, Y. Chen, K. Zheng, T. Pullerits, Z. Liang, *Chemical Society Reviews* **2017**, 46, 5714.
[93] T. Dittrich, F. Lang, O. Shargaieva, J. Rappich, N. H. Nickel, E. Unger, B. Rech, *Applied Physics Letters* **2016**, 109, 073901.
[94] Y. Chen, J. Peng, D. Su, X. Chen, Z. Liang, *ACS Applied Materials & Interfaces* **2015**, 7, 4471.
[95] J. Shi, Y. Li, Y. Li, D. Li, Y. Luo, H. Wu, Q. Meng, *Joule* **2018**, 2, 879.
[96] J. H. Heo, S. H. Im, J. H. Noh, T. N. Mandal, C.-S. Lim, J. A. Chang, Y. H. Lee, H.-j. Kim, A. Sarkar, M. K. Nazeeruddin, M. Grätzel, S. I. Seok, *Nature Photonics* **2013**, 7, 486.
[97] A. Dodabalapur, H. E. Katz, L. Torsi, R. C. Haddon, *Science* **1995**, 269, 1560.
[98] R. A. Kerner, B. P. Rand, *The Journal of Physical Chemistry Letters* **2018**, 9, 132.
[99] J.-H. Im, C.-R. Lee, J.-W. Lee, S.-W. Park, N.-G. Park, *Nanoscale* **2011**, 3, 4088.
[100] W. S. Yang, B.-W. Park, E. H. Jung, N. J. Jeon, Y. C. Kim, D. U. Lee, S. S. Shin, J. Seo, E. K. Kim, J. H. Noh, S. I. Seok, *Science* **2017**, 356, 1376.
[101] D. Yang, R. Yang, K. Wang, C. Wu, X. Zhu, J. Feng, X. Ren, G. Fang, S. Priya, S. Liu, *Nature Communications* **2018**, 9, 3239.
[102] X. Zheng, Y. Hou, C. Bao, J. Yin, F. Yuan, Z. Huang, K. Song, J. Liu, J. Troughton, N. Gasparini, C. Zhou, Y. Lin, D.-J. Xue, B. Chen, A. K. Johnston, N. Wei, M. N. Hedhili,

M. Wei, A. Y. Alsalloum, P. Maity, B. Turedi, C. Yang, D. Baran, T. D. Anthopoulos, Y. Han, Z.-H. Lu, O. F. Mohammed, F. Gao, E. H. Sargent, O. M. Bakr, *Nature Energy* **2020**, 5, 131.

[103] V. Babu, R. Fuentes Pineda, T. Ahmad, A. O. Alvarez, L. A. Castriotta, A. Di Carlo, F. Fabregat-Santiago, K. Wojciechowski, *ACS Applied Energy Materials* **2020**, 3, 5126.

[104] W.-Q. Wu, Q. Wang, Y. Fang, Y. Shao, S. Tang, Y. Deng, H. Lu, Y. Liu, T. Li, Z. Yang, A. Gruverman, J. Huang, *Nature Communications* **2018**, 9, 1625.

[105] C. Huang, P. Lin, N. Fu, C. Liu, B. Xu, K. Sun, D. Wang, X. Zeng, S. Ke, *Chemical Communications* **2019**, 55, 2777.

[106] H.-S. Kim, C.-R. Lee, J.-H. Im, K.-B. Lee, T. Moehl, A. Marchioro, S.-J. Moon, R. Humphry-Baker, J.-H. Yum, J. E. Moser, M. Grätzel, N.-G. Park, *Scientific Reports* **2012**, 2, 591.

[107] L. Gao, T. H. Schloemer, F. Zhang, X. Chen, C. Xiao, K. Zhu, A. Sellinger, *ACS Applied Energy Materials* **2020**, 3, 4492.

[108] F. Zhang, Z. Yao, Y. Guo, Y. Li, J. Bergstrand, C. J. Brett, B. Cai, A. Hajian, Y. Guo, X. Yang, J. M. Gardner, J. Widengren, S. V. Roth, L. Kloo, L. Sun, *Journal of the American Chemical Society* **2019**, 141, 19700.

[109] X. Yin, Z. Song, Z. Li, W. Tang, *Energy & Environmental Science* **2020**, 13, 4057.

[110] P.-K. Kung, M.-H. Li, P.-Y. Lin, Y.-H. Chiang, C.-R. Chan, T.-F. Guo, P. Chen, *Advanced Materials Interfaces* **2018**, 5, 1800882.

[111] M. M. Lee, J. Teuscher, T. Miyasaka, T. N. Murakami, H. J. Snaith, *Science* **2012**, 338, 643.

[112] H. Chen, Z. Wei, H. He, X. Zheng, K. S. Wong, S. Yang, *Advanced Energy Materials* **2016**, 6, 1502087.

[113] S. Liu, W. Huang, P. Liao, N. Pootrakulchote, H. Li, J. Lu, J. Li, F. Huang, X. Shai, X. Zhao, Y. Shen, Y.-B. Cheng, M. Wang, *Journal of Materials Chemistry A* **2017**, 5, 22952.

[114] R. He, X. Huang, M. Chee, F. Hao, P. Dong, *Carbon Energy* **2019**, 1, 109.

[115] M. Hadadian, J.-H. Smått, J.-P. Correa-Baena, *Energy & Environmental Science* **2020**, 13, 1377.

[116] L. Fagiolari, F. Bella, *Energy & Environmental Science* **2019**, 12, 3437.

[117] E. H. Anaraki, A. Kermanpur, L. Steier, K. Domanski, T. Matsui, W. Tress, M. Saliba, A. Abate, M. Grätzel, A. Hagfeldt, J.-P. Correa-Baena, *Energy & Environmental Science* **2016**, 9, 3128.

[118] Y. Zhao, Q. Ye, Z. Chu, F. Gao, X. Zhang, J. You, *ENERGY & ENVIRONMENTAL MATERIALS* **2019**, 2, 93.

[119] F. Yang, J. Liu, X. Wang, K. Tanaka, K. Shinokita, Y. Miyauchi, A. Wakamiya, K. Matsuda, *ACS Applied Materials & Interfaces* **2019**, 11, 15680.

[120] S. Akin, *ACS Applied Materials & Interfaces* **2019**, 11, 39998.

[121] J. Liang, Z. Chen, G. Yang, H. Wang, F. Ye, C. Tao, G. Fang, *ACS Applied Materials & Interfaces* **2019**, 11, 23152.

[122] W. Yang, Y. Yao, C.-Q. Wu, *Journal of Applied Physics* **2015**, 117, 095502.

[123] C.-T. Lin, J. Lee, J. Kim, T. J. Macdonald, J. Ngiam, B. Xu, M. Daboczi, W. Xu, S. Pont, B. Park, H. Kang, J.-S. Kim, D. J. Payne, K. Lee, J. R. Durrant, M. A. McLachlan, *Advanced Functional Materials* **2020**, 30, 1906763.

[124] A. Bag, R. Radhakrishnan, R. Nekovei, R. Jeyakumar, *Solar Energy* **2020**, 196, 177.

[125] M. Rai, L. H. Wong, L. Etgar, *The Journal of Physical Chemistry Letters* **2020**, 11, 8189.

[126] T. Du, W. Xu, S. Xu, S. R. Ratnasingham, C.-T. Lin, J. Kim, J. Briscoe, M. A. McLachlan, J. R. Durrant, *Journal of Materials Chemistry C* **2020**, 8, 12648.

[127] J.-Y. Jeng, Y.-F. Chiang, M.-H. Lee, S.-R. Peng, T.-F. Guo, P. Chen, T.-C. Wen, *Advanced Materials* **2013**, 25, 3727.

[128] X. Liu, Y. Cheng, C. Liu, T. Zhang, N. Zhang, S. Zhang, J. Chen, Q. Xu, J. Ouyang, H. Gong, *Energy & Environmental Science* **2019**, 12, 1622.
[129] J. Tang, D. Jiao, L. Zhang, X. Zhang, X. Xu, C. Yao, J. Wu, Z. Lan, *Solar Energy* **2018**, 161, 100.
[130] D. Liu, Y. Li, J. Yuan, Q. Hong, G. Shi, D. Yuan, J. Wei, C. Huang, J. Tang, M.-K. Fung, *Journal of Materials Chemistry A* **2017**, 5, 5701.
[131] S. A. L. Weber, I. M. Hermes, S.-H. Turren-Cruz, C. Gort, V. W. Bergmann, L. Gilson, A. Hagfeldt, M. Graetzel, W. Tress, R. Berger, *Energy & Environmental Science* **2018**, 11, 2404.
[132] I. M. Dharmadasa, Y. Rahaq, A. E. Alam, *Journal of Materials Science: Materials in Electronics* **2019**, 30, 12851.
[133] D.-H. Kang, N.-G. Park, *Advanced Materials* **2019**, 31, 1805214.
[134] P. Calado, A. M. Telford, D. Bryant, X. Li, J. Nelson, B. C. O'Regan, P. R. F. Barnes, *Nature Communications* **2016**, 7, 13831.
[135] V. Gupta, G. Lucarelli, S. Castro-Hermosa, T. Brown, M. Ottavi, *Nanotechnology* **2020**, 31, 445201.
[136] A. Lewis, J. R. Troughton, B. Smith, J. McGettrick, T. Dunlop, F. De Rossi, A. Pockett, M. Spence, M. J. Carnie, T. M. Watson, C. Charbonneau, *Solar Energy Materials and Solar Cells* **2020**, 209, 110448.
[137] Y. Zou, R. J. Holmes, *Advanced Energy Materials* **2016**, 6, 1501994.
[138] Y. Jiang, Y. Feng, X. Sun, R. Qin, H. Ma, *Journal of Physics D: Applied Physics* **2019**, 52, 385501.
[139] F. Wu, B. Bahrami, K. Chen, S. Mabrouk, R. Pathak, Y. Tong, X. Li, T. Zhang, R. Jian, Q. Qiao, *ACS Applied Materials & Interfaces* **2018**, 10, 25604.
[140] G. A. Nemnes, C. Besleaga, A. G. Tomulescu, A. Palici, L. Pintilie, A. Manolescu, I. Pintilie, *Solar Energy* **2018**, 173, 976.
[141] W. Tress, N. Marinova, T. Moehl, S. M. Zakeeruddin, M. K. Nazeeruddin, M. Grätzel, *Energy & Environmental Science* **2015**, 8, 995.
[142] L. Cojocaru, S. Uchida, K. Tamaki, P. V. V. Jayaweera, S. Kaneko, J. Nakazaki, T. Kubo, H. Segawa, *Scientific Reports* **2017**, 7, 11790.
[143] L. Lin, L. Jiang, Y. Qiu, Y. Yu, *Superlattices and Microstructures* **2017**, 104, 167.
[144] K. Ke, K. K. Kondamareddy, F. Gao, X. Zhang, X. Yuan, *Energy Technology* **2019**, 7, 1900446.
[145] J. Zhou, Z. Ye, J. Hou, J. Wu, Y.-Z. Zheng, X. Tao, *Journal of Materials Chemistry A* **2018**, 6, 22626.
[146] Y. Li, S. Ye, W. Sun, W. Yan, Y. Li, Z. Bian, Z. Liu, S. Wang, C. Huang, *Journal of Materials Chemistry A* **2015**, 3, 18389.
[147] A. Mei, X. Li, L. Liu, Z. Ku, T. Liu, Y. Rong, M. Xu, M. Hu, J. Chen, Y. Yang, M. Grätzel, H. Han, *Science* **2014**, 345, 295.
[148] U. Nwankwo, S. Ngqoloda, A. C. Nkele, C. J. Arendse, K. I. Ozoemena, A. B. C. Ekwealor, R. Jose, M. Maaza, F. I. Ezema, *RSC Advances* **2020**, 10, 13139.
[149] J. Dagar, S. Castro-Hermosa, G. Lucarelli, A. Zampetti, F. Cacialli, T. M. Brown, *IEEE Journal of Photovoltaics* **2019**, 9, 1309.
[150] R. Taheri-Ledari, K. Valadi, A. Maleki, *Progress in Photovoltaics: Research and Applications* **2020**, 28, 956.
[151] W. Ke, G. Fang, J. Wan, H. Tao, Q. Liu, L. Xiong, P. Qin, J. Wang, H. Lei, G. Yang, M. Qin, X. Zhao, Y. Yan, *Nature Communications* **2015**, 6, 6700.
[152] D. Liu, J. Yang, T. L. Kelly, *Journal of the American Chemical Society* **2014**, 136, 17116.
[153] L. Huang, J. Xu, X. Sun, Y. Du, H. Cai, J. Ni, J. Li, Z. Hu, J. Zhang, *ACS Applied Materials & Interfaces* **2016**, 8, 9811.

[154] S. Agarwal, P. R. Nair, *Journal of Applied Physics* **2017**, 122, 163104.
[155] B. S. Kim, G. H. Moon, S. C. Park, J. Jang, Y. S. Kang, *Materials Letters* **2019**, 242, 191.
[156] J. Augustynski, B. Alexander, R. Solarska, *Metal Oxide Photoanodes for Water Splitting*, **2011**.
[157] C. Ros, T. Andreu, J. R. Morante, *Journal of Materials Chemistry A* **2020**, 8, 10625.
[158] C. Li, J. He, Y. Xiao, Y. Li, J.-J. Delaunay, *Energy & Environmental Science* **2020**, 13, 3269.
[159] B. H. R. Suryanto, Y. Wang, R. K. Hocking, W. Adamson, C. Zhao, *Nature Communications* **2019**, 10, 5599.
[160] A. A. Said, J. Xie, Q. Zhang, *Small* **2019**, 15, 1900854.
[161] W. Chen, Y. Shi, Y. Wang, X. Feng, A. B. Djurišić, H. Y. Woo, X. Guo, Z. He, *Nano Energy* **2020**, 68, 104363.
[162] Y. Luo, H. Yang, W. Li, Y. Qin, *ACS Omega* **2019**, 4, 21178.
[163] K. Mahmood, S. Sarwar, M. T. Mehran, *RSC Advances* **2017**, 7, 17044.
[164] T. Kim, J. Lim, S. Song, *Energies* **2020**, 13, 5572.
[165] G. D. Tainter, M. T. Hörantner, L. M. Pazos-Outón, R. D. Lamboll, H. Āboliņš, T. Leijtens, S. Mahesh, R. H. Friend, H. J. Snaith, H. J. Joyce, F. Deschler, *Joule* **2019**, 3, 1301.
[166] H. P. Pasanen, P. Vivo, L. Canil, H. Hempel, T. Unold, A. Abate, N. V. Tkachenko, *The Journal of Physical Chemistry Letters* **2020**, 11, 445.
[167] Z. Wang, X. Zhu, S. Zuo, M. Chen, C. Zhang, C. Wang, X. Ren, Z. Yang, Z. Liu, X. Xu, Q. Chang, S. Yang, F. Meng, Z. Liu, N. Yuan, J. Ding, S. Liu, D. Yang, *Advanced Functional Materials* **2020**, 30, 1908298.
[168] Q. Wali, N. K. Elumalai, Y. Iqbal, A. Uddin, R. Jose, *Renewable and Sustainable Energy Reviews* **2018**, 84, 89.
[169] R. Tagliaferro, D. Gentilini, S. Mastroianni, A. Zampetti, A. Gagliardi, T. M. Brown, A. Reale, A. Di Carlo, *RSC Advances* **2013**, 3, 20273.
[170] J. Kwon, M. J. Im, C. U. Kim, S. H. Won, S. B. Kang, S. H. Kang, I. T. Choi, H. K. Kim, I. H. Kim, J. H. Park, K. J. Choi, *Energy & Environmental Science* **2016**, 9, 3657.
[171] T. Ameri, G. Dennler, C. Lungenschmied, C. J. Brabec, *Energy & Environmental Science* **2009**, 2, 347.
[172] I. J. Park, J. H. Park, S. G. Ji, M.-A. Park, J. H. Jang, J. Y. Kim, *Joule* **2019**, 3, 807.
[173] M. Schnabel, H. Schulte-Huxel, M. Rienäcker, E. L. Warren, P. F. Ndione, B. Nemeth, T. R. Klein, M. F. A. M. van Hest, J. F. Geisz, R. Peibst, P. Stradins, A. C. Tamboli, *Sustainable Energy & Fuels* **2020**, 4, 549.
[174] B. Chen, S.-W. Baek, Y. Hou, E. Aydin, M. De Bastiani, B. Scheffel, A. Proppe, Z. Huang, M. Wei, Y.-K. Wang, E.-H. Jung, T. G. Allen, E. Van Kerschaver, F. P. García de Arquer, M. I. Saidaminov, S. Hoogland, S. De Wolf, E. H. Sargent, *Nature Communications* **2020**, 11, 1257.
[175] F. H. Alharbi, S. Kais, *Renewable and Sustainable Energy Reviews* **2015**, 43, 1073.
[176] R. S. Drago, *The Journal of Physical Chemistry* **1958**, 62, 353.
[177] M. I. Hossain, W. Qarony, S. Ma, L. Zeng, D. Knipp, Y. H. Tsang, *Nano-Micro Letters* **2019**, 11, 58.
[178] M. Jošt, L. Kegelmann, L. Korte, S. Albrecht, *Advanced Energy Materials* **2020**, n/a, 1904102.
[179] L. Mazzarella, Y.-H. Lin, S. Kirner, A. B. Morales-Vilches, L. Korte, S. Albrecht, E. Crossland, B. Stannowski, C. Case, H. J. Snaith, R. Schlatmann, *Advanced Energy Materials* **2019**, 9, 1803241.

[180] C. D. Bailie, M. G. Christoforo, J. P. Mailoa, A. R. Bowring, E. L. Unger, W. H. Nguyen, J. Burschka, N. Pellet, J. Z. Lee, M. Grätzel, R. Noufi, T. Buonassisi, A. Salleo, M. D. McGehee, *Energy & Environmental Science* **2015**, 8, 956.
[181] Q.-D. Dao, R. Tsuji, A. Fujii, M. Ozaki, *Organic Electronics* **2017**, 43, 229.
[182] T. Zhang, M. I. Dar, G. Li, F. Xu, N. Guo, M. Grätzel, Y. Zhao, *Science Advances* **2017**, 3, e1700841.
[183] R. Lin, K. Xiao, Z. Qin, Q. Han, C. Zhang, M. Wei, M. I. Saidaminov, Y. Gao, J. Xu, M. Xiao, A. Li, J. Zhu, E. H. Sargent, H. Tan, *Nature Energy* **2019**, 4, 864.
[184] F. Jiang, T. Liu, B. Luo, J. Tong, F. Qin, S. Xiong, Z. Li, Y. Zhou, *Journal of Materials Chemistry A* **2016**, 4, 1208.
[185] A. Rajagopal, Z. Yang, S. B. Jo, I. L. Braly, P.-W. Liang, H. W. Hillhouse, A. K. Y. Jen, *Advanced Materials* **2017**, 29, 1702140.
[186] M. Konstantakou, T. Stergiopoulos, *Journal of Materials Chemistry A* **2017**, 5, 11518.
[187] K. Galkowski, A. Surrente, M. Baranowski, B. Zhao, Z. Yang, A. Sadhanala, S. Mackowski, S. D. Stranks, P. Plochocka, *ACS Energy Letters* **2019**, 4, 615.
[188] R. Prasanna, T. Leijtens, A. Gold-Parker, B. Conings, A. Babayigit, H. Boyen, M. F. Toney, M. D. McGehee, presented at 2018 IEEE 7th World Conference on Photovoltaic Energy Conversion (WCPEC) (A Joint Conference of 45th IEEE PVSC, 28th PVSEC & 34th EU PVSEC), 10-15 June 2018, **2018**.
[189] C. Wang, Z. Song, C. Li, D. Zhao, Y. Yan, *Advanced Functional Materials* **2019**, 29, 1808801.
[190] A. F. Palmstrom, G. E. Eperon, T. Leijtens, R. Prasanna, S. N. Habisreutinger, W. Nemeth, E. A. Gaulding, S. P. Dunfield, M. Reese, S. Nanayakkara, T. Moot, J. Werner, J. Liu, B. To, S. T. Christensen, M. D. McGehee, M. F. A. M. van Hest, J. M. Luther, J. J. Berry, D. T. Moore, *Joule* **2019**, 3, 2193.
[191] J. Zheng, C. F. J. Lau, H. Mehrvarz, F.-J. Ma, Y. Jiang, X. Deng, A. Soeriyadi, J. Kim, M. Zhang, L. Hu, X. Cui, D. S. Lee, J. Bing, Y. Cho, C. Chen, M. A. Green, S. Huang, A. W. Y. Ho-Baillie, *Energy & Environmental Science* **2018**, 11, 2432.
[192] X. Zheng, A. Y. Alsalloum, Y. Hou, E. H. Sargent, O. M. Bakr, *Accounts of Materials Research* **2020**, 1, 63.
[193] D. P. McMeekin, S. Mahesh, N. K. Noel, M. T. Klug, J. Lim, J. H. Warby, J. M. Ball, L. M. Herz, M. B. Johnston, H. J. Snaith, *Joule* **2019**, 3, 387.
[194] M. De Bastiani, A. S. Subbiah, E. Aydin, F. H. Isikgor, T. G. Allen, S. De Wolf, *Materials Horizons* **2020**, 7, 2791.
[195] R. Liu, C. Liu, S. Fan, *Journal of Materials Chemistry A* **2017**, 5, 23078.
[196] X. Xu, S. Li, H. Zhang, Y. Shen, S. M. Zakeeruddin, M. Graetzel, Y.-B. Cheng, M. Wang, *ACS Nano* **2015**, 9, 1782.
[197] T. Miyasaka, T. N. Murakami, *Applied Physics Letters* **2004**, 85, 3932.
[198] T. Famprikis, P. Canepa, J. A. Dawson, M. S. Islam, C. Masquelier, *Nature Materials* **2019**, 18, 1278.
[199] B. Pal, A. Yasin, R. Kunwar, S. Yang, M. M. Yusoff, R. Jose, *Industrial & Engineering Chemistry Research* **2019**, 58, 654.
[200] S. Xia, X. Wu, Z. Zhang, Y. Cui, W. Liu, *Chem* **2019**, 5, 753.
[201] A. Varzi, R. Raccichini, S. Passerini, B. Scrosati, *Journal of Materials Chemistry A* **2016**, 4, 17251.
[202] A. P. Cohn, W. R. Erwin, K. Share, L. Oakes, A. S. Westover, R. E. Carter, R. Bardhan, C. L. Pint, *Nano Letters* **2015**, 15, 2727.
[203] F. Zhou, Z. Ren, Y. Zhao, X. Shen, A. Wang, Y. Y. Li, C. Surya, Y. Chai, *ACS Nano* **2016**, 10, 5900.
[204] K. Gao, D. Ti, Z. Zhang, *Sustainable Energy & Fuels* **2019**, 3, 1937.

[205] J. Xu, Z. Ku, Y. Zhang, D. Chao, H. J. Fan, *Advanced Materials Technologies* **2016**, 1, 1600074.
[206] J. Ding, W. Hu, E. Paek, D. Mitlin, *Chemical Reviews* **2018**, 118, 6457.
[207] G. Zhu, L. Ma, H. Lin, P. Zhao, L. Wang, Y. Hu, R. Chen, T. Chen, Y. Wang, Z. Tie, Z. Jin, *Nano Research* **2019**, 12, 1713.
[208] L. Dong, W. Yang, W. Yang, Y. Li, W. Wu, G. Wang, *Journal of Materials Chemistry A* **2019**, 7, 13810.
[209] Q. Li, A. Balilonda, A. Ali, R. Jose, F. Zabihi, S. Yang, S. Ramakrishna, M. Zhu, *Solar RRL* **2020**, 4, 2000269.
[210] Q. Wali, F. J. Iftikhar, N. K. Elumalai, Y. Iqbal, S. Yousaf, S. Iqbal, R. Jose, *Current Applied Physics* **2020**, 20, 720.
[211] D. Yang, R. Yang, S. Priya, S. Liu, *Angewandte Chemie International Edition* **2019**, 58, 4466.
[212] B. Susrutha, L. Giribabu, S. P. Singh, *Chemical Communications* **2015**, 51, 14696.
[213] W. Zi, Z. Jin, S. Liu, B. Xu, *Journal of Energy Chemistry* **2018**, 27, 971.
[214] L. Hou, Y. Wang, X. Liu, J. Wang, L. Wang, X. Li, G. Fu, S. Yang, *Journal of Materials Chemistry C* **2018**, 6, 8770.
[215] J. Chung, S. S. Shin, K. Hwang, G. Kim, K. W. Kim, D. S. Lee, W. Kim, B. S. Ma, Y.-K. Kim, T.-S. Kim, J. Seo, *Energy & Environmental Science* **2020**, 13, 4854.
[216] Y. Y. Kim, T.-Y. Yang, R. Suhonen, A. Kemppainen, K. Hwang, N. J. Jeon, J. Seo, *Nature Communications* **2020**, 11, 5146.
[217] T. Bu, J. Li, F. Zheng, W. Chen, X. Wen, Z. Ku, Y. Peng, J. Zhong, Y.-B. Cheng, F. Huang, *Nature Communications* **2018**, 9, 4609.
[218] X. Yu, X. Yan, J. Xiao, Z. Ku, J. Zhong, W. Li, F. Huang, Y. Peng, Y.-B. Cheng, *The Journal of Chemical Physics* **2020**, 153, 014706.
[219] J. Dagar, S. Castro-Hermosa, M. Gasbarri, A. L. Palma, L. Cina, F. Matteocci, E. Calabrò, A. Di Carlo, T. M. Brown, *Nano Research* **2018**, 11, 2669.
[220] S. H. Aung, L. Zhao, K. Nonomura, T. Z. Oo, S. M. Zakeeruddin, N. Vlachopoulos, T. Sloboda, S. Svanström, U. B. Cappel, A. Hagfeldt, M. Grätzel, *Journal of Materials Chemistry A* **2019**, 7, 10729.
[221] S. Castro-Hermosa, G. Lucarelli, M. Top, M. Fahland, J. Fahlteich, T. M. Brown, *Cell Reports Physical Science* **2020**, 1, 100045.
[222] B. Feleki, G. Bex, R. Andriessen, Y. Galagan, F. Di Giacomo, *Materials Today Communications* **2017**, 13, 232.
[223] A. E. Ostfeld, A. C. Arias, *Flexible and Printed Electronics* **2017**, 2, 013001.
[224] T. Tamai, M. Watanabe, Y. Kobayashi, Y. Nakahara, S. Yajima, *RSC Advances* **2017**, 7, 33155.
[225] A. R. Kolahchi, A. Ajji, P. J. Carreau, *AIP Conference Proceedings* **2015**, 1664, 030001.
[226] L. Románszki, S. Klébert, K. Héberger, *ACS Omega* **2020**, 5, 3670.
[227] L. Gao, L. Chao, M. Hou, J. Liang, Y. Chen, H.-D. Yu, W. Huang, *npj Flexible Electronics* **2019**, 3, 4.
[228] F. Yang, J. Liu, H. E. Lim, Y. Ishikura, K. Shinokita, Y. Miyauchi, A. Wakamiya, Y. Murata, K. Matsuda, *The Journal of Physical Chemistry C* **2018**, 122, 17088.
[229] E. Calabrò, F. Matteocci, A. L. Palma, L. Vesce, B. Taheri, L. Carlini, I. Pis, S. Nappini, J. Dagar, C. Battocchio, T. M. Brown, A. Di Carlo, *Solar Energy Materials and Solar Cells* **2018**, 185, 136.
[230] M. J. Carnie, C. Charbonneau, M. L. Davies, J. Troughton, T. M. Watson, K. Wojciechowski, H. Snaith, D. A. Worsley, *Chemical Communications* **2013**, 49, 7893.
[231] S. Sánchez, M. Vallés-Pelarda, J.-A. Alberola-Borràs, R. Vidal, J. J. Jerónimo-Rendón, M. Saliba, P. P. Boix, I. Mora-Seró, *Materials Today* **2019**, 31, 39.
[232] H. Chen, S. Yang, *Advanced Materials* **2017**, 29, 1603994.

[233] F. Brunetti, A. Operamolla, S. Castro-Hermosa, G. Lucarelli, V. Manca, G. M. Farinola, T. M. Brown, *Advanced Functional Materials* **2019**, 29, 1806798.
[234] A. Balilonda, Q. Li, X. Bian, R. Jose, S. Ramakrishna, M. Zhu, F. Zabihi, S. Yang, *Chemical Engineering Journal* **2021**, 410, 128384.
[235] D. Ding, H. Li, H. Yao, L. Liu, B. Tian, C. Su, Y. Wang, Y. Shi, *Journal of Materials Chemistry C* **2019**, 7, 9496.
[236] M. Lee, Y. Ko, Y. Jun, *Journal of Materials Chemistry A* **2015**, 3, 19310.
[237] M. Tebyetekerwa, I. Marriam, Z. Xu, S. Yang, H. Zhang, F. Zabihi, R. Jose, S. Peng, M. Zhu, S. Ramakrishna, *Energy & Environmental Science* **2019**, DOI: 10.1039/C8EE02607F.
[238] V. Hardev, Ubiquitous Energy Certifies New World Record Performance of Transparent Solar Cell, https://www.businesswire.com/news/home/20190320005019/en/Ubiquitous-Energy-Certifies-New-World-Record-Performance, accessed.
[239] K. Pickerel, 9.8% efficient "Transparent" Solar Glass Product ClearView Power Finds Global Glass Manufacturer, https://www.solarpowerworldonline.com/2019/05/9-8-efficient-transparent-solar-glass-product-clearview-power-finds-global-glass-manufacturer/, accessed.
[240] V. Rosenberg, Major Milestone - CPV IGU Prototype Increases Power Output by 33%, http://www.clearvuepv.com/wp-content/uploads/austocks/cpv/2020_05_07_CPV_5e1fe9664b93d6973659f446d560b2c5.pdf, accessed.
[241] V. Rosenberg, ClearVue signs Letter of Intent with Jinmao Green Building Technology http://www.clearvuepv.com/wp-content/uploads/austocks/cpv/2020_04_23_CPV_55e71dd53d878ebca8fac82eed59f798.pdf, accessed.
[242] L. Yuan, Z. Wang, R. Duan, P. Huang, K. Zhang, Q. Chen, N. K. Allam, Y. Zhou, B. Song, Y. Li, *Journal of Materials Chemistry A* **2018**, 6, 19696.
[243] C. Momblona, O. Malinkiewicz, C. Roldán-Carmona, A. Soriano, L. Gil-Escrig, E. Bandiello, M. Scheepers, E. Edri, H. J. Bolink, *APL Materials* **2014**, 2, 081504.
[244] J. Wu, J. Luke, H. K. H. Lee, P. Shakya Tuladhar, H. Cha, S.-Y. Jang, W. C. Tsoi, M. Heeney, H. Kang, K. Lee, T. Kirchartz, J.-S. Kim, J. R. Durrant, *Nature Communications* **2019**, 10, 5159.
[245] G. E. Eperon, V. M. Burlakov, A. Goriely, H. J. Snaith, *ACS Nano* **2014**, 8, 591.
[246] A. Fakharuddin, P. S. Archana, Z. Kalidin, M. M. Yusoff, R. Jose, *RSC Advances* **2013**, 3, 2683.
[247] C. O. Ramírez Quiroz, C. Bronnbauer, I. Levchuk, Y. Hou, C. J. Brabec, K. Forberich, *ACS Nano* **2016**, 10, 5104.
[248] T. Kirchartz, S. Korgitzsch, J. Hüpkes, C. O. R. Quiroz, C. J. Brabec, *ACS Energy Letters* **2018**, 3, 1861.
[249] C.-Y. Chen, J.-H. Chang, K.-M. Chiang, H.-L. Lin, S.-Y. Hsiao, H.-W. Lin, *Advanced Functional Materials* **2015**, 25, 7064.
[250] F. Di Giacomo, V. Zardetto, G. Lucarelli, L. Cinà, A. Di Carlo, M. Creatore, T. M. Brown, *Nano Energy* **2016**, 30, 460.
[251] I. Mathews, S. N. Kantareddy, T. Buonassisi, I. M. Peters, *Joule* **2019**, 3, 1415.
[252] J. Dagar, S. Castro-Hermosa, G. Lucarelli, F. Cacialli, T. M. Brown, *Nano Energy* **2018**, 49, 290.
[253] H. K. H. Lee, J. Barbé, S. M. P. Meroni, T. Du, C.-T. Lin, A. Pockett, J. Troughton, S. M. Jain, F. De Rossi, J. Baker, M. J. Carnie, M. A. McLachlan, T. M. Watson, J. R. Durrant, W. C. Tsoi, *Solar RRL* **2019**, 3, 1800207.

[254] M. Li, C. Zhao, Z.-K. Wang, C.-C. Zhang, H. K. H. Lee, A. Pockett, J. Barbé, W. C. Tsoi, Y.-G. Yang, M. J. Carnie, X.-Y. Gao, W.-X. Yang, J. R. Durrant, L.-S. Liao, S. M. Jain, *Advanced Energy Materials* **2018**, 8, 1801509.
[255] M. H. Ann, J. Kim, M. Kim, G. Alosaimi, D. Kim, N. Y. Ha, J. Seidel, N. Park, J. S. Yun, J. H. Kim, *Nano Energy* **2020**, 68, 104321.
[256] J. Kim, J. H. Jang, E. Choi, S. J. Shin, J.-H. Kim, G. G. Jeon, M. Lee, J. Seidel, J. H. Kim, J. S. Yun, N. Park, *Cell Reports Physical Science* **2020**, 1, 100273.
[257] M.-J. Wu, C.-C. Kuo, L.-S. Jhuang, P.-H. Chen, Y.-F. Lai, F.-C. Chen, *Advanced Energy Materials* **2019**, 9, 1901863.
[258] R. Cheng, C.-C. Chung, H. Zhang, F. Liu, W.-T. Wang, Z. Zhou, S. Wang, A. B. Djurišić, S.-P. Feng, *Advanced Energy Materials* **2019**, 9, 1901980.
[259] Y. Peng, T. N. Huq, J. Mei, L. Portilla, R. A. Jagt, L. G. Occhipinti, J. L. MacManus-Driscoll, R. L. Z. Hoye, V. Pecunia, *Advanced Energy Materials* **2020**, n/a, 2002761.
[260] I. Mathews, S. N. R. Kantareddy, S. Sun, M. Layurova, J. Thapa, J.-P. Correa-Baena, R. Bhattacharyya, T. Buonassisi, S. Sarma, I. M. Peters, *Advanced Functional Materials* **2019**, 29, 1904072.
[261] U. S. E. I. Administration, DOI: https://www.eia.gov/outlooks/aeo/pdf/electricity_generation.pdf, 2020.
[262] M. Cai, Y. Wu, H. Chen, X. Yang, Y. Qiang, L. Han, in *Adv Sci (Weinh)*, Vol. 4, 2017, 1600269.
[263] Z. Li, Y. Zhao, X. Wang, Y. Sun, Z. Zhao, Y. Li, H. Zhou, Q. Chen, *Joule* **2018**, 2, 1559.
[264] M. Powalla, S. Paetel, D. Hariskos, R. Wuerz, F. Kessler, P. Lechner, W. Wischmann, T. M. Friedlmeier, *Engineering* **2017**, 3, 445.
[265] S. U. Nanayakkara, K. Horowitz, A. Kanevce, M. Woodhouse, P. Basore, *Progress in Photovoltaics: Research and Applications* **2017**, 25, 271.
[266] M. Cai, Y. Wu, H. Chen, X. Yang, Y. Qiang, L. Han, *Advanced Science* **2017**, 4, 1600269.
[267] Z. Song, C. L. McElvany, A. B. Phillips, I. Celik, P. W. Krantz, S. C. Watthage, G. K. Liyanage, D. Apul, M. J. Heben, *Energy & Environmental Science* **2017**, 10, 1297.
[268] A. Louwen, W. G. J. H. M. van Sark, A. P. C. Faaij, R. E. I. Schropp, *Nature Communications* **2016**, 7, 13728.
[269] M. Jeong, I. W. Choi, E. M. Go, Y. Cho, M. Kim, B. Lee, S. Jeong, Y. Jo, H. W. Choi, J. Lee, J.-H. Bae, S. K. Kwak, D. S. Kim, C. Yang, *Science* **2020**, 369, 1615.
[270] W. Sha, X. Ren, L. Chen, W. Choy, *Applied Physics Letters* **2015**, 106, 221104.
[271] N. L. Chang, A. W. Y. Ho-Baillie, D. Vak, M. Gao, M. A. Green, R. J. Egan, *Solar Energy Materials and Solar Cells* **2018**, 174, 314.
[272] Z. Song, A. B. Phillips, I. Celik, G. K. Liyanage, D. Zhao, D. Apul, Y. Yan, M. J. Heben, presented at 2018 IEEE 7th World Conference on Photovoltaic Energy Conversion (WCPEC) (A Joint Conference of 45th IEEE PVSC, 28th PVSEC & 34th EU PVSEC), 10-15 June 2018, **2018**.
[273] W. H. Balmain, *The London, Edinburgh, and Dublin Philosophical Magazine and Journal of Science* **1842**, 21, 270.
[274] J. Yin, J. Li, Y. Hang, J. Yu, G. Tai, X. Li, Z. Zhang, W. Guo, *Small* **2016**, 12, 2942.
[275] Q. Wali, F. J. Iftikhar, M. E. Khan, A. Ullah, Y. Iqbal, R. Jose, *Organic Electronics* **2020**, 78, 105590.
[276] X. Zhu, D. Yang, R. Yang, B. Yang, Z. Yang, X. Ren, J. Zhang, J. Niu, J. Feng, S. Liu, *Nanoscale* **2017**, 9, 12316.
[277] C. Wu, K. Wang, X. Feng, Y. Jiang, D. Yang, Y. Hou, Y. Yan, M. Sanghadasa, S. Priya, *Nano Letters* **2019**, 19, 1251.

[278] A. Mei, Y. Sheng, Y. Ming, Y. Hu, Y. Rong, W. Zhang, S. Luo, G. Na, C. Tian, X. Hou, Y. Xiong, Z. Zhang, S. Liu, S. Uchida, T.-W. Kim, Y. Yuan, L. Zhang, Y. Zhou, H. Han, *Joule* **2020**, 4, 2646.
[279] M. H. Futscher, J. M. Lee, L. McGovern, L. A. Muscarella, T. Wang, M. I. Haider, A. Fakharuddin, L. Schmidt-Mende, B. Ehrler, *Materials Horizons* **2019**, 6, 1497.
[280] B. Rivkin, P. Fassl, Q. Sun, A. D. Taylor, Z. Chen, Y. Vaynzof, *ACS Omega* **2018**, 3, 10042.
[281] M. De Bastiani, G. Dell'Erba, M. Gandini, V. D'Innocenzo, S. Neutzner, A. R. S. Kandada, G. Grancini, M. Binda, M. Prato, J. M. Ball, M. Caironi, A. Petrozza, *Advanced Energy Materials* **2016**, 6, 1501453.
[282] J.-W. Lee, S.-G. Kim, J.-M. Yang, Y. Yang, N.-G. Park, *APL Materials* **2019**, 7, 041111.
[283] Y. Yuan, J. Huang, *Accounts of Chemical Research* **2016**, 49, 286.
[284] S. Meloni, T. Moehl, W. Tress, M. Franckevičius, M. Saliba, Y. H. Lee, P. Gao, M. K. Nazeeruddin, S. M. Zakeeruddin, U. Rothlisberger, M. Graetzel, *Nature Communications* **2016**, 7, 10334.
[285] K. Domanski, B. Roose, T. Matsui, M. Saliba, S.-H. Turren-Cruz, J.-P. Correa-Baena, C. R. Carmona, G. Richardson, J. M. Foster, F. De Angelis, J. M. Ball, A. Petrozza, N. Mine, M. K. Nazeeruddin, W. Tress, M. Grätzel, U. Steiner, A. Hagfeldt, A. Abate, *Energy & Environmental Science* **2017**, 10, 604.
[286] J. M. Frost, K. T. Butler, F. Brivio, C. H. Hendon, M. van Schilfgaarde, A. Walsh, *Nano Letters* **2014**, 14, 2584.
[287] H. Zhang, D. Li, J. Cheng, F. Lin, J. Mao, A. K. Y. Jen, M. Grätzel, W. C. H. Choy, *Journal of Materials Chemistry A* **2017**, 5, 3599.
[288] C. Eames, J. M. Frost, P. R. F. Barnes, B. C. O'Regan, A. Walsh, M. S. Islam, *Nature Communications* **2015**, 6, 7497.
[289] J. Haruyama, K. Sodeyama, L. Han, Y. Tateyama, *Journal of the American Chemical Society* **2015**, 137, 10048.
[290] S. Guo, X. Sun, C. Ding, R. Huang, M. Tan, L. Zhang, Q. Luo, F. Li, J. Jin, C.-Q. Ma, *Energy Technology* **2020**, n/a.
[291] Y. Kato, L. K. Ono, M. V. Lee, S. Wang, S. R. Raga, Y. Qi, *Advanced Materials Interfaces* **2015**, 2, 1500195.
[292] H. Zhang, Y. Lv, J. Wang, H. Ma, Z. Sun, W. Huang, *ACS Applied Materials & Interfaces* **2019**, 11, 6022.
[293] S. Kim, S. Bae, S.-W. Lee, K. Cho, K. D. Lee, H. Kim, S. Park, G. Kwon, S.-W. Ahn, H.-M. Lee, Y. Kang, H.-S. Lee, D. Kim, *Scientific Reports* **2017**, 7, 1200.
[294] S. J. Yoon, S. Draguta, J. S. Manser, O. Sharia, W. F. Schneider, M. Kuno, P. V. Kamat, *ACS Energy Letters* **2016**, 1, 290.
[295] S. J. Yoon, M. Kuno, P. V. Kamat, *ACS Energy Letters* **2017**, 2, 1507.
[296] M. C. Brennan, S. Draguta, P. V. Kamat, M. Kuno, *ACS Energy Letters* **2018**, 3, 204.
[297] S. Guarnera, A. Abate, W. Zhang, J. M. Foster, G. Richardson, A. Petrozza, H. J. Snaith, *The Journal of Physical Chemistry Letters* **2015**, 6, 432.
[298] A. F. Gualdrón-Reyes, S. J. Yoon, E. M. Barea, S. Agouram, V. Muñoz-Sanjosé, Á. M. Meléndez, M. E. Niño-Gómez, I. Mora-Seró, *ACS Energy Letters* **2019**, 4, 54.
[299] A. F. Gualdrón-Reyes, S. J. Yoon, I. Mora-Seró, *Current Opinion in Electrochemistry* **2018**, 11, 84.
[300] K. O. Brinkmann, J. Zhao, N. Pourdavoud, T. Becker, T. Hu, S. Olthof, K. Meerholz, L. Hoffmann, T. Gahlmann, R. Heiderhoff, M. F. Oszajca, N. A. Luechinger, D. Rogalla, Y. Chen, B. Cheng, T. Riedl, *Nature Communications* **2017**, 8, 13938.
[301] H. Back, G. Kim, J. Kim, J. Kong, T. K. Kim, H. Kang, H. Kim, J. Lee, S. Lee, K. Lee, *Energy & Environmental Science* **2016**, 9, 1258.

[302] J. You, L. Meng, T.-B. Song, T.-F. Guo, Y. Yang, W.-H. Chang, Z. Hong, H. Chen, H. Zhou, Q. Chen, Y. Liu, N. De Marco, Y. Yang, *Nature Nanotechnology* **2015**, 11, 75.
[303] Z. Li, M. Yang, J.-S. Park, S.-H. Wei, J. J. Berry, K. Zhu, *Chemistry of Materials* **2016**, 28, 284.
[304] Y. Fan, H. Meng, L. Wang, S. Pang, *Solar RRL* **2019**, 3, 1900215.
[305] A. A. Zhumekenov, M. I. Saidaminov, M. A. Haque, E. Alarousu, S. P. Sarmah, B. Murali, I. Dursun, X.-H. Miao, A. L. Abdelhady, T. Wu, O. F. Mohammed, O. M. Bakr, *ACS Energy Letters* **2016**, 1, 32.
[306] C. C. Stoumpos, C. D. Malliakas, M. G. Kanatzidis, *Inorganic Chemistry* **2013**, 52, 9019.
[307] N. Pellet, P. Gao, G. Gregori, T.-Y. Yang, M. K. Nazeeruddin, J. Maier, M. Grätzel, *Angewandte Chemie International Edition* **2014**, 53, 3151.
[308] N. J. Jeon, J. H. Noh, W. S. Yang, Y. C. Kim, S. Ryu, J. Seo, S. I. Seok, *Nature* **2015**, 517, 476.
[309] J. Cho, P. V. Kamat, *Chemistry of Materials* **2020**, 32, 6206.
[310] D. Di Girolamo, N. Phung, F. U. Kosasih, F. Di Giacomo, F. Matteocci, J. A. Smith, M. A. Flatken, H. Köbler, S. H. Turren Cruz, A. Mattoni, L. Cinà, B. Rech, A. Latini, G. Divitini, C. Ducati, A. Di Carlo, D. Dini, A. Abate, *Advanced Energy Materials* **2020**, 10, 2000310.
[311] D. J. Kubicki, M. Saski, S. MacPherson, K. Gałkowski, J. Lewiński, D. Prochowicz, J. J. Titman, S. D. Stranks, *Chemistry of Materials* **2020**, 32, 8129.
[312] S. Dastidar, D. A. Egger, L. Z. Tan, S. B. Cromer, A. D. Dillon, S. Liu, L. Kronik, A. M. Rappe, A. T. Fafarman, *Nano Letters* **2016**, 16, 3563.
[313] N. Rolston, K. A. Bush, A. D. Printz, A. Gold-Parker, Y. Ding, M. F. Toney, M. D. McGehee, R. H. Dauskardt, *Advanced Energy Materials* **2018**, 8, 1802139.
[314] C. Zhu, X. Niu, Y. Fu, N. Li, C. Hu, Y. Chen, X. He, G. Na, P. Liu, H. Zai, Y. Ge, Y. Lu, X. Ke, Y. Bai, S. Yang, P. Chen, Y. Li, M. Sui, L. Zhang, H. Zhou, Q. Chen, *Nature Communications* **2019**, 10, 815.
[315] J. Zhao, Y. Deng, H. Wei, X. Zheng, Z. Yu, Y. Shao, J. E. Shield, J. Huang, *Science Advances* **2017**, 3, eaao5616.
[316] C. Ma, D. Shen, M.-F. Lo, C.-S. Lee, *Angewandte Chemie International Edition* **2018**, 57, 9941.
[317] Z. Ahmad, M. A. Najeeb, R. A. Shakoor, A. Alashraf, S. A. Al-Muhtaseb, A. Soliman, M. K. Nazeeruddin, *Scientific Reports* **2017**, 7, 15406.
[318] X. Xiao, J. Dai, Y. Fang, J. Zhao, X. Zheng, S. Tang, P. N. Rudd, X. C. Zeng, J. Huang, *ACS Energy Letters* **2018**, 3, 684.
[319] Y. Gao, Y. Wu, Y. Liu, M. Lu, L. Yang, Y. Wang, W. W. Yu, X. Bai, Y. Zhang, Q. Dai, *Nanoscale Horizons* **2020**, 5, 1574.
[320] T. Wang, Z. Cheng, Y. Zhou, H. Liu, W. Shen, *Journal of Materials Chemistry A* **2019**, 7, 21730.
[321] G. Liu, H. Zheng, H. Xu, L. Zhang, X. Xu, S. Xu, X. Pan, *Nano Energy* **2020**, 73, 104753.
[322] J. Kim, A. Ho-Baillie, S. Huang, *Solar RRL* **2019**, 3, 1800302.
[323] H. Lu, A. Krishna, S. M. Zakeeruddin, M. Grätzel, A. Hagfeldt, *iScience* **2020**, 23, 101359.
[324] L. Zhang, P. H. L. Sit, *The Journal of Physical Chemistry C* **2015**, 119, 22370.
[325] L. Zhang, P. H. L. Sit, *Journal of Materials Chemistry A* **2019**, 7, 2135.
[326] E. Fabbri, A. Habereder, K. Waltar, R. Kötz, T. J. Schmidt, *Catalysis Science & Technology* **2014**, 4, 3800.
[327] J. Chen, A. Selloni, *The Journal of Physical Chemistry Letters* **2012**, 3, 2808.

[328] M. García-Mota, M. Bajdich, V. Viswanathan, A. Vojvodic, A. T. Bell, J. K. Nørskov, *The Journal of Physical Chemistry C* **2012**, 116, 21077.
[329] G. E. Eperon, G. M. Paternò, R. J. Sutton, A. Zampetti, A. A. Haghighirad, F. Cacialli, H. J. Snaith, *Journal of Materials Chemistry A* **2015**, 3, 19688.
[330] S. Xiao, K. Zhang, S. Zheng, S. Yang, *Nanoscale Horizons* **2020**, 5, 1147.
[331] N. Adhikari, A. Dubey, E. A. Gaml, B. Vaagensmith, K. M. Reza, S. A. A. Mabrouk, S. Gu, J. Zai, X. Qian, Q. Qiao, *Nanoscale* **2016**, 8, 2693.
[332] Y. Rong, X. Hou, Y. Hu, A. Mei, L. Liu, P. Wang, H. Han, *Nature Communications* **2017**, 8, 14555.
[333] X. Gong, M. Li, X.-B. Shi, H. Ma, Z.-K. Wang, L.-S. Liao, *Advanced Functional Materials* **2015**, 25, 6671.
[334] C. Aranda, A. Guerrero, J. Bisquert, *ChemPhysChem* **2019**, 20, 2587.
[335] Y. Shao, Y. Fang, T. Li, Q. Wang, Q. Dong, Y. Deng, Y. Yuan, H. Wei, M. Wang, A. Gruverman, J. Shield, J. Huang, *Energy & Environmental Science* **2016**, 9, 1752.
[336] M. K. Gangishetty, R. W. J. Scott, T. L. Kelly, *Nanoscale* **2016**, 8, 6300.
[337] L. Contreras-Bernal, C. Aranda, M. Valles-Pelarda, T. T. Ngo, S. Ramos-Terrón, J. J. Gallardo, J. Navas, A. Guerrero, I. Mora-Seró, J. Idígoras, J. A. Anta, *The Journal of Physical Chemistry C* **2018**, 122, 5341.
[338] M. E. Kayesh, K. Matsuishi, R. Kaneko, S. Kazaoui, J.-J. Lee, T. Noda, A. Islam, *ACS Energy Letters* **2019**, 4, 278.
[339] D. H. Cao, C. C. Stoumpos, O. K. Farha, J. T. Hupp, M. G. Kanatzidis, *Journal of the American Chemical Society* **2015**, 137, 7843.
[340] J. Rodríguez-Romero, J. Sanchez-Diaz, C. Echeverría-Arrondo, S. Masi, D. Esparza, E. M. Barea, I. Mora-Seró, *ACS Energy Letters* **2020**, 5, 1013.
[341] R. Arai, M. Yoshizawa-Fujita, Y. Takeoka, M. Rikukawa, *CrystEngComm* **2019**, 21, 4529.
[342] A. Z. Chen, M. Shiu, J. H. Ma, M. R. Alpert, D. Zhang, B. J. Foley, D.-M. Smilgies, S.-H. Lee, J. J. Choi, *Nature Communications* **2018**, 9, 1336.
[343] L. Yan, J. Hu, Z. Guo, H. Chen, M. F. Toney, A. M. Moran, W. You, *ACS Applied Materials & Interfaces* **2018**, 10, 33187.
[344] H. Tsai, W. Nie, J.-C. Blancon, C. C. Stoumpos, R. Asadpour, B. Harutyunyan, A. J. Neukirch, R. Verduzco, J. J. Crochet, S. Tretiak, L. Pedesseau, J. Even, M. A. Alam, G. Gupta, J. Lou, P. M. Ajayan, M. J. Bedzyk, M. G. Kanatzidis, A. D. Mohite, *Nature* **2016**, 536, 312.
[345] C. Li, Y. Pan, J. Hu, S. Qiu, C. Zhang, Y. Yang, S. Chen, X. Liu, C. J. Brabec, M. K. Nazeeruddin, Y. Mai, F. Guo, *ACS Energy Letters* **2020**, 5, 1386.
[346] T. Liu, Y. Jiang, M. Qin, J. Liu, L. Sun, F. Qin, L. Hu, S. Xiong, X. Jiang, F. Jiang, P. Peng, S. Jin, X. Lu, Y. Zhou, *Nature Communications* **2019**, 10, 878.
[347] X. Zhang, G. Wu, S. Yang, W. Fu, Z. Zhang, C. Chen, W. Liu, J. Yan, W. Yang, H. Chen, *Small* **2017**, 13, 1700611.
[348] T. Zhou, H. Lai, T. Liu, D. Lu, X. Wan, X. Zhang, Y. Liu, Y. Chen, *Advanced Materials* **2019**, 31, 1901242.
[349] G. Liu, H. Zheng, X. Xu, S. Xu, X. Zhang, X. Pan, S. Dai, *Advanced Functional Materials* **2019**, 29, 1807565.
[350] E. V. Péan, C. S. De Castro, S. Dimitrov, F. De Rossi, S. Meroni, J. Baker, T. Watson, M. L. Davies, *Advanced Functional Materials* **2020**, 30, 1909839.
[351] N. A. Manshor, Q. Wali, K. K. Wong, S. K. Muzakir, A. Fakharuddin, L. Schmidt-Mende, R. Jose, *Physical Chemistry Chemical Physics* **2016**, 18, 21629.
[352] H. Zheng, X. Xu, S. Xu, G. Liu, S. Chen, X. Zhang, T. Chen, X. Pan, *Journal of Materials Chemistry C* **2019**, 7, 4441.

[353] L. Zuo, H. Guo, D. W. deQuilettes, S. Jariwala, N. De Marco, S. Dong, R. DeBlock, D. S. Ginger, B. Dunn, M. Wang, Y. Yang, *Science Advances* **2017**, 3, e1700106.
[354] A. Fakharuddin, M. Seybold, A. Agresti, S. Pescetelli, F. Matteocci, M. I. Haider, S. T. Birkhold, H. Hu, R. Giridharagopal, M. Sultan, I. Mora-Seró, A. Di Carlo, L. Schmidt-Mende, *ACS Applied Materials & Interfaces* **2018**, 10, 42542.
[355] S. Ghosh, R. Singh, A. S. Subbiah, P. P. Boix, I. M. Seró, S. K. Sarkar, *Applied Physics Letters* **2020**, 116, 113502.
[356] B. McKenna, J. R. Troughton, T. M. Watson, R. C. Evans, *RSC Advances* **2017**, 7, 32942.
[357] S. Castro-Hermosa, M. Top, J. Dagar, J. Fahlteich, T. M. Brown, *Advanced Electronic Materials* **2019**, 5, 1800978.
[358] S. Cros, R. de Bettignies, S. Berson, S. Bailly, P. Maisse, N. Lemaitre, S. Guillerez, *Solar Energy Materials and Solar Cells* **2011**, 95, S65.
[359] F. Corsini, G. Griffini, *Journal of Physics: Energy* **2020**, 2, 031002.
[360] S. Zhang, Z. Liu, W. Zhang, Z. Jiang, W. Chen, R. Chen, Y. Huang, Z. Yang, Y. Zhang, L. Han, W. Chen, *Advanced Energy Materials* **2020**, 10, 2001610.
[361] S. N. Habisreutinger, D. P. McMeekin, H. J. Snaith, R. J. Nicholas, *APL Materials* **2016**, 4, 091503.
[362] M. Bonomo, B. Taheri, L. Bonandini, S. Castro-Hermosa, T. M. Brown, M. Zanetti, A. Menozzi, C. Barolo, F. Brunetti, *ACS Applied Materials & Interfaces* **2020**, 12, 54862.
[363] Y. Han, S. Meyer, Y. Dkhissi, K. Weber, J. M. Pringle, U. Bach, L. Spiccia, Y.-B. Cheng, *Journal of Materials Chemistry A* **2015**, 3, 8139.
[364] S. Ma, Y. Bai, H. Wang, H. Zai, J. Wu, L. Li, S. Xiang, N. Liu, L. Liu, C. Zhu, G. Liu, X. Niu, H. Chen, H. Zhou, Y. Li, Q. Chen, *Advanced Energy Materials* **2020**, 10, 1902472.
[365] B. Li, M. Wang, R. Subair, G. Cao, J. Tian, *The Journal of Physical Chemistry C* **2018**, 122, 25260.
[366] R. Cheacharoen, C. C. Boyd, G. F. Burkhard, T. Leijtens, J. A. Raiford, K. A. Bush, S. F. Bent, M. D. McGehee, *Sustainable Energy & Fuels* **2018**, 2, 2398.
[367] J. Martins, S. Emami, R. Madureira, J. Mendes, D. Ivanou, A. Mendes, *Journal of Materials Chemistry A* **2020**, 8, 20037.
[368] J. Fahlteich, M. Fahland, W. Schönberger, N. Schiller, *Thin Solid Films* **2009**, 517, 3075.
[369] H. C. Weerasinghe, Y. Dkhissi, A. D. Scully, R. A. Caruso, Y.-B. Cheng, *Nano Energy* **2015**, 18, 118.
[370] E. Skoplaki, J. A. Palyvos, *Renewable Energy* **2009**, 34, 23.
[371] N.-K. Kim, Y. H. Min, S. Noh, E. Cho, G. Jeong, M. Joo, S.-W. Ahn, J. S. Lee, S. Kim, K. Ihm, H. Ahn, Y. Kang, H.-S. Lee, D. Kim, *Scientific Reports* **2017**, 7, 4645.
[372] T. Duong, Y. Wu, H. Shen, J. Peng, S. Zhao, N. Wu, M. Lockrey, T. White, K. Weber, K. Catchpole, *Solar Energy Materials and Solar Cells* **2018**, 188, 27.
[373] Z. Fan, H. Xiao, Y. Wang, Z. Zhao, Z. Lin, H.-C. Cheng, S.-J. Lee, G. Wang, Z. Feng, W. A. Goddard, Y. Huang, X. Duan, *Joule* **2017**, 1, 548.
[374] D. P. Nenon, J. A. Christians, L. M. Wheeler, J. L. Blackburn, E. M. Sanehira, B. Dou, M. L. Olsen, K. Zhu, J. J. Berry, J. M. Luther, *Energy & Environmental Science* **2016**, 9, 2072.
[375] E. J. Juarez-Perez, Z. Hawash, S. R. Raga, L. K. Ono, Y. Qi, *Energy & Environmental Science* **2016**, 9, 3406.
[376] E. J. Juarez-Perez, L. K. Ono, Y. Qi, *Journal of Materials Chemistry A* **2019**, 7, 16912.
[377] L. Shi, M. P. Bucknall, T. L. Young, M. Zhang, L. Hu, J. Bing, D. S. Lee, J. Kim, T. Wu, N. Takamure, D. R. McKenzie, S. Huang, M. A. Green, A. W. Y. Ho-Baillie, *Science* **2020**, 368, eaba2412.
[378] X. Zheng, C. Wu, S. K. Jha, Z. Li, K. Zhu, S. Priya, *ACS Energy Letters* **2016**, 1, 1014.

[379] C. Zhang, J. F. S. Fernando, K. L. Firestein, J. E. v. Treifeldt, D. Siriwardena, X. Fang, D. Golberg, *APL Materials* **2019**, 7, 071110.
[380] M. Liao, B. Shan, M. Li, *The Journal of Physical Chemistry Letters* **2019**, 10, 1217.
[381] Q. Meng, Y. Chen, Y. Y. Xiao, J. Sun, X. Zhang, C. B. Han, H. Gao, Y. Zhang, H. Yan, *Journal of Materials Science: Materials in Electronics* **2021**, 32, 12784.
[382] G. Abdelmageed, C. Mackeen, K. Hellier, L. Jewell, L. Seymour, M. Tingwald, F. Bridges, J. Z. Zhang, S. Carter, *Solar Energy Materials and Solar Cells* **2018**, 174, 566.
[383] P. H. Svensson, L. Kloo, *Chemical Reviews* **2003**, 103, 1649.
[384] X. Tang, M. Brandl, B. May, I. Levchuk, Y. Hou, M. Richter, H. Chen, S. Chen, S. Kahmann, A. Osvet, F. Maier, H.-P. Steinrück, R. Hock, G. J. Matt, C. J. Brabec, *Journal of Materials Chemistry A* **2016**, 4, 15896.
[385] J. Yang, Q. Hong, Z. Yuan, R. Xu, X. Guo, S. Xiong, X. Liu, S. Braun, Y. Li, J. Tang, C. Duan, M. Fahlman, Q. Bao, *Advanced Optical Materials* **2018**, 6, 1800262.
[386] C. Das, M. Wussler, T. Hellmann, T. Mayer, W. Jaegermann, *Physical Chemistry Chemical Physics* **2018**, 20, 17180.
[387] R.-P. Xu, Y.-Q. Li, T.-Y. Jin, Y.-Q. Liu, Q.-Y. Bao, C. O'Carroll, J.-X. Tang, *ACS Applied Materials & Interfaces* **2018**, 10, 6737.
[388] Y.-B. Lu, W.-Y. Cong, C. Guan, H. Sun, Y. Xin, K. Wang, S. Song, *Journal of Materials Chemistry A* **2019**, 7, 27469.
[389] H. Tsai, R. Asadpour, J.-C. Blancon, C. C. Stoumpos, O. Durand, J. W. Strzalka, B. Chen, R. Verduzco, P. M. Ajayan, S. Tretiak, J. Even, M. A. Alam, M. G. Kanatzidis, W. Nie, A. D. Mohite, *Science* **2018**, 360, 67.
[390] J. P. Bastos, U. W. Paetzold, R. Gehlhaar, W. Qiu, D. Cheyns, S. Surana, V. Spampinato, T. Aernouts, J. Poortmans, *Advanced Energy Materials* **2018**, 8, 1800554.
[391] W. Nie, J.-C. Blancon, A. J. Neukirch, K. Appavoo, H. Tsai, M. Chhowalla, M. A. Alam, M. Y. Sfeir, C. Katan, J. Even, S. Tretiak, J. J. Crochet, G. Gupta, A. D. Mohite, *Nature Communications* **2016**, 7, 11574.
[392] A. J. Neukirch, W. Nie, J.-C. Blancon, K. Appavoo, H. Tsai, M. Y. Sfeir, C. Katan, L. Pedesseau, J. Even, J. J. Crochet, G. Gupta, A. D. Mohite, S. Tretiak, *Nano Letters* **2016**, 16, 3809.
[393] R. Azmi, N. Nurrosyid, S.-H. Lee, M. Al Mubarok, W. Lee, S. Hwang, W. Yin, T. K. Ahn, T.-W. Kim, D. Y. Ryu, Y. R. Do, S.-Y. Jang, *ACS Energy Letters* **2020**, 5, 1396.
[394] G. Niu, W. Li, J. Li, X. Liang, L. Wang, *RSC Advances* **2017**, 7, 17473.
[395] E. L. Unger, E. T. Hoke, C. D. Bailie, W. H. Nguyen, A. R. Bowring, T. Heumüller, M. G. Christoforo, M. D. McGehee, *Energy & Environmental Science* **2014**, 7, 3690.
[396] T. Malinauskas, D. Tomkute-Luksiene, R. Sens, M. Daskeviciene, R. Send, H. Wonneberger, V. Jankauskas, I. Bruder, V. Getautis, *ACS Applied Materials & Interfaces* **2015**, 7, 11107.
[397] X. Sun, F. Wu, C. Zhong, L. Zhu, Z. a. Li, *Chemical Science* **2019**, DOI: 10.1039/C9SC01697J.
[398] G. Xing, N. Mathews, S. Sun, S. S. Lim, Y. M. Lam, M. Grätzel, S. Mhaisalkar, T. C. Sum, *Science* **2013**, 342, 344.
[399] C. R. Kagan, D. B. Mitzi, C. D. Dimitrakopoulos, *Science* **1999**, 286, 945.
[400] T. Leijtens, R. Prasanna, A. Gold-Parker, M. F. Toney, M. D. McGehee, *ACS Energy Letters* **2017**, 2, 2159.
[401] T. C. Jellicoe, J. M. Richter, H. F. J. Glass, M. Tabachnyk, R. Brady, S. E. Dutton, A. Rao, R. H. Friend, D. Credgington, N. C. Greenham, M. L. Böhm, *Journal of the American Chemical Society* **2016**, 138, 2941.
[402] A. L. Abdelhady, M. I. Saidaminov, B. Murali, V. Adinolfi, O. Voznyy, K. Katsiev, E. Alarousu, R. Comin, I. Dursun, L. Sinatra, E. H. Sargent, O. F. Mohammed, O. M. Bakr, *The Journal of Physical Chemistry Letters* **2016**, 7, 295.

[403] Y. Takahashi, R. Obara, Z.-Z. Lin, Y. Takahashi, T. Naito, T. Inabe, S. Ishibashi, K. Terakura, *Dalton Transactions* **2011**, 40, 5563.
[404] D. B. Mitzi, C. A. Feild, Z. Schlesinger, R. B. Laibowitz, *Journal of Solid State Chemistry* **1995**, 114, 159.
[405] Y. Takahashi, R. Obara, K. Nakagawa, M. Nakano, J.-y. Tokita, T. Inabe, *Chemistry of Materials* **2007**, 19, 6312.
[406] J. Cheng, A. Navrotsky, X.-D. Zhou, H. U. Anderson, *Journal of Materials Research* **2011**, 20, 191.
[407] L. N. Quan, M. Yuan, R. Comin, O. Voznyy, E. M. Beauregard, S. Hoogland, A. Buin, A. R. Kirmani, K. Zhao, A. Amassian, D. H. Kim, E. H. Sargent, *Journal of the American Chemical Society* **2016**, 138, 2649.
[408] Z. Deng, F. Wei, F. Brivio, Y. Wu, S. Sun, P. D. Bristowe, A. K. Cheetham, *The Journal of Physical Chemistry Letters* **2017**, 8, 5015.
[409] A. S. Thind, S. Kavadiya, M. Kouhnavard, R. Wheelus, S. B. Cho, L.-Y. Lin, C. Kacica, H. K. Mulmudi, K. A. Unocic, A. Y. Borisevich, G. Pilania, P. Biswas, R. Mishra, *Chemistry of Materials* **2019**, 31, 4769.
[410] A. M. Glass, D. v. d. Linde, T. J. Negran, *Applied Physics Letters* **1974**, 25, 233.
[411] W. T. H. Koch, R. Munser, W. Ruppel, P. Würfel, *Solid State Communications* **1975**, 17, 847.
[412] D. Cao, C. Wang, F. Zheng, W. Dong, L. Fang, M. Shen, *Nano Letters* **2012**, 12, 2803.
[413] M. Qin, K. Yao, Y. C. Liang, *Applied Physics Letters* **2008**, 93, 122904.
[414] G. Gopal Khan, R. Das, N. Mukherjee, K. Mandal, *physica status solidi (RRL) – Rapid Research Letters* **2012**, 6, 312.
[415] I. Grinberg, D. V. West, M. Torres, G. Gou, D. M. Stein, L. Wu, G. Chen, E. M. Gallo, A. R. Akbashev, P. K. Davies, J. E. Spanier, A. M. Rappe, *Nature* **2013**, 503, 509.
[416] R. Nechache, C. Harnagea, S. Li, L. Cardenas, W. Huang, J. Chakrabartty, F. Rosei, *Nature Photonics* **2015**, 9, 61.
[417] Y.-B. Lu, H. Yang, W.-Y. Cong, P. Zhang, H. Guo, *Applied Physics Letters* **2017**, 111, 253902.
[418] M. Qin, K. Yao, Y. C. Liang, *Journal of Applied Physics* **2009**, 105, 061624.
[419] R. Nechache, W. Huang, S. Li, F. Rosei, *Nanoscale* **2016**, 8, 3237.
[420] N. Wu, Y. Wu, D. Walter, H. Shen, T. Duong, D. Grant, C. Barugkin, X. Fu, J. Peng, T. White, K. Catchpole, K. Weber, *Energy Technology* **2017**, 5, 1827.
[421] H. Fu, *Solar Energy Materials and Solar Cells* **2019**, 193, 107.
[422] R. Wang, J. Wang, S. Tan, Y. Duan, Z.-K. Wang, Y. Yang, *Trends in Chemistry* **2019**, 1, 368.
[423] Z. Xiao, Z. Song, Y. Yan, *Advanced Materials* **2019**, 31, 1803792.
[424] E. Jokar, C.-H. Chien, C.-M. Tsai, A. Fathi, E. W.-G. Diau, *Advanced Materials* **2019**, 31, 1804835.
[425] T. Wang, Q. Tai, X. Guo, J. Cao, C.-K. Liu, N. Wang, D. Shen, Y. Zhu, C.-S. Lee, F. Yan, *ACS Energy Letters* **2020**, 5, 1741.
[426] Q. Fu, X. Tang, D. Li, L. Huang, S. Xiao, Y. Chen, T. Hu, *Journal of Materials Chemistry C* **2020**, 8, 7786.
[427] X. Liu, Y. Wang, T. Wu, X. He, X. Meng, J. Barbaud, H. Chen, H. Segawa, X. Yang, L. Han, *Nature Communications* **2020**, 11, 2678.
[428] T. Krishnamoorthy, H. Ding, C. Yan, W. L. Leong, T. Baikie, Z. Zhang, M. Sherburne, S. Li, M. Asta, N. Mathews, S. G. Mhaisalkar, *Journal of Materials Chemistry A* **2015**, 3, 23829.
[429] I. Kopacic, B. Friesenbichler, S. F. Hoefler, B. Kunert, H. Plank, T. Rath, G. Trimmel, *ACS Applied Energy Materials* **2018**, 1, 343.

[430] S. Yue, S. C. McGuire, H. Yan, Y. S. Chu, M. Cotlet, X. Tong, S. S. Wong, *ACS Omega* **2019**, 4, 18219.
[431] X. Chang, D. Marongiu, V. Sarritzu, N. Sestu, Q. Wang, S. Lai, A. Mattoni, A. Filippetti, F. Congiu, A. G. Lehmann, F. Quochi, M. Saba, A. Mura, G. Bongiovanni, *Advanced Functional Materials* **2019**, 29, 1903528.
[432] T. Wu, X. Liu, X. He, Y. Wang, X. Meng, T. Noda, X. Yang, L. Han, *Science China Chemistry* **2020**, 63, 107.
[433] S. A. U. Hasan, D. S. Lee, S. H. Im, K.-H. Hong, *Solar RRL* **2020**, 4, 1900310.
[434] J. Cao, Q. Tai, P. You, G. Tang, T. Wang, N. Wang, F. Yan, *Journal of Materials Chemistry A* **2019**, 7, 26580.
[435] J. H. Heo, J. Kim, H. Kim, S. H. Moon, S. H. Im, K.-H. Hong, *The Journal of Physical Chemistry Letters* **2018**, 9, 6024.
[436] T.-B. Song, T. Yokoyama, S. Aramaki, M. G. Kanatzidis, *ACS Energy Letters* **2017**, 2, 897.
[437] F. Gao, C. Li, L. Qin, L. Zhu, X. Huang, H. Liu, L. Liang, Y. Hou, Z. Lou, Y. Hu, F. Teng, *RSC Advances* **2018**, 8, 14025.
[438] J. Jiang, C. K. Onwudinanti, R. A. Hatton, P. A. Bobbert, S. Tao, *The Journal of Physical Chemistry C* **2018**, 122, 17660.
[439] J. Wu, F. Fang, Z. Zhao, T. Li, R. Ullah, Z. Lv, Y. Zhou, D. Sawtell, *RSC Advances* **2019**, 9, 37119.
[440] R. M. I. Bandara, K. D. G. I. Jayawardena, S. O. Adeyemo, S. J. Hinder, J. A. Smith, H. M. Thirimanne, N. C. Wong, F. M. Amin, B. G. Freestone, A. J. Parnell, D. G. Lidzey, H. J. Joyce, R. A. Sporea, S. R. P. Silva, *Journal of Materials Chemistry C* **2019**, 7, 8389.
[441] J. Yuan, B. Li, C. Hao, *Materials Science in Semiconductor Processing* **2017**, 57, 95.
[442] C. Park, J. Choi, J. Min, K. Cho, *ACS Energy Letters* **2020**, 5, 3285.
[443] Z. Wang, Alex M. Ganose, C. Niu, D. O. Scanlon, *Journal of Materials Chemistry A* **2018**, 6, 5652.
[444] L. Lanzetta, J. M. Marin-Beloqui, I. Sanchez-Molina, D. Ding, S. A. Haque, *ACS Energy Letters* **2017**, 2, 1662.
[445] M. I. Saidaminov, I. Spanopoulos, J. Abed, W. Ke, J. Wicks, M. G. Kanatzidis, E. H. Sargent, *ACS Energy Letters* **2020**, DOI: 10.1021/acsenergylett.0c004021153.
[446] D. Wu, P. Jia, W. Bi, Y. Tang, J. Zhang, B. Song, L. Qin, Z. Lou, Y. Hu, F. Teng, Y. Hou, *Organic Electronics* **2020**, 82, 105728.
[447] D. Ramirez, K. Schutt, Z. Wang, A. J. Pearson, E. Ruggeri, H. J. Snaith, S. D. Stranks, F. Jaramillo, *ACS Energy Letters* **2018**, 3, 2246.
[448] M. Wei, K. Xiao, G. Walters, R. Lin, Y. Zhao, M. I. Saidaminov, P. Todorović, A. Johnston, Z. Huang, H. Chen, A. Li, J. Zhu, Z. Yang, Y.-K. Wang, A. H. Proppe, S. O. Kelley, Y. Hou, O. Voznyy, H. Tan, E. H. Sargent, *Advanced Materials* **2020**, 32, 1907058.
[449] S. Fang, Y. Wang, H. Li, F. Fang, K. Jiang, Z. Liu, H. Li, Y. Shi, *Journal of Materials Chemistry C* **2020**, 8, 4895.
[450] K. Eckhardt, V. Bon, J. Getzschmann, J. Grothe, F. M. Wisser, S. Kaskel, *Chemical Communications* **2016**, 52, 3058.
[451] Y. Li, K. Yang, *Energy & Environmental Science* **2019**, 12, 2233.
[452] X. Xu, Y. Zhong, Z. Shao, *Trends in Chemistry* **2019**, 1, 410.
[453] J. Zhou, X. Rong, M. S. Molokeev, X. Zhang, Z. Xia, *Journal of Materials Chemistry A* **2018**, 6, 2346.
[454] C. Li, Z. Song, C. Chen, C. Xiao, B. Subedi, S. P. Harvey, N. Shrestha, K. K. Subedi, L. Chen, D. Liu, Y. Li, Y.-W. Kim, C.-s. Jiang, M. J. Heben, D. Zhao, R. J. Ellingson, N. J. Podraza, M. Al-Jassim, Y. Yan, *Nature Energy* **2020**, 5, 768.

[455] S. Shao, J. Dong, H. Duim, G. H. ten Brink, G. R. Blake, G. Portale, M. A. Loi, *Nano Energy* **2019**, 60, 810.
[456] H. Kim, Y. H. Lee, T. Lyu, J. H. Yoo, T. Park, J. H. Oh, *Journal of Materials Chemistry A* **2018**, 6, 18173.
[457] T. Yokoyama, Y. Nishitani, Y. Miyamoto, S. Kusumoto, R. Uchida, T. Matsui, K. Kawano, T. Sekiguchi, Y. Kaneko, *ACS Applied Materials & Interfaces* **2020**, 12, 27131.
[458] Y. Miyamoto, S. Kusumoto, T. Yokoyama, Y. Nishitani, T. Matsui, T. Kouzaki, R. Nishikubo, A. Saeki, Y. Kaneko, *ACS Applied Nano Materials* **2020**, 3, 11650.
[459] Z. Wan, H. Lai, S. Ren, R. He, Y. Jiang, J. Luo, Q. Chen, X. Hao, Y. Wang, J. Zhang, L. Wu, D. Zhao, *Journal of Energy Chemistry* **2021**, 57, 147.
[460] X. Li, X. Zhong, Y. Hu, B. Li, Y. Sheng, Y. Zhang, C. Weng, M. Feng, H. Han, J. Wang, *The Journal of Physical Chemistry Letters* **2017**, 8, 1804.
[461] K. Ahmad, S. M. Mobin, *Energy Technology* **2020**, 8, 1901185.
[462] L. Xie, B. Chen, F. Zhang, Z. Zhao, X. Wang, L. Shi, Y. Liu, L. Huang, R. Liu, B. Zou, Y. Wang, *Photon. Res.* **2020**, 8, 768.
[463] A. M. Elseman, A. E. Shalan, S. Sajid, M. M. Rashad, A. M. Hassan, M. Li, *ACS Applied Materials & Interfaces* **2018**, 10, 11699.
[464] D. Cortecchia, H. A. Dewi, J. Yin, A. Bruno, S. Chen, T. Baikie, P. P. Boix, M. Grätzel, S. Mhaisalkar, C. Soci, N. Mathews, *Inorganic Chemistry* **2016**, 55, 1044.
[465] D. B. Khadka, Y. Shirai, M. Yanagida, K. Miyano, *Journal of Materials Chemistry C* **2019**, 7, 8335.
[466] M.-C. Tang, D. Barrit, R. Munir, R. Li, J. M. Barbé, D.-M. Smilgies, S. Del Gobbo, T. D. Anthopoulos, A. Amassian, *Solar RRL* **2019**, 3, 1800305.
[467] Y. Yang, C. Liu, M. Cai, Y. Liao, Y. Ding, S. Ma, X. Liu, M. Guli, S. Dai, M. K. Nazeeruddin, *ACS Applied Materials & Interfaces* **2020**, 12, 17062.
[468] K. M. Boopathi, P. Karuppuswamy, A. Singh, C. Hanmandlu, L. Lin, S. A. Abbas, C. C. Chang, P. C. Wang, G. Li, C. W. Chu, *Journal of Materials Chemistry A* **2017**, 5, 20843.
[469] Z. Jin, Z. Zhang, J. Xiu, H. Song, T. Gatti, Z. He, *Journal of Materials Chemistry A* **2020**, 8, 16166.
[470] P. K. Nayak, S. Mahesh, H. J. Snaith, D. Cahen, *Nature Reviews Materials* **2019**, 4, 269.
[471] N. Wang, Y. Zhang, P. Zeng, Y. Hu, F. Li, M. Liu, *Journal of Applied Physics* **2020**, 128, 044504.
[472] J. Lu, S.-C. Chen, Q. Zheng, *ACS Applied Energy Materials* **2018**, 1, 5872.
[473] Z. Xiao, W. Meng, J. Wang, D. B. Mitzi, Y. Yan, *Materials Horizons* **2017**, 4, 206.
[474] B. Saparov, F. Hong, J.-P. Sun, H.-S. Duan, W. Meng, S. Cameron, I. G. Hill, Y. Yan, D. B. Mitzi, *Chemistry of Materials* **2015**, 27, 5622.
[475] B. Saparov, D. B. Mitzi, *Chemical Reviews* **2016**, 116, 4558.
[476] M. Harilal, B. Vidyadharan, I. I. Misnon, G. M. Anilkumar, A. Lowe, J. Ismail, M. M. Yusoff, R. Jose, *ACS Applied Materials & Interfaces* **2017**, 9, 10730.
[477] Q. Wali, A. Fakharuddin, I. Ahmed, M. H. Ab Rahim, J. Ismail, R. Jose, *Journal of Materials Chemistry A* **2014**, 2, 17427.
[478] B. Vidyadharan, I. I. Misnon, J. Ismail, M. M. Yusoff, R. Jose, *Journal of Alloys and Compounds* **2015**, 633, 22.
[479] G. Volonakis, M. R. Filip, A. A. Haghighirad, N. Sakai, B. Wenger, H. J. Snaith, F. Giustino, *The Journal of Physical Chemistry Letters* **2016**, 7, 1254.
[480] Y.-J. Li, T. Wu, L. Sun, R.-X. Yang, L. Jiang, P.-F. Cheng, Q.-Q. Hao, T.-J. Wang, R.-F. Lu, W.-Q. Deng, *RSC Advances* **2017**, 7, 35175.
[481] V. K. Ravi, N. Singhal, A. Nag, *Journal of Materials Chemistry A* **2018**, 6, 21666.
[482] X.-G. Zhao, D. Yang, J.-C. Ren, Y. Sun, Z. Xiao, L. Zhang, *Joule* **2018**, 2, 1662.

[483] M. R. Filip, S. Hillman, A. A. Haghighirad, H. J. Snaith, F. Giustino, *The Journal of Physical Chemistry Letters* **2016**, 7, 2579.
[484] A. H. Slavney, T. Hu, A. M. Lindenberg, H. I. Karunadasa, *Journal of the American Chemical Society* **2016**, 138, 2138.
[485] S. E. Creutz, E. N. Crites, M. C. De Siena, D. R. Gamelin, *Nano Letters* **2018**, 18, 1118.
[486] S. Khalfin, Y. Bekenstein, *Nanoscale* **2019**, 11, 8665.
[487] E. T. McClure, M. R. Ball, W. Windl, P. M. Woodward, *Chemistry of Materials* **2016**, 28, 1348.
[488] F. Liu, D. Marongiu, R. Pau, V. Sarritzu, Q. Wang, S. Lai, A. G. Lehmann, F. Quochi, M. Saba, A. Mura, G. Bongiovanni, A. Mattoni, C. Caddeo, A. Bosin, A. Filippetti, *EcoMat* **2020**, 2, e12017.
[489] W. J. Mir, T. Sheikh, H. Arfin, Z. Xia, A. Nag, *NPG Asia Materials* **2020**, 12, 9.
[490] G. Longo, S. Mahesh, L. R. V. Buizza, A. D. Wright, A. J. Ramadan, M. Abdi-Jalebi, P. K. Nayak, L. M. Herz, H. J. Snaith, *ACS Energy Letters* **2020**, 5, 2200.
[491] G. A. Mousdis, V. Gionis, G. C. Papavassiliou, C. P. Raptopoulou, A. Terzis, *Journal of Materials Chemistry* **1998**, 8, 2259.
[492] L.-Y. Bi, Y.-Q. Hu, M.-Q. Li, T.-L. Hu, H.-L. Zhang, X.-T. Yin, W.-X. Que, M. S. Lassoued, Y.-Z. Zheng, *Journal of Materials Chemistry A* **2019**, 7, 19662.
[493] P. Han, X. Mao, S. Yang, F. Zhang, B. Yang, D. Wei, W. Deng, K. Han, *Angewandte Chemie International Edition* **2019**, 58, 17231.
[494] F. Wei, Z. Deng, S. Sun, F. Zhang, D. M. Evans, G. Kieslich, S. Tominaka, M. A. Carpenter, J. Zhang, P. D. Bristowe, A. K. Cheetham, *Chemistry of Materials* **2017**, 29, 1089.
[495] M. Roknuzzaman, C. Zhang, K. Ostrikov, A. Du, H. Wang, L. Wang, T. Tesfamichael, *Scientific Reports* **2019**, 9, 718.
[496] N. Rajeev Kumar, R. Radhakrishnan, *Materials Letters* **2018**, 227, 289.
[497] M. Pehl, A. Arvesen, F. Humpenöder, A. Popp, E. G. Hertwich, G. Luderer, *Nature Energy* **2017**, 2, 939.
[498] P. Wu, X. Ma, J. Ji, Y. Ma, *Energy Procedia* **2017**, 105, 1289.
[499] H. Schaefer, G. Hagedorn, *Renewable Energy* **1992**, 2, 159.
[500] F. Kreith, P. Norton, D. Brown, *Energy* **1990**, 15, 1181.
[501] D. Mulvaney, Solar Energy Isn't Always as Green as You Think, https://spectrum.ieee.org/green-tech/solar/solar-energy-isnt-always-as-green-as-you-think, accessed.
[502] A. E. Cha, Solar Energy Firms Leave Waste Behind in Chine, https://www.washingtonpost.com/wp-dyn/content/article/2008/03/08/AR2008030802595.html, accessed.
[503] Z. Shi, A. H. Jayatissa, *Materials (Basel)* **2018**, 11.
[504] D. Zhou, T. Zhou, Y. Tian, X. Zhu, Y. Tu, *Journal of Nanomaterials* **2018**, 2018, 15.
[505] S. Razza, S. Castro-Hermosa, A. Di Carlo, T. M. Brown, *APL Materials* **2016**, 4, 091508.
[506] C. Tao, S. Neutzner, L. Colella, S. Marras, A. R. Srimath Kandada, M. Gandini, M. D. Bastiani, G. Pace, L. Manna, M. Caironi, C. Bertarelli, A. Petrozza, *Energy & Environmental Science* **2015**, 8, 2365.
[507] C.-G. Park, W.-G. Choi, S. Na, T. Moon, *Electronic Materials Letters* **2019**, 15, 56.
[508] Y.-H. Chiang, M. Anaya, S. D. Stranks, *ACS Energy Letters* **2020**, 5, 2498.
[509] J. M. Ball, L. Buizza, H. C. Sansom, M. D. Farrar, M. T. Klug, J. Borchert, J. Patel, L. M. Herz, M. B. Johnston, H. J. Snaith, *ACS Energy Letters* **2019**, 4, 2748.
[510] J. Li, H. Wang, X. Y. Chin, H. A. Dewi, K. Vergeer, T. W. Goh, J. W. M. Lim, J. H. Lew, K. P. Loh, C. Soci, T. C. Sum, H. J. Bolink, N. Mathews, S. Mhaisalkar, A. Bruno, *Joule* **2020**, 4, 1035.

[511] S. Tafazoli, N. Timasi, E. Nouri, M. R. Mohammadi, *CrystEngComm* **2018**, 20, 4428.
[512] S. Chen, L. Lei, S. Yang, Y. Liu, Z.-S. Wang, *ACS Applied Materials & Interfaces* **2015**, 7, 25770.
[513] D. B. Mitzi, M. T. Prikas, K. Chondroudis, *Chemistry of Materials* **1999**, 11, 542.
[514] J.-M. Ting, N. Z. Huang, *Carbon* **2001**, 39, 835.
[515] S. Faÿ, J. Steinhauser, S. Nicolay, C. Ballif, *Thin Solid Films* **2010**, 518, 2961.
[516] A. Yanguas-Gil, N. Kumar, Y. Yang, J. R. Abelson, *Journal of Vacuum Science & Technology A* **2009**, 27, 1244.
[517] P. Luo, S. Zhou, W. Xia, J. Cheng, C. Xu, Y. Lu, *Advanced Materials Interfaces* **2017**, 4, 1600970.
[518] H. M. Yates, J. L. Hodgkinson, S. M. P. Meroni, D. Richards, T. M. Watson, *Surface and Coatings Technology* **2020**, 385, 125423.
[519] Q. Chen, H. Zhou, Z. Hong, S. Luo, H.-S. Duan, H.-H. Wang, Y. Liu, G. Li, Y. Yang, *Journal of the American Chemical Society* **2014**, 136, 622.
[520] M. M. Tavakoli, L. Gu, Y. Gao, C. Reckmeier, J. He, A. L. Rogach, Y. Yao, Z. Fan, *Scientific Reports* **2015**, 5, 14083.
[521] M. R. Leyden, Y. Jiang, Y. Qi, *Journal of Materials Chemistry A* **2016**, 4, 13125.
[522] P. Luo, Z. Liu, W. Xia, C. Yuan, J. Cheng, Y. Lu, *ACS Applied Materials & Interfaces* **2015**, 7, 2708.
[523] G. Kim, S. An, S.-K. Hyeong, S.-K. Lee, M. Kim, N. Shin, *Chemistry of Materials* **2019**, 31, 8212.
[524] A. Fakharuddin, L. Schmidt-Mende, G. Garcia-Belmonte, R. Jose, I. Mora-Sero, *Advanced Energy Materials* **2017**, 7, 1700623.
[525] S. Castro-Hermosa, L. Wouk, I. S. Bicalho, L. de Queiroz Corrêa, B. de Jong, L. Cinà, T. M. Brown, D. Bagnis, *Nano Research* **2021**, 14, 1034.
[526] Z. Yang, C.-C. Chueh, F. Zuo, J. H. Kim, P.-W. Liang, A. K. Y. Jen, *Advanced Energy Materials* **2015**, 5, 1500328.
[527] J. H. Kim, S. T. Williams, N. Cho, C.-C. Chueh, A. K. Y. Jen, *Advanced Energy Materials* **2015**, 5, 1401229.
[528] D. Wang, J. Zheng, X. Wang, J. Gao, W. Kong, C. Cheng, B. Xu, *Journal of Energy Chemistry* **2019**, 38, 207.
[529] K. Liao, C. Li, L. Xie, Y. Yuan, S. Wang, Z. Cao, L. Ding, F. Hao, *Nano-Micro Letters* **2020**, 12, 156.
[530] J. Zhang, T. Bu, J. Li, H. Li, Y. Mo, Z. Wu, Y. Liu, X.-L. Zhang, Y.-B. Cheng, F. Huang, *Journal of Materials Chemistry A* **2020**, 8, 8447.
[531] W. Kong, G. Wang, J. Zheng, H. Hu, H. Chen, Y. Li, M. Hu, X. Zhou, C. Liu, B. N. Chandrashekar, A. Amini, J. Wang, B. Xu, C. Cheng, *Solar RRL* **2018**, 2, 1700214.
[532] S. Wang, Z. Ma, B. Liu, W. Wu, Y. Zhu, R. Ma, C. Wang, *Solar RRL* **2018**, 2, 1800034.
[533] Z. Bi, X. Rodríguez-Martínez, C. Aranda, E. Pascual-San-José, A. R. Goñi, M. Campoy-Quiles, X. Xu, A. Guerrero, *Journal of Materials Chemistry A* **2018**, 6, 19085.
[534] C. Li, J. Yin, R. Chen, X. Lv, X. Feng, Y. Wu, J. Cao, *Journal of the American Chemical Society* **2019**, 141, 6345.
[535] Y. Zhong, R. Munir, J. Li, M.-C. Tang, M. R. Niazi, D.-M. Smilgies, K. Zhao, A. Amassian, *ACS Energy Letters* **2018**, 3, 1078.
[536] M. K. Kim, H. S. Lee, S. R. Pae, D.-J. Kim, J.-Y. Lee, I. Gereige, S. Park, B. Shin, *Journal of Materials Chemistry A* **2018**, 6, 24911.
[537] A. Reale, L. La Notte, L. Salamandra, G. Polino, G. Susanna, T. M. Brown, F. Brunetti, A. Di Carlo, *Energy Technology* **2015**, 3, 385.
[538] T.-T. Duong, T.-D. Tran, Q.-T. Le, *Journal of Materials Science: Materials in Electronics* **2019**, 30, 11027.

[539] J. E. Bishop, J. A. Smith, D. G. Lidzey, *ACS Applied Materials & Interfaces* **2020**, 12, 48237.
[540] H. Back, J. Kim, G. Kim, T. Kyun Kim, H. Kang, J. Kong, S. Ho Lee, K. Lee, *Solar Energy Materials and Solar Cells* **2016**, 144, 309.
[541] I. A. Howard, T. Abzieher, I. M. Hossain, H. Eggers, F. Schackmar, S. Ternes, B. S. Richards, U. Lemmer, U. W. Paetzold, *Advanced Materials* **2019**, 31, 1806702.
[542] R. Patidar, D. Burkitt, K. Hooper, D. Richards, T. Watson, *Materials Today Communications* **2020**, 22, 100808.
[543] H. Eggers, F. Schackmar, T. Abzieher, Q. Sun, U. Lemmer, Y. Vaynzof, B. S. Richards, G. Hernandez-Sosa, U. W. Paetzold, *Advanced Energy Materials* **2020**, 10, 1903184.
[544] Z. Liang, S. Zhang, X. Xu, N. Wang, J. Wang, X. Wang, Z. Bi, G. Xu, N. Yuan, J. Ding, *RSC Advances* **2015**, 5, 60562.
[545] Y.-C. Huang, C.-S. Tsao, H.-C. Cha, C.-M. Chuang, C.-J. Su, U. S. Jeng, C.-Y. Chen, *Scientific Reports* **2016**, 6, 20062.
[546] S. Das, B. Yang, G. Gu, P. C. Joshi, I. N. Ivanov, C. M. Rouleau, T. Aytug, D. B. Geohegan, K. Xiao, *ACS Photonics* **2015**, 2, 680.
[547] N. K. Roy, D. Behera, O. G. Dibua, C. S. Foong, M. A. Cullinan, *Microsystems & Nanoengineering* **2019**, 5, 64.
[548] H.-Y. Park, K. Kim, D. Y. Kim, S.-K. Choi, S. M. Jo, S.-Y. Jang, *Journal of Materials Chemistry* **2011**, 21, 4457.
[549] T. Zhang, X. Zhao, D. Yang, X. Yang, *Energy Technology* **2018**, 6, 171.
[550] M. Yang, Z. Li, M. O. Reese, O. G. Reid, D. H. Kim, S. Siol, T. R. Klein, Y. Yan, J. J. Berry, M. F. A. M. van Hest, K. Zhu, *Nature Energy* **2017**, 2, 17038.
[551] L. Gao, K. Huang, C. Long, F. Zeng, B. Liu, J. Yang, *Applied Physics A* **2020**, 126, 452.
[552] A. Vijayan, M. B. Johansson, S. Svanström, U. B. Cappel, H. Rensmo, G. Boschloo, *ACS Applied Energy Materials* **2020**, 3, 4331.
[553] D. Burkitt, R. Patidar, P. Greenwood, K. Hooper, J. McGettrick, S. Dimitrov, M. Colombo, V. Stoichkov, D. Richards, D. Beynon, M. Davies, T. Watson, *Sustainable Energy & Fuels* **2020**, 4, 3340.
[554] D. Burkitt, P. Greenwood, K. Hooper, D. Richards, V. Stoichkov, D. Beynon, E. Jewell, T. Watson, *MRS Advances* **2019**, 4, 1399.
[555] G. Cotella, J. Baker, D. Worsley, F. De Rossi, C. Pleydell-Pearce, M. Carnie, T. Watson, *Solar Energy Materials and Solar Cells* **2017**, 159, 362.
[556] Y.-C. Huang, C.-F. Li, Z.-H. Huang, P.-H. Liu, C.-S. Tsao, *Solar Energy* **2019**, 177, 255.
[557] S. Razza, F. Di Giacomo, F. Matteocci, L. Cinà, A. L. Palma, S. Casaluci, P. Cameron, A. D'Epifanio, S. Licoccia, A. Reale, T. M. Brown, A. Di Carlo, *Journal of Power Sources* **2015**, 277, 286.
[558] J. B. Whitaker, D. H. Kim, Bryon W. Larson, F. Zhang, J. J. Berry, M. F. A. M. van Hest, K. Zhu, *Sustainable Energy & Fuels* **2018**, 2, 2442.
[559] G. Mincuzzi, A. L. Palma, A. Di Carlo, T. M. Brown, *ChemElectroChem* **2016**, 3, 9.
[560] S. M. P. Meroni, K. E. A. Hooper, T. Dunlop, J. A. Baker, D. Worsley, C. Charbonneau, T. M. Watson, *Energies* **2020**, 13.
[561] S. Moon, J. Yum, L. Löfgren, A. Walter, L. Sansonnens, M. Benkhaira, S. Nicolay, J. Bailat, C. Ballif, *IEEE Journal of Photovoltaics* **2015**, 5, 1087.
[562] M. Yang, D. H. Kim, T. R. Klein, Z. Li, M. O. Reese, B. J. Tremolet de Villers, J. J. Berry, M. F. A. M. van Hest, K. Zhu, *ACS Energy Letters* **2018**, 3, 322.
[563] L. Qiu, Z. Liu, L. K. Ono, Y. Jiang, D.-Y. Son, Z. Hawash, S. He, Y. Qi, *Advanced Functional Materials* **2019**, 29, 1806779.
[564] A. L. Palma, F. Matteocci, A. Agresti, S. Pescetelli, E. Calabrò, L. Vesce, S. Christiansen, M. Schmidt, A. D. Carlo, *IEEE Journal of Photovoltaics* **2017**, 7, 1674.

[565] S. K. Karunakaran, G. M. Arumugam, W. Yang, S. Ge, S. N. Khan, X. Lin, G. Yang, *Journal of Materials Chemistry A* **2019**, 7, 13873.
[566] D. Raptis, V. Stoichkov, S. M. P. Meroni, A. Pockett, C. A. Worsley, M. Carnie, D. A. Worsley, T. Watson, *Current Applied Physics* **2020**, 20, 619.
[567] J. Burschka, N. Pellet, S.-J. Moon, R. Humphry-Baker, P. Gao, M. K. Nazeeruddin, M. Grätzel, *Nature* **2013**, 499, 316.
[568] S.-G. Li, K.-J. Jiang, M.-J. Su, X.-P. Cui, J.-H. Huang, Q.-Q. Zhang, X.-Q. Zhou, L.-M. Yang, Y.-L. Song, *Journal of Materials Chemistry A* **2015**, 3, 9092.
[569] C. Liang, P. Li, H. Gu, Y. Zhang, F. Li, Y. Song, G. Shao, N. Mathews, G. Xing, *Solar RRL* **2018**, 2, 1700217.
[570] H. Huang, J. Shi, L. Zhu, D. Li, Y. Luo, Q. Meng, *Nano Energy* **2016**, 27, 352.
[571] F. Di Giacomo, S. Shanmugam, H. Fledderus, B. J. Bruijnaers, W. J. H. Verhees, M. S. Dorenkamper, S. C. Veenstra, W. Qiu, R. Gehlhaar, T. Merckx, T. Aernouts, R. Andriessen, Y. Galagan, *Solar Energy Materials and Solar Cells* **2018**, 181, 53.
[572] J. Ávila, C. Momblona, P. P. Boix, M. Sessolo, H. J. Bolink, *Joule* **2017**, 1, 431.
[573] M. Park, W. Cho, G. Lee, S. C. Hong, M.-c. Kim, J. Yoon, N. Ahn, M. Choi, *Small* **2019**, 15, 1804005.
[574] J.-A. Alberola-Borràs, R. Vidal, E. J. Juárez-Pérez, E. Mas-Marzá, A. Guerrero, I. Mora-Seró, *Solar Energy Materials and Solar Cells* **2018**, 179, 169.
[575] J.-A. Alberola-Borràs, J. A. Baker, F. De Rossi, R. Vidal, D. Beynon, K. E. A. Hooper, T. M. Watson, I. Mora-Seró, *iScience* **2018**, 9, 542.
[576] R. Vidal, J.-A. Alberola-Borràs, S. N. Habisreutinger, J.-L. Gimeno-Molina, D. T. Moore, T. H. Schloemer, I. Mora-Seró, J. J. Berry, J. M. Luther, *Nature Sustainability* **2020**, DOI: 10.1038/s41893-020-00645-8.
[577] R. Swartwout, R. Patidir, E. Belliveau, B. Dou, D. Beynon, P. Greenwood, N. Moody, D. deQuilettes, M. Bawendi, T. Watson, V. Bulovic, DOI: 10.26434/chemrxiv.13221851.v1, ChemRxiv, 2020.
[578] B. Chen, Z. J. Yu, S. Manzoor, S. Wang, W. Weigand, Z. Yu, G. Yang, Z. Ni, X. Dai, Z. C. Holman, J. Huang, *Joule* **2020**, 4, 850.
[579] B. Chen, Z. Yu, K. Liu, X. Zheng, Y. Liu, J. Shi, D. Spronk, P. N. Rudd, Z. Holman, J. Huang, *Joule* **2019**, 3, 177.
[580] S. Tong, Y. E. von Schirnding, T. Prapamontol, *Bulletin of the World Health Organization* **2000**, 78, 1068.
[581] K. Koller, T. Brown, A. Spurgeon, L. Levy, *Environmental Health Perspectives* **2004**, 112, 987.
[582] B. P. Lanphear, T. D. Matte, J. Rogers, R. P. Clickner, B. Dietz, R. L. Bornschein, P. Succop, K. R. Mahaffey, S. Dixon, W. Galke, M. Rabinowitz, M. Farfel, C. Rohde, J. Schwartz, P. Ashley, D. E. Jacobs, *Environmental Research* **1998**, 79, 51.
[583] H. W. Mielke, P. L. Reagan, *Environmental health perspectives* **1998**, 106 Suppl 1, 217.
[584] P.-Y. Chen, J. Qi, M. T. Klug, X. Dang, P. T. Hammond, A. M. Belcher, *Energy & Environmental Science* **2014**, 7, 3659.
[585] R. Jose, S. K. Panigrahi, R. A. Patil, Y. Fernando, S. Ramakrishna, *Materials Circular Economy* **2020**, 2, 8.
[586] R. Jose, S. Ramakrishna, *Materials Circular Economy* **2021**, 3, 1.
[587] J. M. Kadro, A. Hagfeldt, *Joule* **2017**, 1, 29.
[588] A. Ambrosini, *MRS Bulletin* **2020**, 45, 989.
[589] J. Yakiangngam, P. Ruankham, S. Choopun, A. Intaniwet, *Journal of Physics: Conference Series* **2018**, 1144, 012029.
[590] J. Derksen, H. Sangjun, C. Jung-Hoon, presented at 1999 IEEE International Symposium on Semiconductor Manufacturing Conference Proceedings (Cat No.99CH36314), 11-13 Oct. 1999, **1999**.

[591] B. Augustine, K. Remes, G. S. Lorite, J. Varghese, T. Fabritius, *Solar Energy Materials and Solar Cells* **2019**, 194, 74.
[592] J. M. Kadro, N. Pellet, F. Giordano, A. Ulianov, O. Müntener, J. Maier, M. Grätzel, A. Hagfeldt, *Energy & Environmental Science* **2016**, 9, 3172.
[593] A. K. Jena, Y. Numata, M. Ikegami, T. Miyasaka, *Journal of Materials Chemistry A* **2018**, 6, 2219.
[594] P. Chhillar, B. P. Dhamaniya, V. Dutta, S. K. Pathak, *ACS Omega* **2019**, 4, 11880.
[595] J. Carolus, T. Merckx, Z. Purohit, B. Tripathi, H.-G. Boyen, T. Aernouts, W. De Ceuninck, B. Conings, M. Daenen, *Solar RRL* **2019**, 3, 1900226.
[596] R. Jose, S. Ramakrishna, *Applied Materials Today* **2018**, 10, 127.
[597] C.-J. Yu, *Journal of Physics: Energy* **2019**, 1, 022001.
[598] Q. Sun, W.-J. Yin, S.-H. Wei, *Journal of Materials Chemistry C* **2020**, 8, 12012.
[599] I. E. Castelli, J. M. García-Lastra, K. S. Thygesen, K. W. Jacobsen, *APL Materials* **2014**, 2, 081514.
[600] N. Wazzan, R. M. El-Shishtawy, A. Irfan, *Theoretical Chemistry Accounts* **2017**, 137, 9.
[601] R. Jacobs, G. Luo, D. Morgan, *Advanced Functional Materials* **2019**, 29, 1804354.
[602] H. Wang, G. Gou, J. Li, *Nano Energy* **2016**, 22, 507.
[603] G. Haidari, *AIP Advances* **2019**, 9, 085028.
[604] A. Seidu, L. Himanen, J. Li, P. Rinke, *New Journal of Physics* **2019**, 21, 083018.
[605] C. Kim, T. D. Huan, S. Krishnan, R. Ramprasad, *Scientific Data* **2017**, 4, 170057.
[606] Q. Xu, Z. Li, M. Liu, W.-J. Yin, *The Journal of Physical Chemistry Letters* **2018**, 9, 6948.
[607] S. Ahmad, C. George, D. J. Beesley, J. J. Baumberg, M. De Volder, *Nano Letters* **2018**, 18, 1856.
[608] FuelCellsWorks, South Korea: Work Begins on World's Largest Hydrogen Fuel Cell Power Plant, https://fuelcellsworks.com/news/south-korea-work-begins-on-worlds-largest-hydrogen-fuel-cell-power-plant-commissioned/, accessed.
[609] LogicEnergy, How a Fuel Cell power plant works, https://www.logicenergyusa.com/fuel-cell/how-a-fuel-cell-power-plant-works, accessed.
[610] H. Ahmad, S. K. Kamarudin, L. J. Minggu, M. Kassim, *Renewable and Sustainable Energy Reviews* **2015**, 43, 599.
[611] Y. Li, Y.-K. Peng, L. Hu, J. Zheng, D. Prabhakaran, S. Wu, T. J. Puchtler, M. Li, K.-Y. Wong, R. A. Taylor, S. C. E. Tsang, *Nature Communications* **2019**, 10, 4421.
[612] K. Takanabe, *ACS Catalysis* **2017**, 7, 8006.
[613] Q. Wang, K. Domen, *Chemical Reviews* **2020**, 120, 919.
[614] H. Idriss, *Catalysis Science & Technology* **2020**, 10, 304.
[615] S. F. Hoefler, R. Zettl, D. Knez, G. Haberfehlner, F. Hofer, T. Rath, G. Trimmel, H. M. R. Wilkening, I. Hanzu, *ACS Sustainable Chemistry & Engineering* **2020**, 8, 19155.
[616] B. D. Boruah, B. Wen, S. Nagane, X. Zhang, S. D. Stranks, A. Boies, M. De Volder, *ACS Energy Letters* **2020**, 5, 3132.
[617] B. D. Boruah, A. Mathieson, B. Wen, C. Jo, F. Deschler, M. De Volder, *Nano Letters* **2020**, 20, 5967.
[618] E. Velilla, F. Jaramillo, I. Mora-Seró, *Nature Energy* **2021**, 6, 54.
[619] J. Barbé, A. Pockett, V. Stoichkov, D. Hughes, H. K. H. Lee, M. Carnie, T. Watson, W. C. Tsoi, *Journal of Materials Chemistry C* **2020**, 8, 1715.
[620] M. V. Khenkin, E. A. Katz, A. Abate, G. Bardizza, J. J. Berry, C. Brabec, F. Brunetti, V. Bulović, Q. Burlingame, A. Di Carlo, R. Cheacharoen, Y.-B. Cheng, A. Colsmann, S. Cros, K. Domanski, M. Dusza, C. J. Fell, S. R. Forrest, Y. Galagan, D. Di Girolamo, M. Grätzel, A. Hagfeldt, E. von Hauff, H. Hoppe, J. Kettle, H. Köbler, M. S. Leite, S.

Liu, Y.-L. Loo, J. M. Luther, C.-Q. Ma, M. Madsen, M. Manceau, M. Matheron, M. McGehee, R. Meitzner, M. K. Nazeeruddin, A. F. Nogueira, Ç. Odabaşı, A. Osherov, N.-G. Park, M. O. Reese, F. De Rossi, M. Saliba, U. S. Schubert, H. J. Snaith, S. D. Stranks, W. Tress, P. A. Troshin, V. Turkovic, S. Veenstra, I. Visoly-Fisher, A. Walsh, T. Watson, H. Xie, R. Yıldırım, S. M. Zakeeruddin, K. Zhu, M. Lira-Cantu, *Nature Energy* **2020**, 5, 35.

[621] L. Meng, J. You, Y. Yang, *Nature Communications* **2018**, 9, 5265.

[622] J. Ambrose, in *Oxford PV says tech based on perovskite crystal can generate almost a third more electricity*, The Guardian, 2020.

[623] M. Kim, C. W. Bark, *Thin Solid Films* **2020**, 700, 137888.

[624] P. You, G. Li, G. Tang, J. Cao, F. Yan, *Energy & Environmental Science* **2020**, 13, 1187.

[625] H. Kanda, N. Shibayama, A. J. Huckaba, Y. Lee, S. Paek, N. Klipfel, C. Roldán-Carmona, V. I. E. Queloz, G. Grancini, Y. Zhang, M. Abuhelaiqa, K. T. Cho, M. Li, M. D. Mensi, S. Kinge, M. K. Nazeeruddin, *Energy & Environmental Science* **2020**, 13, 1222.

[626] K. T. Cho, S. Paek, G. Grancini, C. Roldán-Carmona, P. Gao, Y. Lee, M. K. Nazeeruddin, *Energy & Environmental Science* **2017**, 10, 621.

[627] X. Chen, M. Ding, T. Luo, T. Ye, C. Zhao, Y. Zhao, W. Zhang, H. Chang, *ACS Applied Energy Materials* **2020**, 3, 2975.

[628] J. Chen, J.-Y. Seo, N.-G. Park, *Advanced Energy Materials* **2018**, 8, 1702714.

[629] J. Ye, H. Zheng, L. Zhu, G. Liu, X. Zhang, T. Hayat, X. Pan, S. Dai, *Solar RRL* **2017**, 1, 1700125.

[630] S. Bai, P. Da, C. Li, Z. Wang, Z. Yuan, F. Fu, M. Kawecki, X. Liu, N. Sakai, J. T.-W. Wang, S. Huettner, S. Buecheler, M. Fahlman, F. Gao, H. J. Snaith, *Nature* **2019**, 571, 245.

[631] D.-J. Xue, Y. Hou, S.-C. Liu, M. Wei, B. Chen, Z. Huang, Z. Li, B. Sun, A. H. Proppe, Y. Dong, M. I. Saidaminov, S. O. Kelley, J.-S. Hu, E. H. Sargent, *Nature Communications* **2020**, 11, 1514.

[632] F. Fu, T. Feurer, Thomas P. Weiss, S. Pisoni, E. Avancini, C. Andres, S. Buecheler, Ayodhya N. Tiwari, *Nature Energy* **2016**, 2, 16190.

[633] M. He, B. Li, X. Cui, B. Jiang, Y. He, Y. Chen, D. O'Neil, P. Szymanski, M. A. Ei-Sayed, J. Huang, Z. Lin, *Nature Communications* **2017**, 8, 16045.

[634] J. Yi, J. Zhuang, X. Liu, H. Wang, Z. Ma, D. Huang, Z. Guo, H. Li, *Journal of Alloys and Compounds* **2020**, 830, 154710.

[635] Y. Li, Z. Zhang, Y. Zhou, L. Xie, N. Gao, X. Lu, X. Gao, J. Gao, L. Shui, S. Wu, J. Liu, *Applied Surface Science* **2020**, 513, 145790.

[636] H. Liu, P. Zhang, F. Wang, C. Jia, Y. Chen, *Solar Energy* **2020**, 198, 335.

[637] M. Adnan, J. K. Lee, *RSC Advances* **2020**, 10, 5454.

[638] J.-Y. Seo, H.-S. Kim, S. Akin, M. Stojanovic, E. Simon, M. Fleischer, A. Hagfeldt, S. M. Zakeeruddin, M. Grätzel, *Energy & Environmental Science* **2018**, 11, 2985.

[639] K. Choi, J. Lee, H. I. Kim, C. W. Park, G.-W. Kim, H. Choi, S. Park, S. A. Park, T. Park, *Energy & Environmental Science* **2018**, 11, 3238.

[640] S. Suragtkhuu, O. Tserendavag, U. Vandandoo, A. S. R. Bati, M. Bat-Erdene, J. G. Shapter, M. Batmunkh, S. Davaasambuu, *RSC Advances* **2020**, 10, 9133.

[641] T. Zhang, M. Long, M. Qin, X. Lu, S. Chen, F. Xie, L. Gong, J. Chen, M. Chu, Q. Miao, Z. Chen, W. Xu, P. Liu, W. Xie, J.-b. Xu, *Joule* **2018**, 2, 2706.

[642] Y. Jiang, J. Yuan, Y. Ni, J. Yang, Y. Wang, T. Jiu, M. Yuan, J. Chen, *Joule* **2018**, 2, 1356.

[643] H. Tsai, W. Nie, J.-C. Blancon, C. C. Stoumpos, R. Asadpour, B. Harutyunyan, A. J. Neukirch, R. Verduzco, J. J. Crochet, S. Tretiak, L. Pedesseau, J. Even, M. A. Alam, G.

Gupta, J. Lou, P. M. Ajayan, M. J. Bedzyk, M. G. Kanatzidis, A. D. Mohite, *Nature* **2016**, 536, 312.
[644] Z. Wang, Q. Lin, F. P. Chmiel, N. Sakai, L. M. Herz, H. J. Snaith, *Nature Energy* **2017**, 2, 17135.
[645] M. Stolterfoht, C. M. Wolff, J. A. Márquez, S. Zhang, C. J. Hages, D. Rothhardt, S. Albrecht, P. L. Burn, P. Meredith, T. Unold, D. Neher, *Nature Energy* **2018**, 3, 847.
[646] D. Zhao, Y. Yu, C. Wang, W. Liao, N. Shrestha, C. R. Grice, A. J. Cimaroli, L. Guan, R. J. Ellingson, K. Zhu, X. Zhao, R.-G. Xiong, Y. Yan, *Nature Energy* **2017**, 2, 17018.
[647] H. Back, G. Kim, H. Kim, C.-Y. Nam, J. Kim, Y. R. Kim, T. Kim, B. Park, J. R. Durrant, K. Lee, *Energy & Environmental Science* **2020**, 13, 840.
[648] H.-H. Huang, Y.-C. Shih, L. Wang, K.-F. Lin, *Energy & Environmental Science* **2019**, 12, 1265.
[649] X. He, T. Wu, X. Liu, Y. Wang, X. Meng, J. Wu, T. Noda, X. Yang, Y. Moritomo, H. Segawa, L. Han, *Journal of Materials Chemistry A* **2020**, 8, 2760.
[650] J. T.-W. Wang, Z. Wang, S. Pathak, W. Zhang, D. W. deQuilettes, F. Wisnivesky-Rocca-Rivarola, J. Huang, P. K. Nayak, J. B. Patel, H. A. Mohd Yusof, Y. Vaynzof, R. Zhu, I. Ramirez, J. Zhang, C. Ducati, C. Grovenor, M. B. Johnston, D. S. Ginger, R. J. Nicholas, H. J. Snaith, *Energy & Environmental Science* **2016**, 9, 2892.
[651] W. Feng, C. Zhang, J.-X. Zhong, L. Ding, W.-Q. Wu, *Chemical Communications* **2020**, 56, 5006.
[652] F. Wang, X. Jiang, H. Chen, Y. Shang, H. Liu, J. Wei, W. Zhou, H. He, W. Liu, Z. Ning, *Joule* **2018**, 2, 2732.
[653] Y. Lin, Y. Bai, Y. Fang, Z. Chen, S. Yang, X. Zheng, S. Tang, Y. Liu, J. Zhao, J. Huang, *The Journal of Physical Chemistry Letters* **2018**, 9, 654.
[654] C. Ma, C. Leng, Y. Ji, X. Wei, K. Sun, L. Tang, J. Yang, W. Luo, C. Li, Y. Deng, S. Feng, J. Shen, S. Lu, C. Du, H. Shi, *Nanoscale* **2016**, 8, 18309.
[655] J.-H. Lee, D. G. Lee, H. S. Jung, H. H. Lee, H.-K. Kim, *Journal of Alloys and Compounds* **2020**, DOI: https://doi.org/10.1016/j.jallcom.2020.155531155531.
[656] H. Cheng, Y. Li, M. Zhang, K. Zhao, Z.-S. Wang, *ChemSusChem* **2020**, n/a.
[657] R. Prasanna, T. Leijtens, S. P. Dunfield, J. A. Raiford, E. J. Wolf, S. A. Swifter, J. Werner, G. E. Eperon, C. de Paula, A. F. Palmstrom, C. C. Boyd, M. F. A. M. van Hest, S. F. Bent, G. Teeter, J. J. Berry, M. D. McGehee, *Nature Energy* **2019**, 4, 939.
[658] D. Papadatos, D. Sygkridou, E. Stathatos, *Materials Letters* **2020**, 268, 127621.
[659] J. Kim, G. Lee, K. Lee, H. Yu, J. W. Lee, C.-M. Yoon, S. G. Kim, S. K. Kim, J. Jang, *Chemical Communications* **2020**, 56, 535.
[660] S. Ye, H. Rao, Z. Zhao, L. Zhang, H. Bao, W. Sun, Y. Li, F. Gu, J. Wang, Z. Liu, Z. Bian, C. Huang, *Journal of the American Chemical Society* **2017**, 139, 7504.
[661] L. Fan, S. Liu, Y. Lei, R. Qi, L. Guo, X. Yang, Q. Meng, Q. Dai, Z. Zheng, *ACS Applied Materials & Interfaces* **2019**, 11, 45568.
[662] K. A. Bush, S. Manzoor, K. Frohna, Z. J. Yu, J. A. Raiford, A. F. Palmstrom, H.-P. Wang, R. Prasanna, S. F. Bent, Z. C. Holman, M. D. McGehee, *ACS Energy Letters* **2018**, 3, 2173.
[663] K. A. Bush, A. F. Palmstrom, Z. J. Yu, M. Boccard, R. Cheacharoen, J. P. Mailoa, D. P. McMeekin, R. L. Z. Hoye, C. D. Bailie, T. Leijtens, I. M. Peters, M. C. Minichetti, N. Rolston, R. Prasanna, S. Sofia, D. Harwood, W. Ma, F. Moghadam, H. J. Snaith, T. Buonassisi, Z. C. Holman, S. F. Bent, M. D. McGehee, *Nature Energy* **2017**, 2, 17009.
[664] M. Jošt, E. Köhnen, A. B. Morales-Vilches, B. Lipovšek, K. Jäger, B. Macco, A. Al-Ashouri, J. Krč, L. Korte, B. Rech, R. Schlatmann, M. Topič, B. Stannowski, S. Albrecht, *Energy & Environmental Science* **2018**, 11, 3511.

[665] F. Sahli, J. Werner, B. A. Kamino, M. Bräuninger, R. Monnard, B. Paviet-Salomon, L. Barraud, L. Ding, J. J. Diaz Leon, D. Sacchetto, G. Cattaneo, M. Despeisse, M. Boccard, S. Nicolay, Q. Jeangros, B. Niesen, C. Ballif, *Nature Materials* **2018**, 17, 820.
[666] M. Jošt, T. Bertram, D. Koushik, J. A. Marquez, M. A. Verheijen, M. D. Heinemann, E. Köhnen, A. Al-Ashouri, S. Braunger, F. Lang, B. Rech, T. Unold, M. Creatore, I. Lauermann, C. A. Kaufmann, R. Schlatmann, S. Albrecht, *ACS Energy Letters* **2019**, 4, 583.
[667] A. R. Uhl, Z. Yang, A. K. Y. Jen, H. W. Hillhouse, *Journal of Materials Chemistry A* **2017**, 5, 3214.
[668] D. Zhao, C. Chen, C. Wang, M. M. Junda, Z. Song, C. R. Grice, Y. Yu, C. Li, B. Subedi, N. J. Podraza, X. Zhao, G. Fang, R.-G. Xiong, K. Zhu, Y. Yan, *Nature Energy* **2018**, 3, 1093.
[669] T. Leijtens, R. Prasanna, K. A. Bush, G. E. Eperon, J. A. Raiford, A. Gold-Parker, E. J. Wolf, S. A. Swifter, C. C. Boyd, H.-P. Wang, M. F. Toney, S. F. Bent, M. D. McGehee, *Sustainable Energy & Fuels* **2018**, 2, 2450.
[670] Z. Song, D. Zhao, C. Chen, R. H. Ahangharnejhad, C. Li, K. Ghimire, N. J. Podraza, M. J. Heben, K. Zhu, Y. Yan, presented at 2019 IEEE 46th Photovoltaic Specialists Conference (PVSC), 16-21 June 2019, **2019**.
[671] Z. Li, S. Wu, J. Zhang, K. C. Lee, H. Lei, F. Lin, Z. Wang, Z. Zhu, A. K. Y. Jen, *Advanced Energy Materials* **2020**, 10, 2000361.
[672] S. Pisoni, F. Fu, T. Feurer, M. Makha, B. Bissig, S. Nishiwaki, A. N. Tiwari, S. Buecheler, *Journal of Materials Chemistry A* **2017**, 5, 13639.
[673] S. Pisoni, R. Carron, T. Moser, T. Feurer, F. Fu, S. Nishiwaki, A. N. Tiwari, S. Buecheler, *NPG Asia Materials* **2018**, 10, 1076.
[674] L. Kranz, A. Abate, T. Feurer, F. Fu, E. Avancini, J. Löckinger, P. Reinhard, S. M. Zakeeruddin, M. Grätzel, S. Buecheler, A. N. Tiwari, *The Journal of Physical Chemistry Letters* **2015**, 6, 2676.
[675] F. Fu, T. Feurer, T. Jäger, E. Avancini, B. Bissig, S. Yoon, S. Buecheler, A. N. Tiwari, *Nature Communications* **2015**, 6, 8932.
[676] H. Shen, T. Duong, J. Peng, D. Jacobs, N. Wu, J. Gong, Y. Wu, S. K. Karuturi, X. Fu, K. Weber, X. Xiao, T. P. White, K. Catchpole, *Energy & Environmental Science* **2018**, 11, 394.
[677] J. Tong, Z. Song, D. H. Kim, X. Chen, C. Chen, A. F. Palmstrom, P. F. Ndione, M. O. Reese, S. P. Dunfield, O. G. Reid, J. Liu, F. Zhang, S. P. Harvey, Z. Li, S. T. Christensen, G. Teeter, D. Zhao, M. M. Al-Jassim, M. F. A. M. van Hest, M. C. Beard, S. E. Shaheen, J. J. Berry, Y. Yan, K. Zhu, *Science* **2019**, 364, 475.
[678] S. U. Ryu, Z. Abbas, A. Cho, H. Lee, C. E. Song, H. K. Lee, S. K. Lee, W. S. Shin, S.-J. Moon, T. Park, H. I. Kim, J.-C. Lee, *Advanced Energy Materials* **2020**, 10, 1903846.
[679] R. Kang, S. Park, Y. K. Jung, D. C. Lim, M. J. Cha, J. H. Seo, S. Cho, *Advanced Energy Materials* **2018**, 8, 1702165.
[680] Q. Zhang, X. Wan, F. Liu, B. Kan, M. Li, H. Feng, H. Zhang, T. P. Russell, Y. Chen, *Advanced Materials* **2016**, 28, 7008.
[681] Z. Zheng, S. Zhang, J. Zhang, Y. Qin, W. Li, R. Yu, Z. Wei, J. Hou, *Advanced Materials* **2016**, 28, 5133.
[682] M. F. Vildanova, A. B. Nikolskaia, S. S. Kozlov, O. I. Shevaleevskiy, L. L. Larina, *Technical Physics Letters* **2018**, 44, 126.
[683] Y. Dang, Y. Zhou, X. Liu, D. Ju, S. Xia, H. Xia, X. Tao, *Angewandte Chemie International Edition* **2016**, 55, 3447.
[684] X. Meng, J. Lin, X. Liu, X. He, Y. Wang, T. Noda, T. Wu, X. Yang, L. Han, *Advanced Materials* **2019**, 31, 1903721.

[685] Y. Liao, H. Liu, W. Zhou, D. Yang, Y. Shang, Z. Shi, B. Li, X. Jiang, L. Zhang, L. N. Quan, R. Quintero-Bermudez, B. R. Sutherland, Q. Mi, E. H. Sargent, Z. Ning, *Journal of the American Chemical Society* **2017**, 139, 6693.
[686] D. H. Cao, C. C. Stoumpos, T. Yokoyama, J. L. Logsdon, T.-B. Song, O. K. Farha, M. R. Wasielewski, J. T. Hupp, M. G. Kanatzidis, *ACS Energy Letters* **2017**, 2, 982.
[687] M. Chen, M.-G. Ju, H. F. Garces, A. D. Carl, L. K. Ono, Z. Hawash, Y. Zhang, T. Shen, Y. Qi, R. L. Grimm, D. Pacifici, X. C. Zeng, Y. Zhou, N. P. Padture, *Nature Communications* **2019**, 10, 16.
[688] M. Abulikemu, S. Ould-Chikh, X. Miao, E. Alarousu, B. Murali, G. O. Ngongang Ndjawa, J. Barbé, A. El Labban, A. Amassian, S. Del Gobbo, *Journal of Materials Chemistry A* **2016**, 4, 12504.
[689] B.-W. Park, B. Philippe, X. Zhang, H. Rensmo, G. Boschloo, E. M. J. Johansson, *Advanced Materials* **2015**, 27, 6806.
[690] M. B. Johansson, H. Zhu, E. M. J. Johansson, *The Journal of Physical Chemistry Letters* **2016**, 7, 3467.
[691] J.-C. Hebig, I. Kühn, J. Flohre, T. Kirchartz, *ACS Energy Letters* **2016**, 1, 309.
[692] P. C. Harikesh, H. K. Mulmudi, B. Ghosh, T. W. Goh, Y. T. Teng, K. Thirumal, M. Lockrey, K. Weber, T. M. Koh, S. Li, S. Mhaisalkar, N. Mathews, *Chemistry of Materials* **2016**, 28, 7496.
[693] Z. Deng, F. Wei, S. Sun, G. Kieslich, A. K. Cheetham, P. D. Bristowe, *Journal of Materials Chemistry A* **2016**, 4, 12025.
[694] G. García-Espejo, D. Rodríguez-Padrón, R. Luque, L. Camacho, G. de Miguel, *Nanoscale* **2019**, 11, 16650.
[695] S. Nair, M. Deshpande, V. Shah, S. Ghaisas, S. Jadkar, *Journal of Physics: Condensed Matter* **2019**, 31, 445902.
[696] F. Wei, Z. Deng, S. Sun, F. Xie, G. Kieslich, D. M. Evans, M. A. Carpenter, P. D. Bristowe, A. K. Cheetham, *Materials Horizons* **2016**, 3, 328.
[697] P. Cheng, T. Wu, Y. Li, L. Jiang, W. Deng, K. Han, *New Journal of Chemistry* **2017**, 41, 9598.
[698] C. Zhang, L. Gao, S. Teo, Z. Guo, Z. Xu, S. Zhao, T. Ma, *Sustainable Energy & Fuels* **2018**, 2, 2419.
[699] Z. Zhang, C. Wu, D. Wang, G. Liu, Q. Zhang, W. Luo, X. Qi, X. Guo, Y. Zhang, Y. Lao, B. Qu, L. Xiao, Z. Chen, *Organic Electronics* **2019**, 74, 204.
[700] X. Yang, Y. Chen, P. Liu, H. Xiang, W. Wang, R. Ran, W. Zhou, Z. Shao, *Advanced Functional Materials* **2020**, 30, 2001557.
[701] A. Karmakar, M. S. Dodd, S. Agnihotri, E. Ravera, V. K. Michaelis, *Chemistry of Materials* **2018**, 30, 8280.
[702] T. T. Tran, J. R. Panella, J. R. Chamorro, J. R. Morey, T. M. McQueen, *Materials Horizons* **2017**, 4, 688.
[703] B. Vargas, E. Ramos, E. Pérez-Gutiérrez, J. C. Alonso, D. Solis-Ibarra, *Journal of the American Chemical Society* **2017**, 139, 9116.
[704] N. Matsushita, H. Kitagawa, N. Kojima, *ChemInform* **1997**, 28.
[705] X. J. Liu, K. Matsuda, Y. Moritomo, A. Nakamura, N. Kojima, *Physical Review B* **1999**, 59, 7925.
[706] X.-G. Zhao, D. Yang, Y. Sun, T. Li, L. Zhang, L. Yu, A. Zunger, *Journal of the American Chemical Society* **2017**, 139, 6718.
[707] W. Lee, S. Hong, S. Kim, *The Journal of Physical Chemistry C* **2019**, 123, 2665.
[708] G. Volonakis, A. A. Haghighirad, R. L. Milot, W. H. Sio, M. R. Filip, B. Wenger, M. B. Johnston, L. M. Herz, H. J. Snaith, F. Giustino, *The Journal of Physical Chemistry Letters* **2017**, 8, 772.

[709] B. Liu, S. Wang, Z. Ma, J. Ma, R. Ma, C. Wang, *Applied Surface Science* **2019**, 467-468, 708.
[710] S. Sidhik, A. C. Pasarán, C. Rosiles Pérez, T. López-Luke, E. De la Rosa, *Journal of Materials Chemistry C* **2018**, 6, 7880.
[711] M. Nukunudompanich, G. Budiutama, K. Suzuki, K. Hasegawa, M. Ihara, *CrystEngComm* **2020**, 22, 2718.
[712] Y.-K. Ren, S.-D. Liu, B. Duan, Y.-F. Xu, Z.-Q. Li, Y. Huang, L.-H. Hu, J. Zhu, S.-Y. Dai, *Journal of Alloys and Compounds* **2017**, 705, 205.
[713] P.-W. Liang, C.-Y. Liao, C.-C. Chueh, F. Zuo, S. T. Williams, X.-K. Xin, J. Lin, A. K. Y. Jen, *Advanced Materials* **2014**, 26, 3748.
[714] H. Zhou, Q. Chen, G. Li, S. Luo, T.-b. Song, H.-S. Duan, Z. Hong, J. You, Y. Liu, Y. Yang, *Science* **2014**, 345, 542.
[715] Y. Wen, Y.-G. Tang, G.-Q. Yan, *AIP Advances* **2018**, 8, 095226.
[716] J.-H. Im, H.-S. Kim, N.-G. Park, *APL Materials* **2014**, 2, 081510.
[717] D. Bi, S.-J. Moon, L. Häggman, G. Boschloo, L. Yang, E. M. J. Johansson, M. K. Nazeeruddin, M. Grätzel, A. Hagfeldt, *RSC Advances* **2013**, 3, 18762.
[718] S. Ito, S. Tanaka, H. Nishino, *The Journal of Physical Chemistry Letters* **2015**, 6, 881.
[719] Z. Xiao, C. Bi, Y. Shao, Q. Dong, Q. Wang, Y. Yuan, C. Wang, Y. Gao, J. Huang, *Energy & Environmental Science* **2014**, 7, 2619.
[720] F. Shao, L. Xu, Z. Tian, Y. Xie, Y. Wang, P. Sheng, D. Wang, F. Huang, *RSC Advances* **2016**, 6, 42377.
[721] C.-H. Chiang, C.-G. Wu, *ACS Nano* **2018**, 12, 10355.
[722] M. Liu, M. B. Johnston, H. J. Snaith, *Nature* **2013**, 501, 395.
[723] L. Qiu, S. He, Y. Jiang, D.-Y. Son, L. K. Ono, Z. Liu, T. Kim, T. Bouloumis, S. Kazaoui, Y. Qi, *Journal of Materials Chemistry A* **2019**, 7, 6920.
[724] V.-D. Tran, S. V. N. Pammi, V.-D. Dao, H.-S. Choi, S.-G. Yoon, *Journal of Alloys and Compounds* **2018**, 747, 703.
[725] P.-S. Shen, J.-S. Chen, Y.-H. Chiang, M.-H. Li, T.-F. Guo, P. Chen, *Advanced Materials Interfaces* **2016**, 3, 1500849.
[726] J. Yin, H. Qu, J. Cao, H. Tai, J. Li, N. Zheng, *Journal of Materials Chemistry A* **2016**, 4, 13203.
[727] M.-C. Tang, Y. Fan, D. Barrit, X. Chang, H. X. Dang, R. Li, K. Wang, D.-M. Smilgies, S. Liu, S. De Wolf, T. D. Anthopoulos, K. Zhao, A. Amassian, *Journal of Materials Chemistry A* **2020**, 8, 1095.
[728] Y. Galagan, F. Di Giacomo, H. Gorter, G. Kirchner, I. de Vries, R. Andriessen, P. Groen, *Advanced Energy Materials* **2018**, 8, 1801935.
[729] D. Lee, Y.-S. Jung, Y.-J. Heo, S. Lee, K. Hwang, Y.-J. Jeon, J.-E. Kim, J. Park, G. Y. Jung, D.-Y. Kim, *ACS Applied Materials & Interfaces* **2018**, 10, 16133.
[730] F. Mathies, H. Eggers, B. S. Richards, G. Hernandez-Sosa, U. Lemmer, U. W. Paetzold, *ACS Applied Energy Materials* **2018**, 1, 1834.
[731] F. Mathies, B. S. Richards, G. Hernandez-Sosa, U. Lemmer, U. W. Paetzold, presented at 2018 IEEE 7th World Conference on Photovoltaic Energy Conversion (WCPEC) (A Joint Conference of 45th IEEE PVSC, 28th PVSEC & 34th EU PVSEC), 10-15 June 2018, **2018**.
[732] Y. Y. Kim, E. Y. Park, T.-Y. Yang, J. H. Noh, T. J. Shin, N. J. Jeon, J. Seo, *Journal of Materials Chemistry A* **2018**, 6, 12447.
[733] W. Qiu, T. Merckx, M. Jaysankar, C. Masse de la Huerta, L. Rakocevic, W. Zhang, U. W. Paetzold, R. Gehlhaar, L. Froyen, J. Poortmans, D. Cheyns, H. J. Snaith, P. Heremans, *Energy & Environmental Science* **2016**, 9, 484.
[734] J. Seo, S. Park, Y. Chan Kim, N. J. Jeon, J. H. Noh, S. C. Yoon, S. I. Seok, *Energy & Environmental Science* **2014**, 7, 2642.

[735] J. Borchert, R. L. Milot, J. B. Patel, C. L. Davies, A. D. Wright, L. Martínez Maestro, H. J. Snaith, L. M. Herz, M. B. Johnston, *ACS Energy Letters* **2017**, 2, 2799.
[736] M. Shtein, *Doctoral* Princeton University, **2004**.
[737] L. Hoffmann, K. O. Brinkmann, J. Malerczyk, D. Rogalla, T. Becker, D. Theirich, I. Shutsko, P. Görrn, T. Riedl, *ACS Applied Materials & Interfaces* **2018**, 10, 6006.
[738] J. Feng, Y. Jiao, H. Wang, X. Zhu, Y. Sun, M. Du, Y. Cao, D. Yang, S. Liu, *Energy & Environmental Science* **2021**, 14, 3035.
[739] L. Gu, S. Wang, X. Fang, D. Liu, Y. Xu, N. Yuan, J. Ding, *ACS Applied Materials & Interfaces* **2020**, 12, 33870.
[740] Y. Jiang, M. R. Leyden, L. Qiu, S. Wang, L. K. Ono, Z. Wu, E. J. Juarez-Perez, Y. Qi, *Advanced Functional Materials* **2018**, 28, 1703835.
[741] A. T. Mallajosyula, K. Fernando, S. Bhatt, A. Singh, B. W. Alphenaar, J.-C. Blancon, W. Nie, G. Gupta, A. D. Mohite, *Applied Materials Today* **2016**, 3, 96.
[742] F. De Rossi, J. A. Baker, D. Beynon, K. E. A. Hooper, S. M. P. Meroni, D. Williams, Z. Wei, A. Yasin, C. Charbonneau, E. H. Jewell, T. M. Watson, *Advanced Materials Technologies* **2018**, 3, 1800156.
[743] G. B. Adugna, S. Y. Abate, W.-T. Wu, Y.-T. Tao, *ACS Applied Materials & Interfaces* **2021**, 13, 25926.
[744] J. E. Bishop, C. D. Read, J. A. Smith, T. J. Routledge, D. G. Lidzey, *Scientific Reports* **2020**, 10, 6610.
[745] L. Cai, L. Liang, J. Wu, B. Ding, L. Gao, B. Fan, *Journal of Semiconductors* **2017**, 38, 014006.
[746] Z. Yang, W. Zhang, S. Wu, H. Zhu, Z. Liu, Z. Liu, Z. Jiang, R. Chen, J. Zhou, Q. Lu, Z. Xiao, L. Shi, H. Chen, L. K. Ono, S. Zhang, Y. Zhang, Y. Qi, L. Han, W. Chen, *Science Advances* **2021**, 7, eabg3749.

**Ling Jin Kiong** is a PhD candidate in the Nanostructured Renewable Energy Materials Laboratory, Faculty of Industrial Sciences & Technology at Universiti Malaysia Pahang. He received his MS from Universiti Malaysia Pahang in Advanced Materials. His research interests include interfacial studies and materials development through ab-initio calculation and their applications in the self-rechargeable photobattery.

**Pradeep Kumar Koyadan Kizhakkedath** is the President of Research and Development at Rextone Industries Ltd, Vadodara India. At Rextone, which is the largest inkjet ink manufacturing company in India, he handles the development of next generation of inkjet inks, coatings, pigments and dyes synthesis and modification. Prior to the present role he has worked in Dow Chemicals, Mumbai, Hewlett Packard, San Diego, California and Oak Ridge National Laboratory, Oak Ridge, Tennessee, USA. Dr Pradeep Koyadan earned his PhD Chemistry from University of Tennessee, Knoxville USA, M Tech from Indian Institute of technology, Delhi and MSc from Andhra University.

**Trystan M. Watson** started his academic career with a Chemistry degree at Swansea University before transferring in 2001 to the College of Engineering to carry out a Doctorate in Steel Technology. In 2007 Trystan took up a post-doctoral research position on the development of dye-sensitized solar cells on metal substrates. In 2011 Trystan became the lead of the photovoltaics scale-up activity at the SPECIFIC Innovation and Knowledge Centre, developing infrastructure for the printing and coating of solar cells onto metal, glass and plastic. His current research area is thin film printed PV in particular perovskite with a specialism in developing new technologies for the manufacture of these functional materials including deposition and curing processes.

**Iván Mora-Seró** received his Ph.D. degree in physics in 2004. He is full professor at the Universitat Jaume I de Castelló, Spain, and he is leading the Group of Advanced Semiconductors in the Institute of Advanced Materials (INAM). His research is focused on crystal growth, nanostructured devices, transport and recombination properties, photocatalysis, characterization, and development of PV and optoelectronic devices. Recent research activities are focused on new concepts for PV conversion and light emission (LEDs and light amplifiers) based on nanoscaled devices and semiconductor

materials following two main lines: semiconductor quantum dots and halide perovskites.

**Lukas Schmidt-Mende** received his Ph.D. from the University of Cambridge, UK on organic solar cells. Afterward, he worked as a Postdoc at EPF Lausanne on dye-sensitized solar cells and as Research Fellow at the Materials Science Department, University of Cambridge, UK, focusing on metal oxide nanostructures for hybrid solar cells. In 2007, he became Professor at the LMU Munich, continuing his work on hybrid solar cells. Since 2011, he has been Professor at the University of Konstanz in the Department of Physics, where his research focus is based on fundamental studies of metal oxide nanostructures and organic, hybrid, and perovskite solar cells.

**Thomas M. Brown** investigated polymer OLEDs for his PhD at the Cavendish Laboratory, University of Cambridge. From 2001– 2005 he developed OTFTs and E-Paper as Senior Engineer with Plastic Logic Ltd. In 2005 he was recipient of a ‘‘Re-entry’’ Fellowship awarded by the Italian Ministry of University and Research and is Associate Professor at the University of Rome-Tor Vergata. Cofounder of the Centre for Hybrid and Organic Solar Energy, and Associate Editor of Solar Energy, his current research in perovskite solar cells focuses on a variety of flexible substrates, light harvesting in indoor environments, and processing with greener solvents.

**Rajan Jose** supervises the Nanostructured Renewable Energy Materials Laboratory in the Universiti Malaysia Pahang (UMP) and is the Dean of Research (Technology) at UMP. He investigated nanostructured perovskites for microwave and superconducting electronics during his doctoral research at the Council of Scientific and Industrial Research (CSIR), Trivandrum, India and has received PhD degree in the year 2002. He has contributed to the science and engineering of diverse range of materials including metals and alloys, luminescent quantum dots for biological and energy applications, glass and glass ceramics for quantum electronics, and electrochemical materials for energy conversion and storage. Most of his research is on the structure – property relationship in materials for a desired device functionality.